CANADA

ACTIVATION ANALYSIS WITH A NEUTRON GENERATOR

HUGH P. DIBBS

EPARTMENT OF MINES AND
ECHNICAL SURVEYS, OTTAWA

MINES BRANCH

RESEARCH REPORT

R 155

Price $1.25

MINERAL SCIENCES DIVISION

FEBRUARY 1965

Available by mail from the Queen's Printer, Ottawa,
and at the following Canadian Government bookshops:

OTTAWA
Daly Building, Corner Mackenzie and Rideau

TORONTO
Mackenzie Building, 36 Adelaide St. East

MONTREAL
Aeterna-Vie Building, 1182 St. Catherine St. West

or through your bookseller

A deposit copy of this publication is also available
for reference in public libraries across Canada

Price $1.25 Catalogue No. M38-1/155

Price subject to change without notice

ROGER DUHAMEL, F.R.S.C.
Queen's Printer and Controller of Stationery
Ottawa, Canada
1965

Mines Branch Research Report R 155

ACTIVATION ANALYSIS WITH A NEUTRON GENERATOR

by

Hugh P. Dibbs*

SYNOPSIS

An account is given of an activation analysis system using a neutron generator as a neutron source. The shielding requirements for high-energy neutrons and the experimental irradiation facilities are described. Activation yields have been calculated, under defined conditions, for all stable nuclides that on irradiation with 14 MeV neutrons or with thermal neutrons produce gamma-emitting isotopes. Experimental measurements have also been made to determine the sensitivity of detection of sixty-six elements. The gamma-ray spectra resulting from a number of these empirical determinations are presented.

---

*Senior Scientific Officer, Mineral Physics, Mineral Sciences Division, Mines Branch, Department of Mines and Technical Surveys, Ottawa, Canada.

Direction des mines

Rapport de recherches R 155

ANALYSE PAR ACTIVATION À L'AIDE D'UN GÉNÉRATEUR DE NEUTRONS

par

Hugh P. Dibbs*

RÉSUMÉ

L'auteur décrit une méthode d'analyse par activation à l'aide d'un générateur neutronique émettant ces particules, les caractéristiques des écrans qu'exige l'emploi de neutrons de grande énergie, et les installations d'irradiation expérimentale. Il a calculé les rendements d'activation sous des conditions déterminées pour tous les nuclides stables qui, soumis à une irradiation de neutrons d'une énergie de 14 MeV ou de neutrons d'énergie thermique, forment des isotopes émettant des rayons γ. Des mesures d'essai ont été également effectuées en vue de déterminer la sensibilité de soixante-six éléments détecteurs. L'auteur présente les spectres de rayonnement γ obtenus au cours d'un certain nombre de ces déterminations empiriques.

*Agent scientifique senior, Physique des minéraux, Division des sciences minérales, Direction des mines, ministère des Mines et des Relevés techniques, Ottawa, Canada.

CONTENTS

FIGURES

TABLES

INTRODUCTION

Neutron activation analysis is an analytical technique that has gained wide acceptance in recent years as a very sensitive method for the quantitative determination of a large number of elements (1-3). The method depends upon the fact that most elements become radioactive on neutron bombardment. The radioactive isotopes that are formed are unstable, and decay to a stable ground state with the emission of beta and/or gamma radiation of characteristic energies, and with definite half-lives: factors that usually allow unambiguous characterisation of a radioisotope. Although, in principle, activation analysis is an absolute method of analysis, in practice the method is almost always performed on a comparison basis. Thus, if a given element is being determined in a sample, a known weight of the element, as a standard, is usually irradiated simultaneously.

Following the neutron irradiation, a comparison of the activity induced in the known weight of the standard with the activity from the same isotope in the sample, gives a quantitative measure of the weight of the element in the sample. In many cases, particularly where the concentration of the element of interest is low, it is necessary for counting purposes to separate chemically the isotope of interest from the (radioactive) matrix. This separation may be performed by conventional chemical techniques, normally after the addition of an inactive carrier (4).

Activation analysis differs from most conventional analytical methods in that it is based on a nuclear interaction and is not concerned with the behaviour of the outer electron shells of atoms. The method is thus independent of the chemical (or physical) state of the target element and provides a true elemental analytical technique. An important corollary of activation analysis being a nuclear phenomenon is that, since the nuclear properties of an element (in terms of neutron activation cross sections and half-lives of product isotopes) are unrelated to its chemical properties, elements that are very similar chemically (and hence difficult to determine by chemical methods) may often be readily determined by activation analysis.

The high sensitivity associated with activation analysis is a result of two factors. Firstly, the uncharged nature of the neutron, which means that there is a negligible energy barrier for the neutron-nucleus interaction, and secondly, the availability of very-high-flux thermal neutron reactors together with the relatively high probability of neutron-nucleus interaction at thermal neutron energies (0.025 eV). In all cases where high analytical sensitivity is required, it is necessary to use a reactor as a neutron source. However, the need to use a reactor places severe restrictions on many laboratories

that wish to perform neutron activation analysis. Ready access to a reactor facility is not always possible and logistic difficulties often preclude the use of short-lived isotopes unless an on-site experiment can be arranged. Moreover, the very high analytical sensitivity that is available using a reactor is not always required to perform many useful activation analysis studies. A number of alternative neutron sources, other than reactors, are available. Their characteristics are listed, together with a typical high-flux reactor, in Table 1.

TABLE 1

Outputs Available from Various Neutron Sources

Source	Neutron Production Method	Neutron Output or Flux	Average Neutron Energy at Given Output or Flux
1 curie Sb/Be	Be-9(γ, n)Be-8	1.3×10^6 n/sec	0.025 MeV
1 curie Am/Be	Be-9(α, n)C-12	2.5×10^6 n/sec	4.5 MeV
1 curie Ra/Be	Be-9(α, n)C-12	1.3×10^7 n/sec	4.0 MeV
Van de Graaf Accelerator	Be-9(d, n)B-10	2.5×10^8 n/cm^2-sec*	0.025 eV
Cockroft-Walton Accelerator	H-3(d, n)He-4	10^{11} n/sec	14 MeV
Reactor (N.R.U., Chalk River)	U fission	2×10^{14} n/cm^2-sec*	0.025 eV

*Neutron flux following thermalisation.

None of these sources can approach a reactor in terms of neutron output, but they do provide relatively low-cost neutron sources that may be under the control of the individual laboratory. The Cockroft-Walton accelerator, referred to in Table 1, provides perhaps the most versatile laboratory source. Neutrons are produced according to the reaction

$$H\text{-}2 + H\text{-}3 = He\text{-}4 + n + 17.6 \text{ MeV}$$

by accelerating a beam of deuterium ions and causing them to impinge on a tritium-containing target. This type of accelerator (or neutron generator, as it is commonly called) is now available commercially from a number of manufacturers. Although the neutron output of the generator is many orders of magnitude lower than a reactor's, the output is nevertheless significantly higher than the neutron output from the currently available isotopic neutron sources. An interesting feature of the neutron generator, using the (d, T)

reaction, is that it produces essentially mono-energetic 14 MeV neutrons. This energy is greater than the average binding energy per nucleon in the nucleus, for all but a few low Z elements. It is thus possible, with 14 MeV neutrons, to induce reactions in which one or more nucleons are emitted from the nucleus, i.e. reactions of the type:

$$ {}^{A}_{Z}M + n \rightarrow {}^{A-1}_{Z}M + 2n $$

$$ {}^{A}_{Z}M + n \rightarrow {}^{A}_{Z-1}N + p $$

$$ {}^{A}_{Z}M + n \rightarrow {}^{A-3}_{Z-2}P + \alpha $$

where Z = number of protons in the target nucleus and A = number of protons and neutrons in the target nucleus.

With thermal neutron activation (neutron energy 0.025 eV), which is the usual activation process in a reactor, reactions are nearly always of the type:

$$ {}^{A}_{Z}M + n \rightarrow {}^{A+1}_{Z}M + \gamma $$

The 14 MeV neutrons produced by a neutron generator may, of course, be slowed to thermal energies with a suitable moderator, such as water.

It is the purpose of this report to describe the application of a neutron generator to laboratory activation analysis, using both 14 MeV neutrons and also thermal neutrons. Until recently the use of 14 MeV neutrons in activation analysis has been restricted almost entirely to the determination of oxygen (5), with very few references to the determination of other elements (6, 7). This situation has arisen, in part, from a lack of a suitable mono-energetic, high-energy neutron source. Although large fluxes of high-energy neutrons are present in a thermal neutron reactor, their use is limited, because of the high activity induced in most elements from the intense thermal neutron background in the reactor. If it is desired to use the fast neutrons in a reactor for activation analysis, special precautions have to be taken to minimise this background effect (8). For certain elements, e.g. oxygen, silicon, iron and lead, fast neutron activation (i.e. with 14 MeV

neutrons) is a more favourable technique for analysis than thermal neutron activation, and, for oxygen in particular, allows a determination to be made that is not practical with a thermal neutron source.

NEUTRON GENERATOR

The neutron generator used in this work was a Model 150-IHV generator, manufactured by the Texas Nuclear Company, Austin, Texas. It consists of three separate components: the positive-ion accelerator section and vacuum pumps, a 150 kV power supply, and a control console. Appropriate cables interconnect these units and allow flexibility as to their relative locations. A maximum beam current of one milliampere at a 150 kV accelerating potential is specified for the generator.

A schematic drawing of the accelerator-section is given in Figure 1. It operates under high-vacuum conditions. Following initial evacuation of the system to about one micron with a rotary oil pump, the rotary pump is valved-off and pumping is continued with an electronic-ion pump. The electronic-ion pump is ideal for accelerator applications, since the absence of a pumping fluid ensures that contamination of the system cannot occur. A molecular-sieve trap was used between the rotary pump and the accelerator to prevent the back-diffusion of oil vapour from the rotary pump, which can cause contamination of the electrodes in the electronic-ion pump. The exhaust of the rotary pump was vented to the outside of the building. A static vacuum of about 2×10^{-7} mm is normally achieved. To produce neutrons, deuterium is admitted to the ion-source bottle through a heated palladium "leak", until a pressure of about 6×10^{-6} mm is reached. The deuterium is then ionised by the application of a radio frequency field, through two metal rings capacitatively coupled to the ion bottle. The ion source is of a modified Oak Ridge design (9) and gives an atomic-ion to molecular-ion ratio of about 9 to 1. Depending on the beam current required, a potential of up to 5 kV is applied to the ion bottle and the D^+ ions extracted, through the canal, into the accelerator tube. For beam currents greater than 100 microamperes, a solenoid coil around the base of the ion bottle is energised to increase the D^+ ion-field in the vicinity of the extraction canal. Air is blown through the high voltage (terminal) section of the generator to cool the ion source and associated voltage supplies. The area around the solenoid coil becomes very warm during extended operation. The small blower installed on the generator was found to be inadequate to provide cooling for this section and was replaced by a much more powerful, 100 cfm axial fan. After acceleration, the D^+ ions pass through a field-free region (drift tube) and impinge on a water-cooled tritium target. This target is 1.25 inches in diameter and consists of a thin titanium layer ($\sim$1 mg/cm^2) evaporated onto

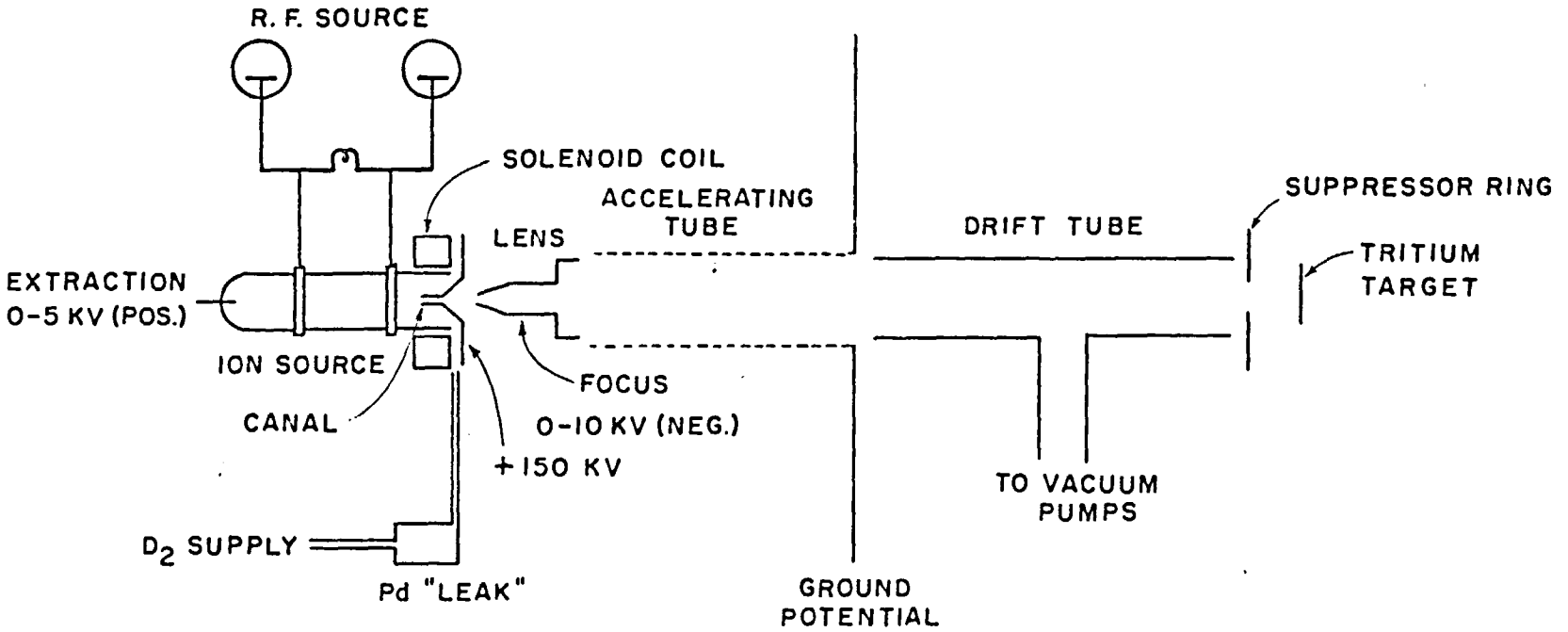

FIGURE 1. SCHEMATIC DIAGRAM OF NEUTRON GENERATOR.

a 0.01-inch-thick copper backing. Between 3-5 curies/in.^{2} of tritium are contained in the titanium layer, the active diameter of the target being one inch. A suppressor ring, at -100V, is placed close to the target to prevent electrons being attracted back to the accelerator tube and causing damage to the accelerator electrodes. The size of the beam on the target may be varied up to about 0.5 inch diameter by means of a focus control. The settings of the deuterium supply, extraction, focus, and high-voltage supply, are controlled from the control console. Preliminary familiarisation with the operation of the generator is performed using hydrogen and a blank target. The beam itself can readily be seen in a darkened room at beam currents above 100 microamperes.

The lifetime of the tritium target, i.e. the time during which the target will produce a useful neutron output, is an important aspect of generator operation. Although one tritium atom is lost for each neutron produced, a further and much more significant loss of tritium occurs both from deuterium-atom displacement of tritium in the target and probably also from a certain amount of thermal decomposition of the tritium-containing surface layer of the target. The actual chemical state of tritium in the target is a matter of some doubt and much of it may be present as chemi-sorbed tritium. Calculations indicate that considerably less than 1% of the tritium in the target is used to produce neutrons, the balance being dispersed in the vacuum system. Various half-lives for tritium targets have been reported and are of the order of 1-4 hours at one milliampere beam current (10, 11). At lower beam currents the half-life of the target is longer. It has been our experience that considerable differences occur in the operating lives of targets. Thus, of two new targets, each of about the same total activity and superficial appearance, one may give a much poorer operating life than the other. The relatively limited life of a target means that extended irradiations (i.e. for many hours) at high beam currents are not practical and this has placed an emphasis, in activation analysis with a neutron generator, on product isotopes of short half-lives.

Although the active diameter of the target is one inch, it is not possible to use the edge of the target for neutron production and hence this edge portion is wasted. A number of targets have been prepared in which only the central area is active. These targets were made relatively cheaply (about $15 each) from a tritium-strip target, 0.625 inch wide and 10 inches long, obtained from the Radiochemical Centre, Amersham, England. Sections, 0.5 inch long, were cut from the strip and soft-soldered on the centre of a 1.25 inch diameter disc of O.F.H.C. (oxygen-free, high-conductivity) copper. Loss of tritium during the soldering operation was negligible.

Because of the heat liberated on the target surface (150 watts at 150 kV accelerating potential and one milliampere beam current), adequate water cooling of the target is necessary. In fact, without water cooling a hole may be rapidly burned through the target. As a safeguard against this

possibility, a simple water control device, based on the design of Houghton (12), was placed in the output cooling line from the target. If for any reason the water supply fails, or drops below a predetermined value, the high-voltage supply (and hence the beam current) is automatically switched off.

NEUTRON SHIELDING

The high penetrating power of 14 MeV neutrons, together with their low biological tolerance (Table 2), means that a neutron generator requires a fairly massive shield for personnel protection. As will be seen in Table 2, the biological hazard associated with neutrons decreases with decrease in neutron energy.

TABLE 2

Maximum Permissible Exposure for Neutrons as a Function of Neutron Energy (13)

Neutron Energy	Flux (n/cm^2-sec) to give 100 mrem in 40 hr
0.025 eV (Thermal)	670
0.1 MeV	80
1.0 MeV	18
10 MeV	17
14 MeV	10

The shielding of high-energy neutrons is based upon decreasing the neutron energy by multiple collisions to epithermal or thermal energies, followed by capture(14). Hydrogeneous materials such as water, paraffin or polyethylene provide excellent thermalising media (15). Hydrogen also possesses a useful thermal neutron absorption cross section (σ =0.33b) through the reaction H + n = D + γ. The most effective form of shielding is that which can be arranged as close as possible to the tritium target in order to degrade the neutrons in energy before they can diffuse over large distances. Since neutrons are emitted isotropically from the target, it is necessary to make the geometry of this shielding as close as possible to 4 pi. Water has many advantages as a shielding medium; it is cheap, coherent and non-inflammable, but it does have the disadvantage of requiring a suitable container. Figure 2 illustrates the shielding used in the immediate vicinity of

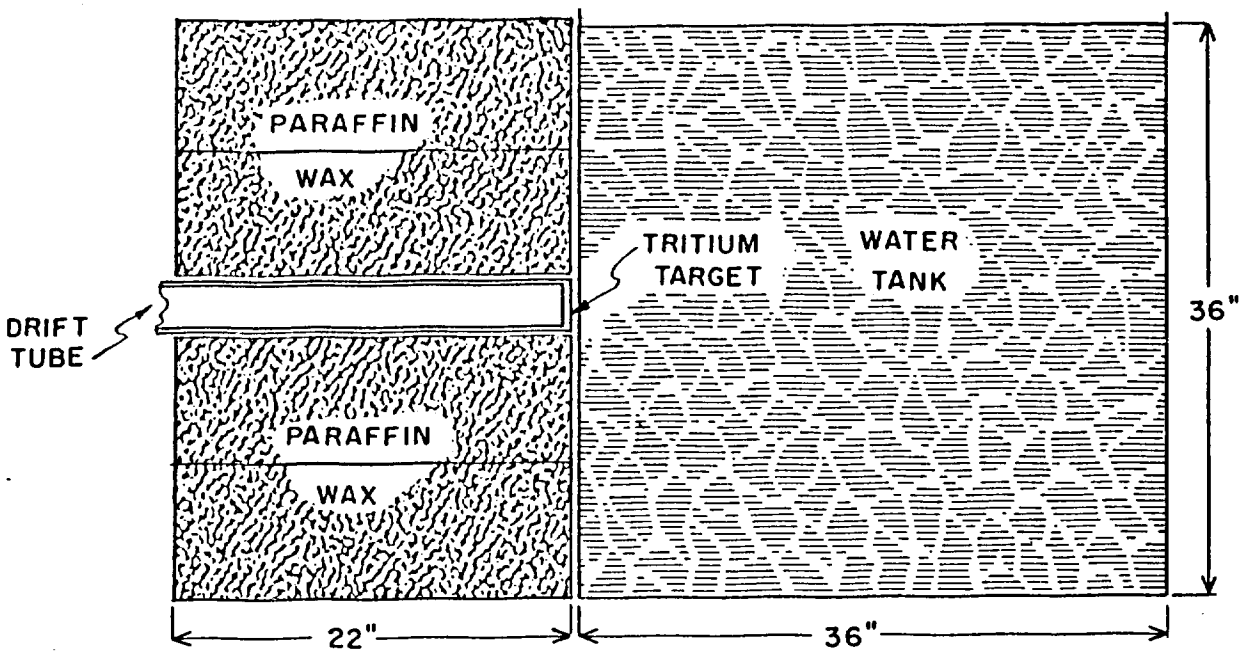

FIGURE 2. SHIELDING AROUND TRITIUM TARGET OF THE NEUTRON GENERATOR.

the target. The water-cooling cap around the tritium target touches the outside surface of the water tank. This three-feet-cube tank has two functions: it acts as a thermalising medium when thermal neutron irradiations are required, and it also acts as a bulk shield for neutrons emitted in the forward hemisphere. For fast neutron irradiations, the sample holder or pneumatic transfer tube (see page 18) is placed against the inner side of the water tank directly in-line with the target. For thermal neutron irradiations the sample holder is moved about 4.5 cm from the target. Plywood boxes, filled with paraffin wax, act as a shield for neutrons emitted in the rear hemisphere. These boxes may be very easily removed to change a target and afterwards replaced in their original positions. Leakage of neutrons still occurs through this primary shield, particularly through the drift tube section of the accelerator which penetrates the boxes of wax and which cannot be shielded. To allow greater shielding to be placed around the drift tube without interfering with the rest of the accelerator, the drift tube was increased in length by fifteen inches.

The external shielding of the generator is shown schematically in Figure 3. The walls are built of standard, commercially available, solid concrete building blocks (nominal dimensions, 4" x 8" x 16"). These blocks are cheap (25 cents each), reproducible in size, and easily obtainable. They may also be stacked with a minimum of skill, albeit with considerable effort. The walls were built so that vertical cracks between the blocks were staggered and did not coincide. Each alternate column of blocks was mounted on a half-inch layer of plywood, so that horizontal cracks between adjacent columns of blocks also did not coincide. Approximately 4500 blocks were used in the shielding walls. Two of the walls around the generator did not require shielding as they were outside walls of the building and below ground level. The initial roof shielding consisted of a three-feet-thick layer of lumber (built from 2" x 8" x 12' lengths) supported by one shielding wall of the room and by an eight inch I beam (mounted on four pillars) on the other side of the room. Lumber has the advantage of being self-supporting and of reasonable hydrogen content. However, it was found that neutron-leakage occurred to the laboratory directly above the neutron generator. An additional eight-inch layer of concrete and ten inches of water (contained in plastic tanks) were added to the roof to reduce the field to acceptable levels. Fast neutron dose-rate readings around the shield were taken with a calibrated fast neutron monitor (Nucleonic Corporation of America, Model FN 2B). The readings obtained at various positions around the shield, for a fast neutron flux of 5×10^8 n/cm^2-sec, are given in brackets in Figure 3. As the generator normally operates for only a relatively small part of the working week, dose-rates higher than those listed in Table 2 could be experienced and still maintain the weekly dose below tolerance level. All personnel associated with the operation of the generator are supplied with fast neutron film badges, the readings of which have always been well below tolerance levels.

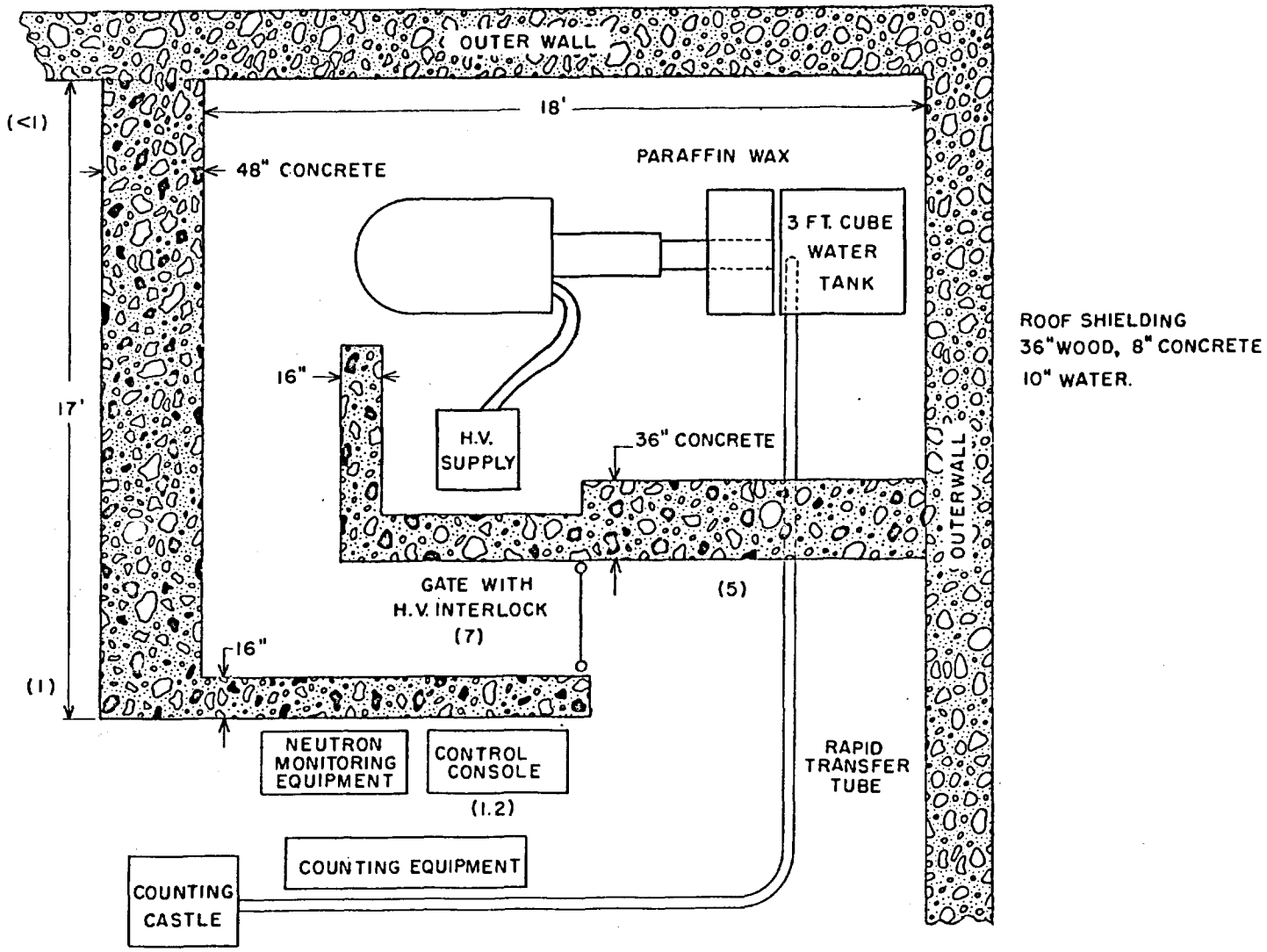

FIGURE 3. SHIELDING FOR NEUTRON GENERATOR.

A high-voltage supply interlock was installed on the gate of the generator room, as a safeguard for personnel inadvertently entering the room while the generator was operating. If the gate is opened the high-voltage supply (and hence the neutron output of the generator) is automatically switched off.

A view of the external shielding of the generator room is given in Figure 4, and a view of the inside of the generator room in Figure 5.

The counting equipment used for the measurement of gamma-ray spectra is situated only a few feet from the outer shielding wall of the generator room. When the generator is operating, a neutron-induced background is found in the NaI (Tl) scintillation crystal. This background arises from the prompt gamma radiation emitted in the vicinity of crystal, following the capture of low-energy neutrons that have diffused through the concrete shielding of the generator room. A shielded enclosure for the NaI (Tl) scintillation crystal (Figure 6) was built to minimise this background. The inner lead shield is constructed after the Chalk River design (16) and is enclosed by two inches of boron-loaded paraffin wax and by an eight-inch-thick layer of concrete blocks. The concrete blocks were soaked overnight in a saturated solution of boric acid before installation. Boron has a high thermal neutron absorption cross section and emits relatively non-penetrating 0.48 MeV gamma radiation following neutron capture.

In certain cases, e.g. the determination of small concentrations of oxygen (5), it is necessary to count a sample immediately after the irradiation has ended and to remove completely the neutron-induced background before counting begins. In the present system, neutron production was stopped instantly at the end of the irradiation by tripping the generator beam switch, which de-energises the radio frequency supply to the ion source.

FLUX DISTRIBUTION

In order to obtain the best utilisation of the neutron output of the generator, it is necessary to know the neutron energy distribution in the water tank, as a function of distance from the tritium target. This distribution was measured, for both fast and thermal neutrons, by foil activation techniques. For fast neutron measurements copper foils were used, and the positron activity resulting from the Cu63 (n, 2n) Cu62 reaction was measured with a single-channel gamma-ray spectrometer. For the measurement of the thermal neutron flux distribution, indium foils were used and the beta particles from the In115 (n, γ) In 116^{m} reaction were measured with a thin window Geiger-Müller counter.

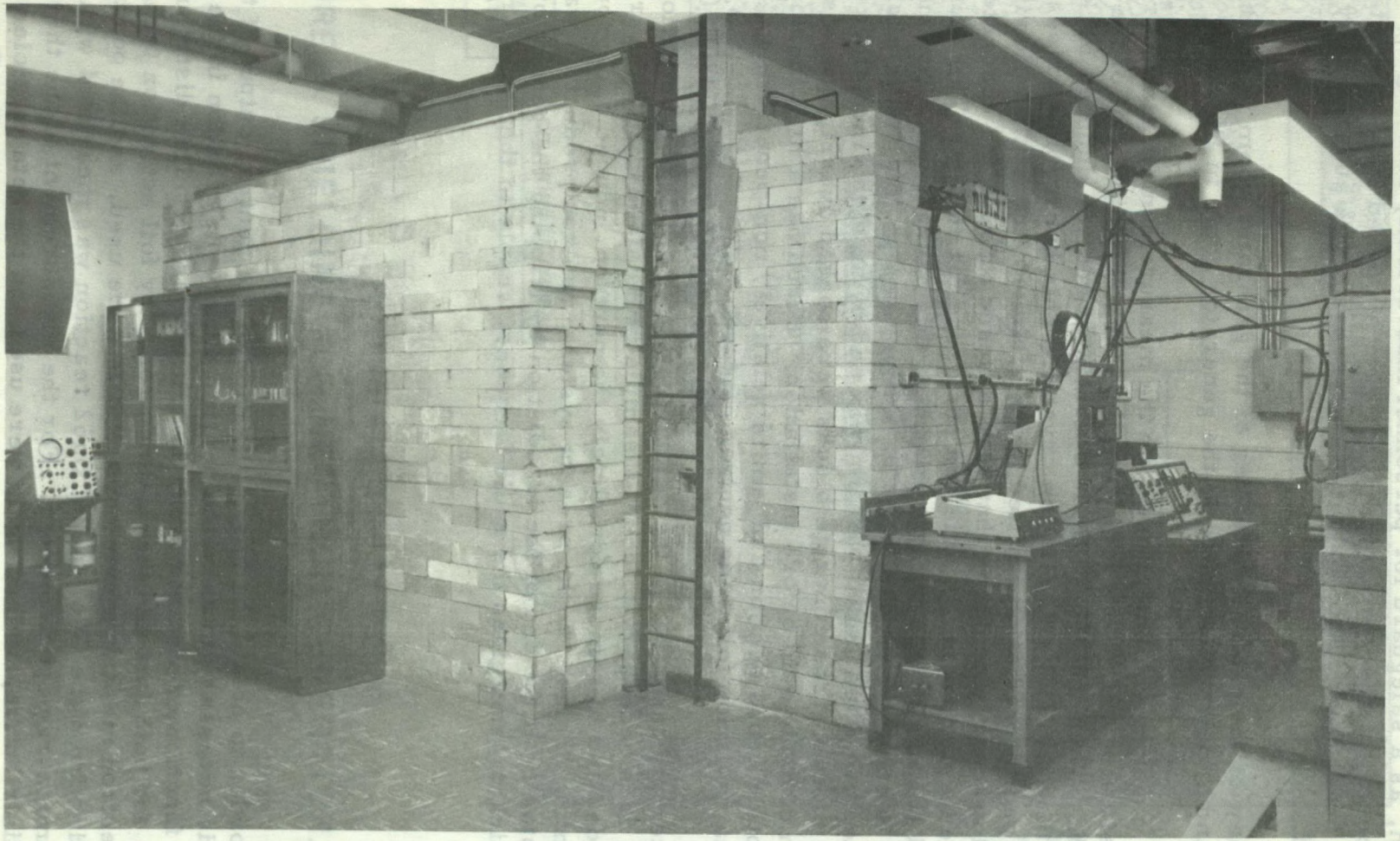

FIGURE 4. EXTERNAL VIEW OF NEUTRON GENERATOR SHIELD.

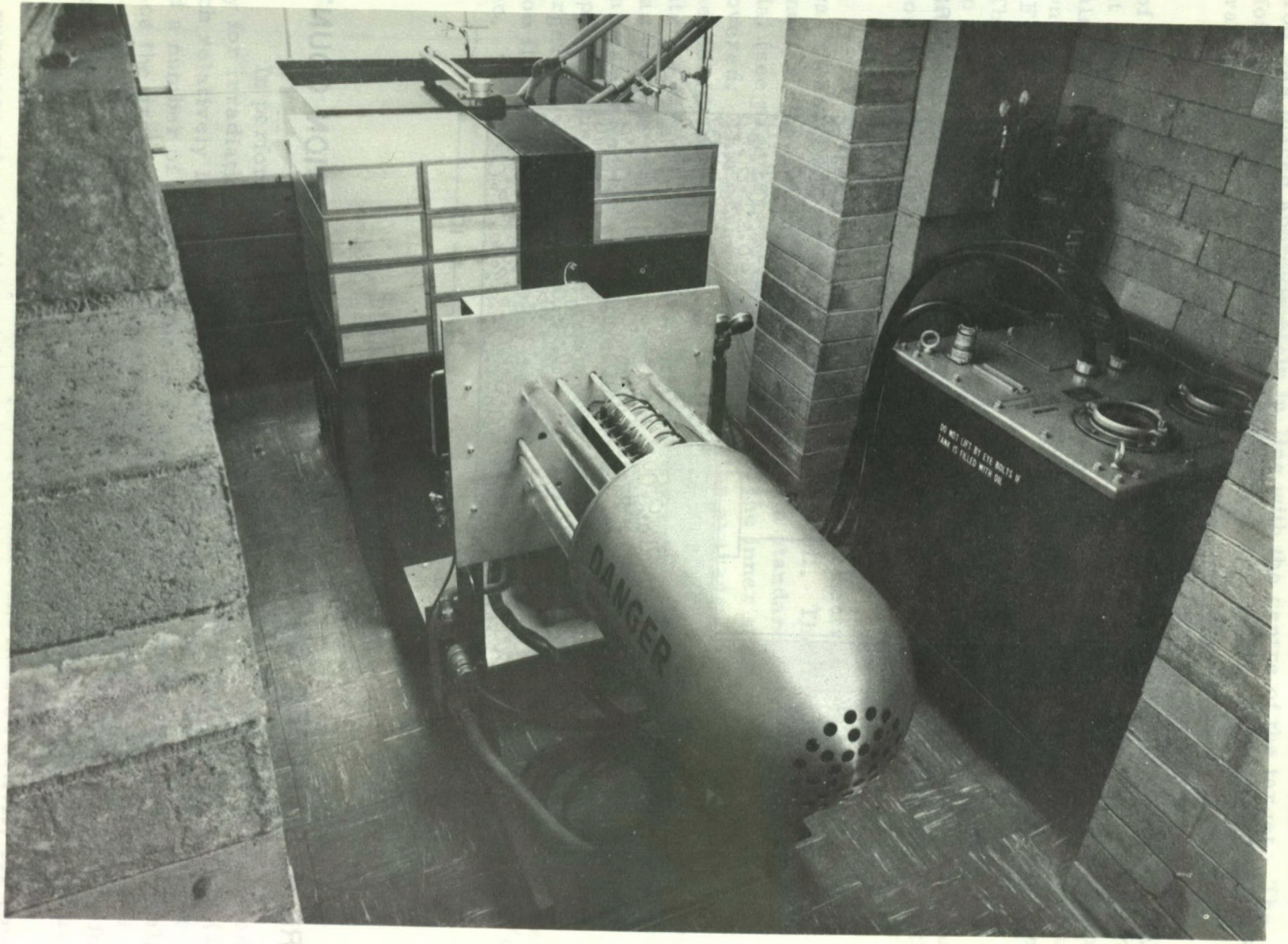

FIGURE 5. INTERNAL VIEW OF NEUTRON GENERATOR ROOM.

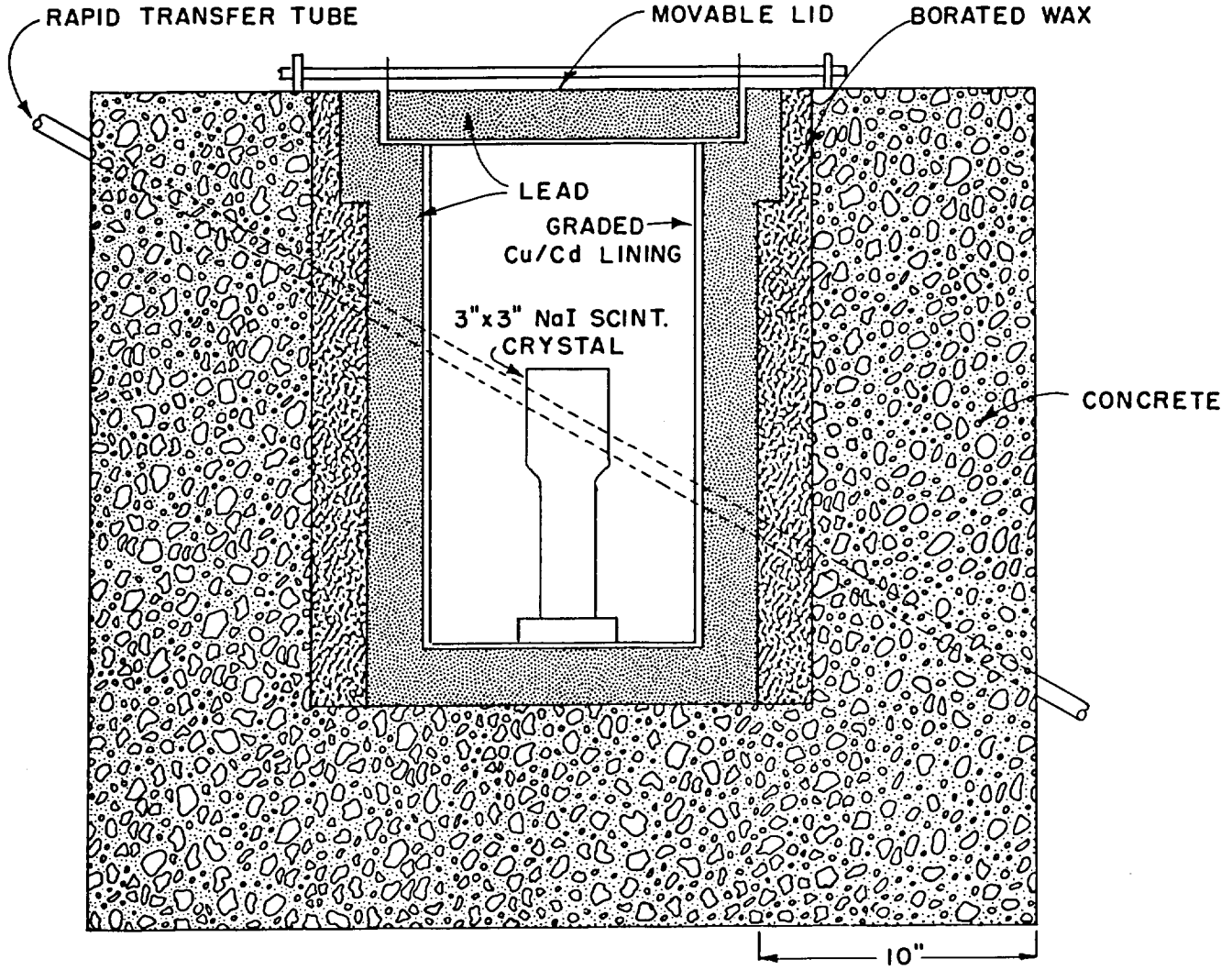

FIGURE 6. SHIELDED ENCLOSURE FOR SCINTILLATION COUNTER.

The foils for each measurement were mounted, parallel to the target, in regularly spaced slots cut in a 0.4 inch diameter Lucite rod. The rod was placed approximately in line with the centre of the target. The foils were then irradiated for a sufficient time to give an adequate count-rate for the foil farthest from the target.

Figure 7 shows the distribution of the fast neutron flux with thickness of the water moderator. The fast flux decreases rapidly with distance and it is therefore necessary to have accurate positioning of the sample, which also should be as close as possible to the target. The thermal neutron flux, on the other hand, goes through a broad maximum at about 4.5 cm of water (Figure 8), so that accurate positioning in this case is not as important. The cadmium ratio, that is, the ratio of the activity induced in a bare foil to the activity induced in a foil covered with a 0.04" thick layer of cadmium (which absorbs all neutrons of energy less than 0.4 eV), was about 7.5 at the position of maximum thermal flux.

The absolute flux available at the fast neutron irradiation position was measured by activating a thin copper foil. The foil was placed as an annular ring around the inner surface of a standard polythene irradiation vial (see page 20), so that the whole of the inner surface of the vial was covered. This arrangement allowed the average flux over the vial to be measured, rather than a maximum flux over a small area immediately opposite the target. After irradiation, the positron activity from the copper-62 was counted with a 3" x 3" NaI (Tl) scintillation detector. The detector was calibrated with a sodium-22 source, previously measured absolutely by 4 pi β - γ counting. The maximum, average fast neutron flux from a new target was about 6×10^8 n/cm^2-sec. The maximum, average thermal neutron flux at about 5 cm from the target is estimated to be about 1×10^8 n/cm^2-sec.

IRRADIATION FACILITIES

In performing activation analysis with a nuclear reactor it is customary for irradiation times to be of the order of a number of hours or days (17). Such relatively long irradiations are not possible with a neutron generator and a number of short irradiations are both more practical and economical. Since the growth law for the formation of induced activity, as a function of irradiation time (18), favours the more rapid build-up of induced activity for short-lived isotopes, rather than for long-lived isotopes, emphasis in neutron generator operation is placed on isotopes of short half-lives. Short irradiations are also adequate to produce sufficient induced activity for counting purposes when dealing with macro amounts (i.e. grams) of a given target element, although the half-life of the product isotope may be relatively

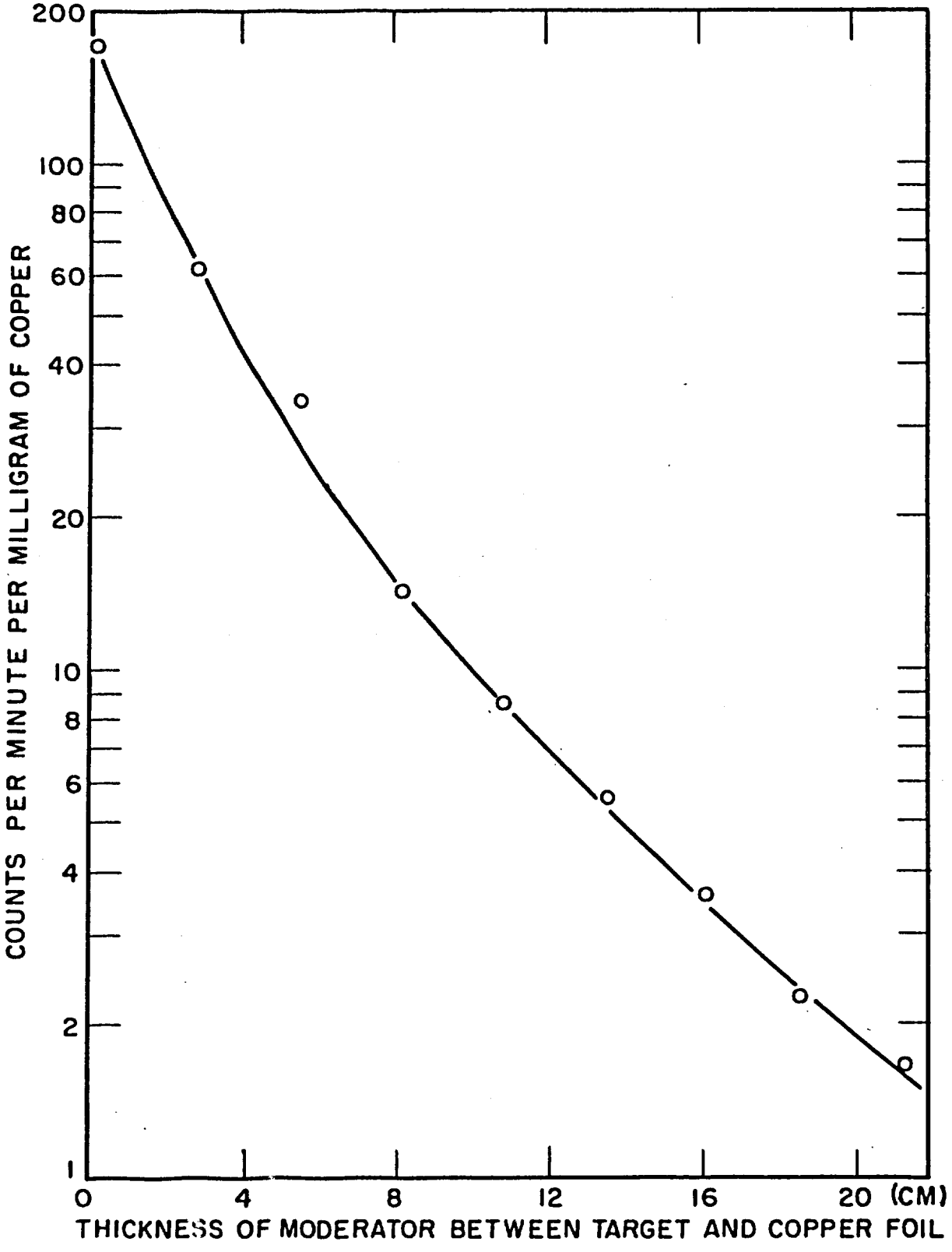

FIGURE 7. DISTRIBUTION OF FAST NEUTRON FLUX, WITH DISTANCE, IN WATER MODERATOR.

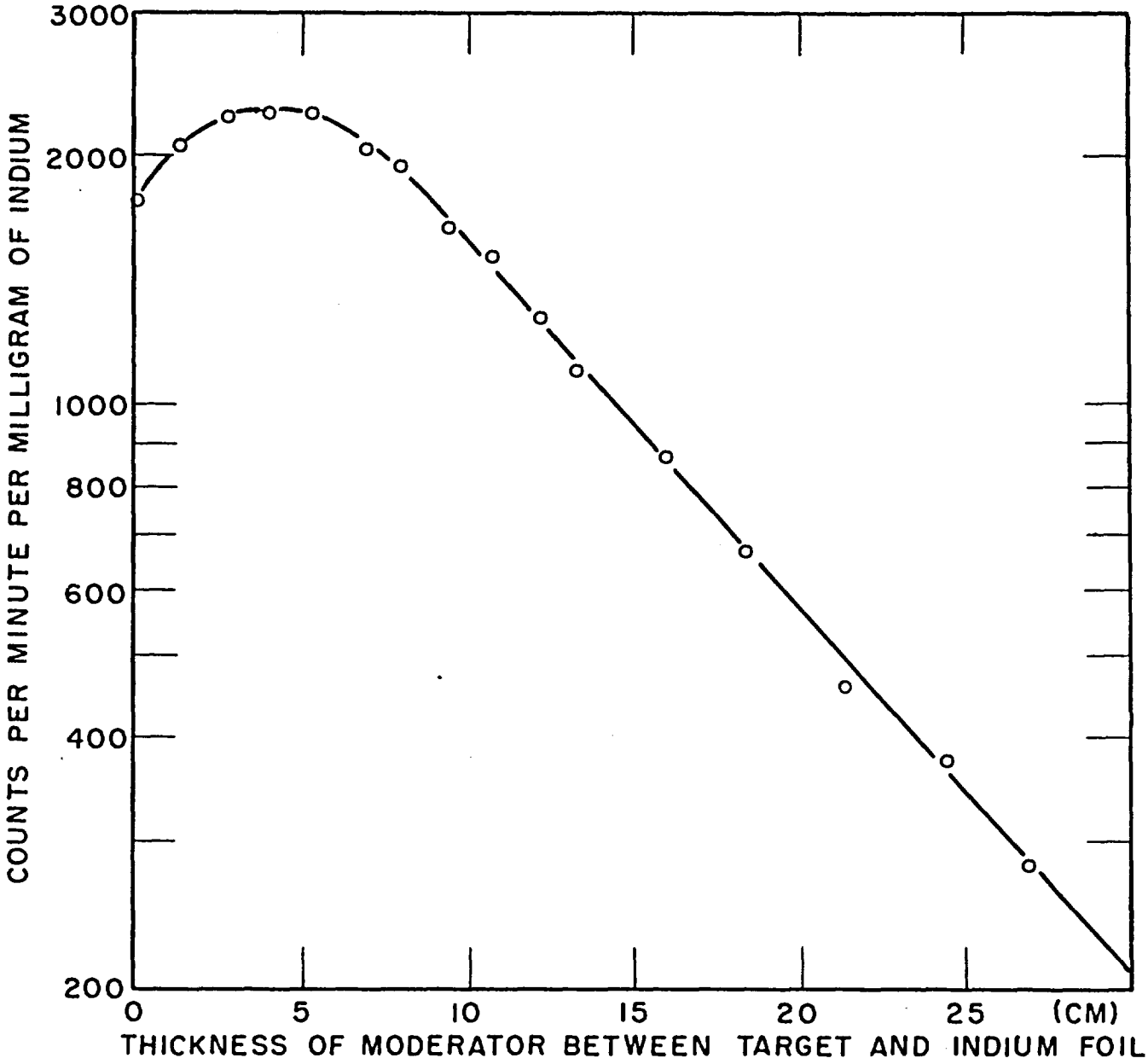

FIGURE 8. DISTRIBUTION OF THERMAL NEUTRON FLUX, WITH DISTANCE, IN WATER MODERATOR.

long.

In all cases involving a product isotope of short half-life, it is necessary to irradiate the sample after the neutron output of the generator has been adjusted to the required value. If the sample were placed in an irradiation position and then the neutron flux adjusted, the sample would receive a varying flux during the irradiation period. As a result of the varying flux, the build-up of activity during successive irradiations of other samples and standards would be an indeterminate function of irradiation time. It would not be possible, under these conditions, to normalise the induced activity to the neutron flux for the different irradiations. With product isotopes of short half-lives it is also mandatory that the sample should be counted as soon as possible after the irradiation has ended, in order to minimise decay time losses. For short irradiations, a pneumatic transfer system has been constructed that permits a sample to be transferred rapidly and reproducibly between the irradiation position and a counter.

Where the half-life of the product isotope is fairly long, counting with a minimum decay time following irradiation is not so significant. For this type of sample, a rotating rack irradiation facility has been used that allows the simultaneous irradiation of up to four samples. With both the pneumatic transfer system and the rotating rack facility, a cadmium sleeve can be placed around the sample to minimise thermal neutron effects during fast neutron irradiation. A description of both types of facility will now be given.

Pneumatic Transfer System

This system is shown in Figure 9. The transfer tube is made of 3/4" ID, Schedule 80 polyvinyl chloride tubing. This tubing is quite rigid but may be bent by wrapping a heating tape over about an eighteen-inch section and gently bending when the tubing becomes pliable (80-90°C). Dry air, at a pressure of 60 psi, is used to blow the sample into the irradiation position and, after irradiation, to return it for counting. The air pressure, for each transfer, is admitted to the system through a solenoid valve (Versa Products Company, Inc. Model VSG-4322). This type of valve is well suited for use with a transfer facility. When it is not energised there is a direct path from (a) to (e) (Figure 9). Thus the air being admitted to the transfer tubing through the other solenoid valve can escape through port (e). The same procedure operates with the valves in the opposite mode for the reverse transfer. A minimum pressure of 40 psi is required to operate the valves. The time during which each valve is open is controlled by a timer (Industrial Timer Corporation, Model PAB-6S) that may be set to 0.1 second. Transit times for the 35 feet of travel between the irradiation position and the counting position are somewhat dependent on sample weight and are normally in the range of 0.4 - 0.8 second. For very heavy samples, the air pressure may be increased to maintain transit times in this range.

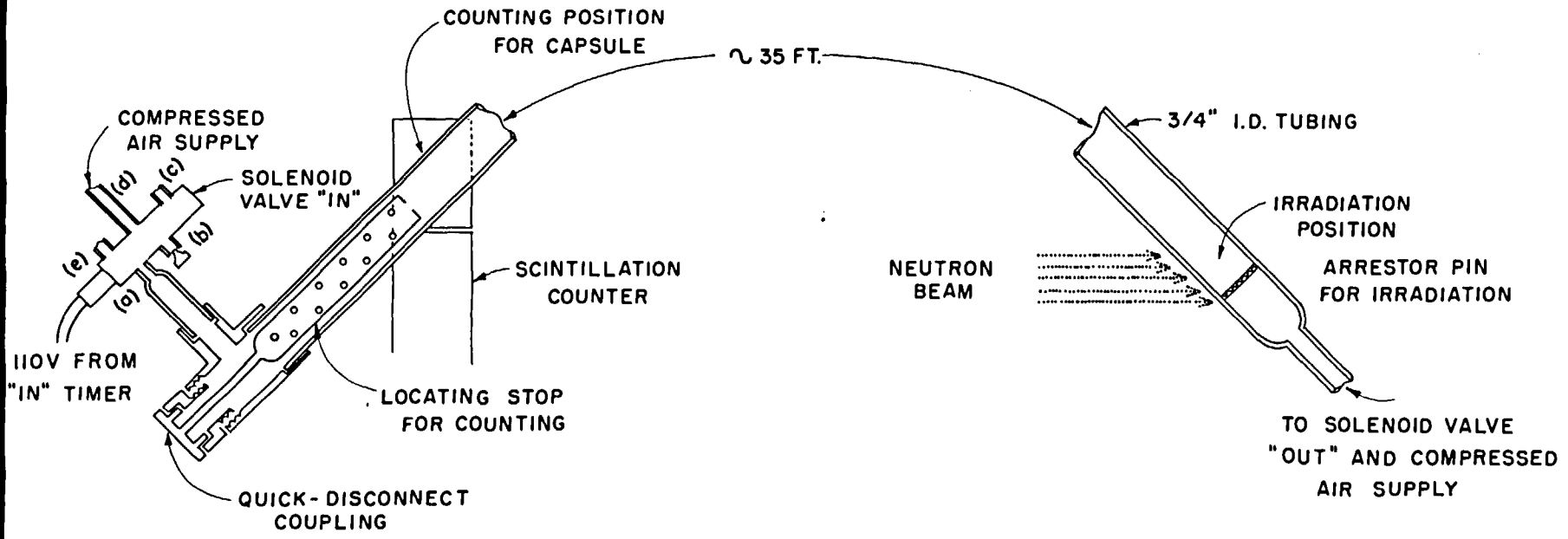

FIGURE 9. PNEUMATIC TRANSFER IRRADIATION AND COUNTING SYSTEM.

The sample containers used in the transfer system were polythene vials with a nominal capacity of 5 ml. These vials are cheap, reproducible in size, and contain negligible impurities. Vials of similar capacity were obtained from two suppliers: A.D. Wood, Ltd., London, England, and Olympic Plastic Co., Inc., Los Angeles, U.S.A. The vials from A.D. Wood, Ltd. were preferred because of their somewhat lower oxygen content. After filling with a sample, the lids of the vials are heat-sealed with a small soldering iron.

In order to ensure reproducible positioning of the sample vial in the neutron beam and beside the scintillation counter, the transfer tube in these positions is inclined at an angle of 35°. This removes the possibility of the sample bouncing back from these stop positions at the completion of either transfer. The transfer system has been used successfully for many hundreds of irradiations and has been found to be very reliable.

Activation analysis experiments requiring short irradiations in the pneumatic facility usually involve successive irradiations, for the same time, of a number of samples and standards. Although the time of these irradiations may be regulated by complete manual control of the IN and OUT solenoid valves, it is more accurate to have a control circuit that will provide a reproducible, pre-set irradiation cycle. Two separate control circuits were designed for this purpose. One circuit allows irradiation times of up to 55 minutes to be selected, while the other, which was built specifically for automatic control in the determination of oxygen (via 7.14 second nitrogen-16), has a fixed irradiation time of 40 seconds. This automatic control circuit also switches on the counting equipment at the end of the irradiation cycle to measure the induced activity in the sample. Apart from the determination of oxygen, this control circuit has been found useful for other short-lived isotopes with half-lives comparable to nitrogen-16, e.g. gold-197^m, phosphorus-34, and hafnium-178^m.

The pre-set time control circuit is shown in Figure 10. To operate this circuit, the required irradiation time is set on the X-Ray Timer, and switches (c), (d), and the neutron scaler switch are closed. The irradiation cycle is then started by momentary closure of the spring-loaded switch (a). This DPDT switch performs two functions:

(1) It closes the latching relay L.R. 2 (Potter and Brumfield, PC Series, Type 11A). This relay opens the stop-start circuit in the neutron scaler, to monitor the relative neutron flux received by the sample during irradiation.

(2) It also closes an electrically-actuated clutch in the IN timer that causes 110V to be applied to the IN solenoid valve (for the time set on the IN timer - normally about 0.5 second) to send the capsule into the irradiation position beside the neutron generator.

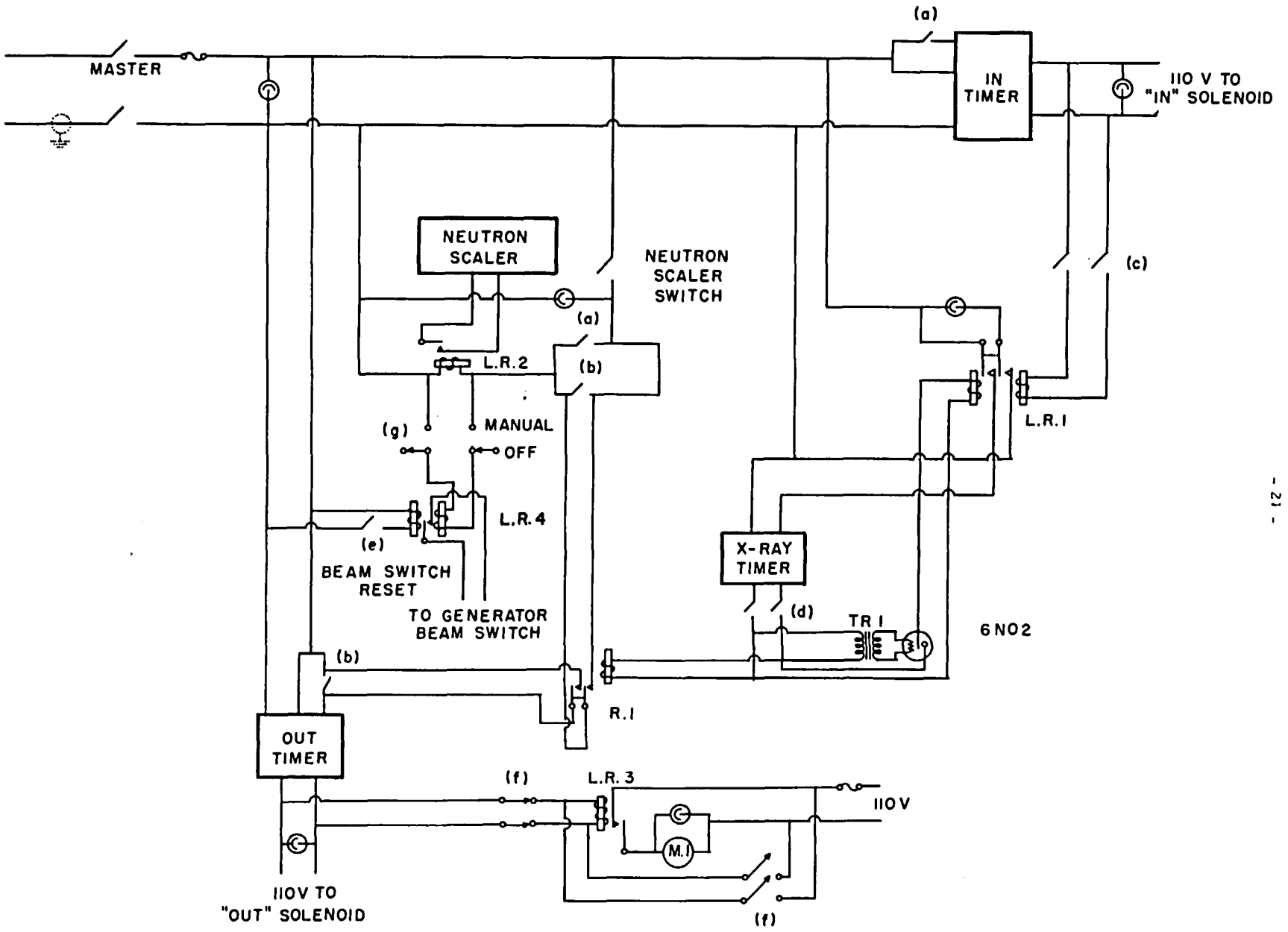

FIGURE 10. CIRCUIT DIAGRAM FOR PRE-SET TIME CONTROL CIRCUIT.

The 110V supply from the IN timer also switches the double-coil latching relay L.R.1 (Potter and Brumfield, KB Series, Type 17AG) that applies 110V to start the X-Ray Timer. A pilot light is used on a normally closed set of contacts in this relay to indicate that the relay is in the correct latching position for the irradiation cycle. During the irradiation period, this "ready light" goes off. When the irradiation time (as set on the X-Ray Timer) has elapsed, the X-Ray Timer switches off. A cam-actuated Micro Switch, mounted in the Timer, then closes and gives 110V at the output of the Timer. This 110V is used to:

(1) Close relay R.1. When R.1 closes, switch (b) is shorted and the OUT timer energised to send the capsule from the irradiation position; also, the relay L.R.2 is simultaneously energised to stop the neutron scaler. If switch (g) is in the manual position, the generator beam switch will be tripped at this time, which will stop the neutron-induced background on the scintillation counter.

(2) Apply 12.6V, through the filament transformer TR1, to the heater of the 6NO2 tube. This thermal delay tube is designed to operate at a heater voltage of 6V and nominally to remain open for two seconds. However, it was found that with a 12.6V heater supply, the tube would close in about 0.4 second.

When the thermal delay switch in the 6NO2 tube closes, 110V is placed on the other coil of relay L.R.1, which then switches to its initial position and disconnects the 110V supply voltage, through the X-Ray Timer, to TR1 and relay R.1. The control circuit has now returned to its original position and may be used for another irradiation.

In certain instances, when measuring the rate of decay of a particular sample, it is necessary to know accurately the time from the end of irradiation. For this purpose an elapsed time meter (M.1) is started, through the latching relay L.R.3, at the same time that the OUT solenoid is energised to send the capsule from the irradiation position. This relay may be re-set with switch (f).

If complete manual control of the irradiation cycle is desired, the pre-set time control functions may be by-passed by leaving switches (c) and (d) open. The capsule is then returned after the irradiation by manually closing switch (b). Manual operation is very convenient as a pre-irradiation check on the transit times of capsules of different weights.

The neutron generator is frequently used for the determination of oxygen. A control circuit that permits the irradiation, monitoring, and counting sequences to be performed automatically is shown in Figure 11. The operation of the circuit is controlled by an Industrial Timer Corporation multi-cam timer (Model RC3 with an A-18 gear train). This unit consists of

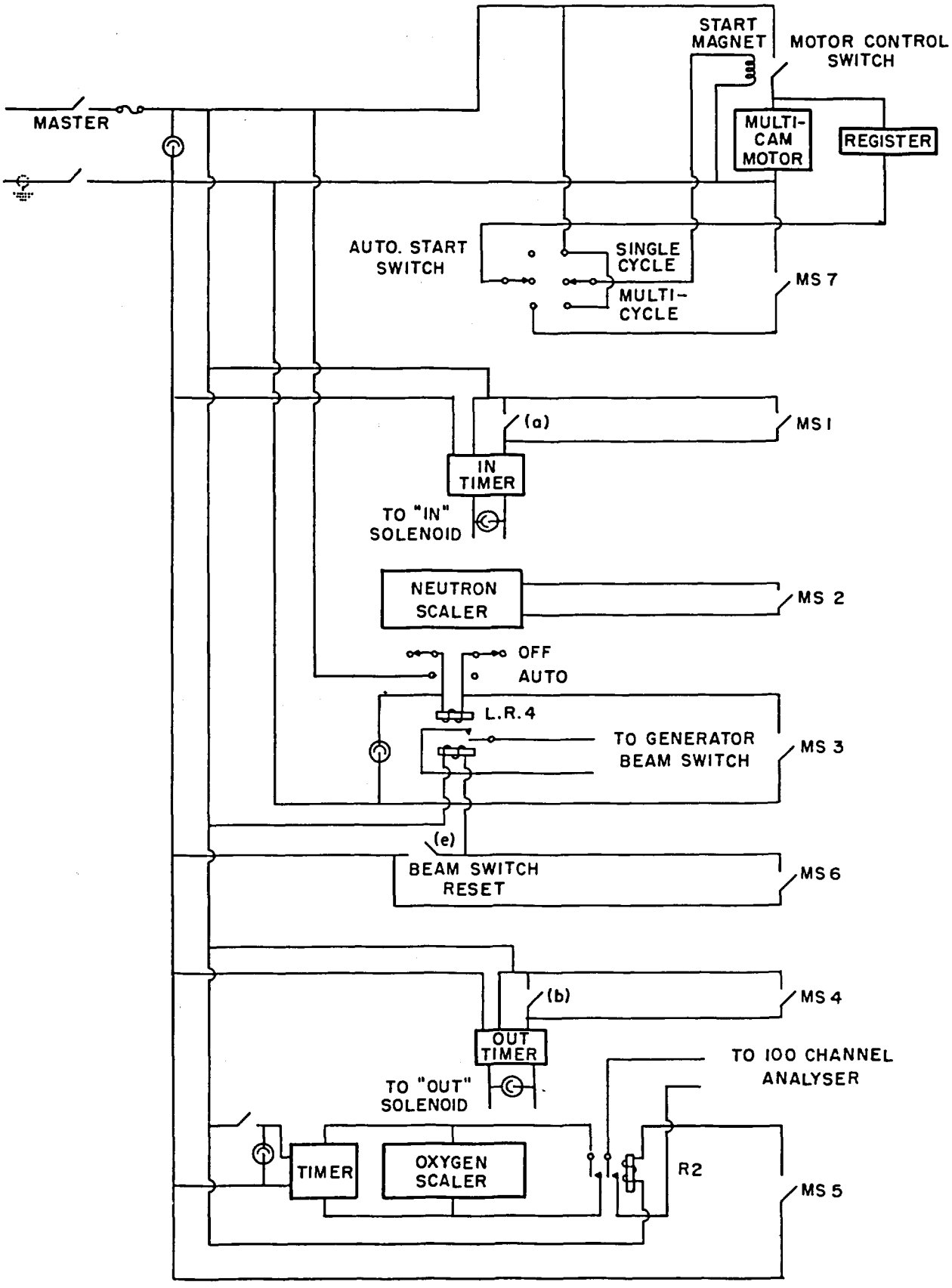

FIGURE II. CIRCUIT DIAGRAM FOR AUTOMATIC CONTROL CIRCUIT.

a 2 rpm synchronous motor and gear-train assembly, that drives a shaft through one revolution in ninety seconds. Seven adjustable cams are mounted on the shaft, each of which opens or closes a Micro Switch (MS1 to MS7) for any selected portion of the operating cycle between about one second and eighty-nine seconds. The motor is started by a momentary pulse of current, which energises a starting magnet, and stops after one revolution. For continuous re-cycling, the starting magnet is maintained energised for as many cycles as required.

After starting the multi-cam timer motor, through momentary closure of the auto-start switch, the following sequence of operations is performed, each operation being controlled by a cam/Micro Switch combination. The particular Micro Switch used is shown in brackets.

(1) Start the IN timer, to energise the IN solenoid valve, to send the capsule into the irradiation position (MS 1).

(2) Start the neutron scaler, to monitor the neutron flux, when the capsule arrives in the irradiation position (MS 2).

(3) At the end of the irradiation period, start the OUT timer, to energise the OUT solenoid valve, to send the capsule to the counting position (MS 4).

(4) At the end of the irradiation period, stop the neutron scaler (MS 2).

(5) When the capsule is beside the scintillation counter, start the counting equipment (MS 5).

(6) Switch off the counting equipment after the counting period (MS 5).

(7) When the auto-start switch is in the multi-cycle mode, record the number of cycles run on a mechanical register (MS 7).

(8) When it is necessary to switch off the generator during the counting period, energise the double-coil latching relay L.R.4, to switch off the generator beam switch (MS 3). (This occurs when the beam switch is set in auto position.)

(9) Reset the beam switch at the end of the counting period, by energising the other coil of L.R.4, so that the generator is ready for a further run (MS 6).

The cams on the multi-cam timer were adjusted to the time schedule shown in Table 3.

TABLE 3

Cam/Micro Switch Time Settings for Auto Control Circuit

Operation Number	Function	Cam/Micro Switch Combination	Time from Start (seconds)
1	Start IN timer	MS 1	2
2	Start neutron scaler	MS 2	3
3	Start OUT timer	MS 4	43
4	Stop neutron scaler	MS 2	43
5	Start scintillation counter	MS 5	44.5
6	Stop scintillation counter	MS 5	84.5
7	Activate mechanical register	MS 7	86.5
8	Beam switch off	MS 3	44
9	Beam switch reset	MS 6	86

A delay period was allowed between operations 3 and 5 that is longer than the normal transit time of the capsule from the irradiation position to the counting position. This was done so that any capsule that arrived in the counting position more slowly than usual was still counted correctly. The reproducibility of the control system was checked by the use of two 60c/s sources to simulate the output of the neutron monitor and of the scintillation counter. The reproducibility was found to be better than 0.1%. By placing the auto-start switch in the multi-cycle position, the system will re-cycle for as many times as desired. The re-cycling is useful in building up a statistically significant count in samples of low oxygen content.

In practice, both the pre-set time control circuit and the automatic control circuit were incorporated into a single control circuit shown in Figure 12.

Rotating Rack Assembly

When fairly long irradiations are required, it is uneconomical in terms of target life to use the pneumatic facility that can accommodate only one sample at a time. For this type of irradiation, a vertically-mounted rotating rack assembly was used that allows up to four samples to be irradiated simultaneously. The rack is positioned in the water tank, close to the target, and is rotated by a 12 rpm motor. Nitrogen activation tests, conducted with ammonium nitrate samples, showed that good flux uniformity (about $\pm$ 4%) was achieved for all four samples. A disadvantage with the rack is that the average distance of a sample from the target is greater than with only one sample in the pneumatic facility and a decrease in sensitivity results.

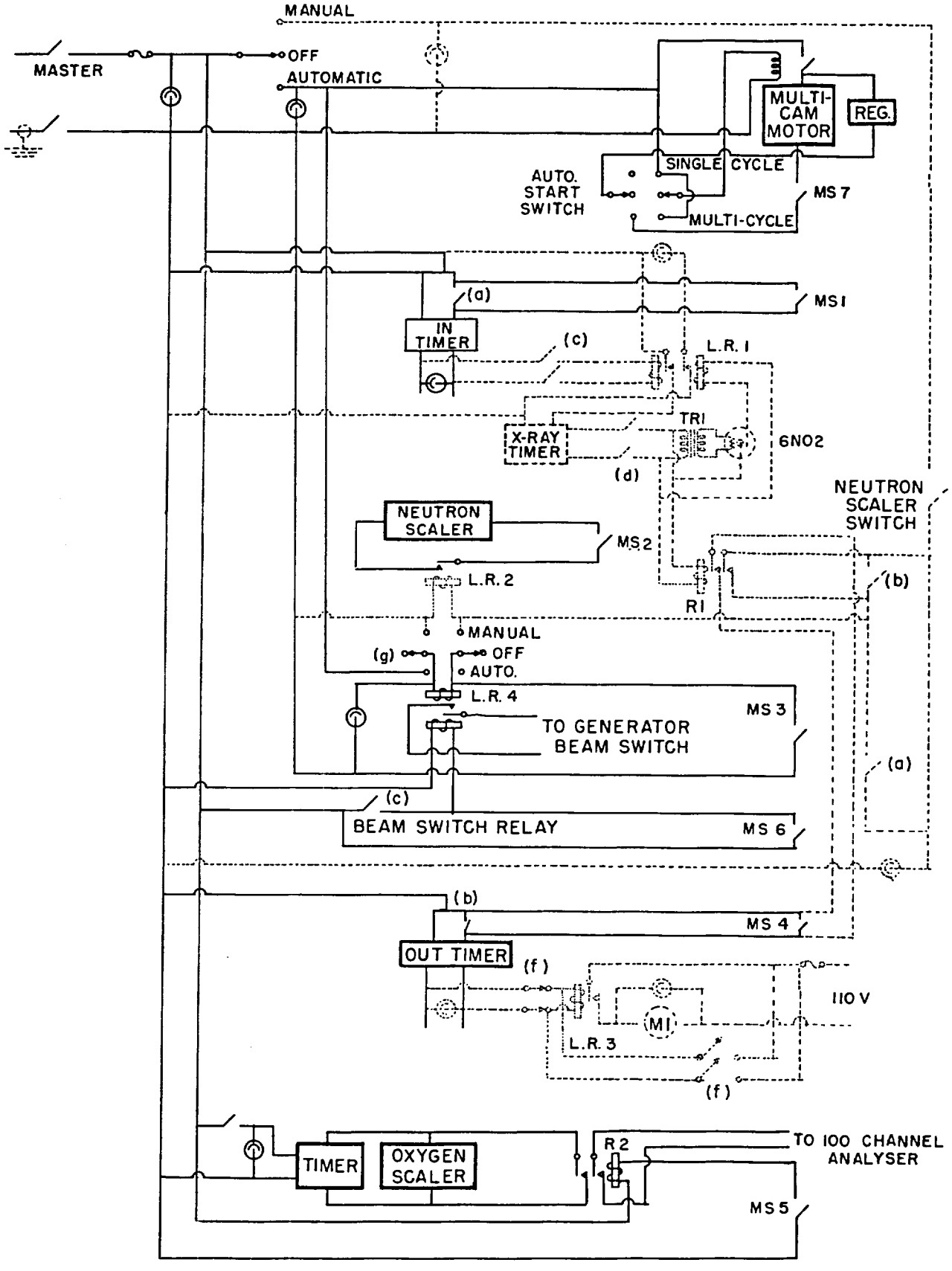

---- PRE-SET TIME CIRCUIT

FIGURE 12. CIRCUIT DIAGRAM FOR AUTOMATIC AND PRE-SET TIME CONTROL CIRCUITS.

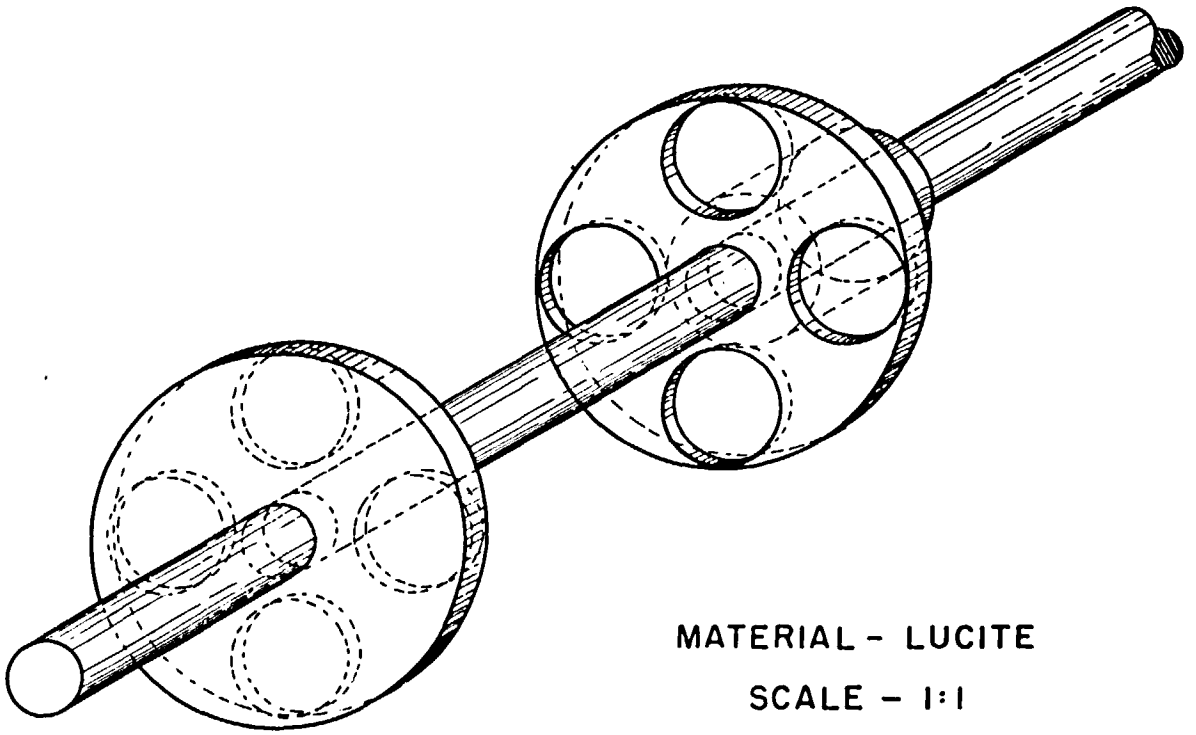

FIGURE 13. ROTATING RACK IRRADIATION FACILITY.

FLUX MONITORING

A comparison of the activity induced in a sample with the same activity induced in a standard during separate irradiations, requires an accurate knowledge of the relative neutron flux received by the sample and the standard. A number of methods may be used to monitor the neutron output of a generator during irradiation, including associated alpha particle measurement (19) and the measurement of the output of various types of counters placed close to the generator (20, 21). The method adopted in this work was to measure the output of a large boron trifluoride counter (Chalk River Type BP 11B) mounted in the shielding wall around the generator. The output of this counter is fed to a scaler and, also, through a counting-rate meter to a chart recorder situated by the operating console (Figure 14). The trace on the chart recorder serves to guide the operator as to the approximate neutron output of the generator, and the scaler gives an accurate integral measurement of the neutron flux during an irradiation. The performance of the boron trifluoride counter and associated counting equipment was checked periodically with a one milligram radium-beryllium neutron source (output 1.3×10^4n/sec) mounted in a position of reproducible geometry beside the counter.

There is a potential source of error in the use of the integral flux measurement technique for the normalisation of induced activity, that becomes significant when the irradiation time is greater than about 20% of the half-life of the product isotope. For the integral counting method to provide accurate normalisation, it is implicitly assumed that the neutron flux is constant during the irradiation period. However, slight variations in beam intensity, or some movement of the beam over areas of the target of different tritium concentrations, can cause the neutron output of the generator to vary by several per cent during an irradiation. In addition, for long irradiations there is a gradual decrease in neutron output, at a given beam current, through tritium depletion in the target. The rate of formation of induced activity (at a constant neutron flux) has an exponential time dependence given by $\left(1-e^{-\frac{0.693 \times T}{t_{1/2}}}\right)$, where T is the irradiation time and $t_{1/2}$ is the half-life of the product isotope. The integral counting method, on the other hand, has a linear time dependence and it is only for $T/t_{1/2} \leq 0.2$ that the growth of activity is approximately linear with time. Thus, any variations in the neutron output during an irradiation will influence the integral neutron measurement and the actual amount of induced activity to different extents. For accurate relative flux measurements, particularly when the irradiation

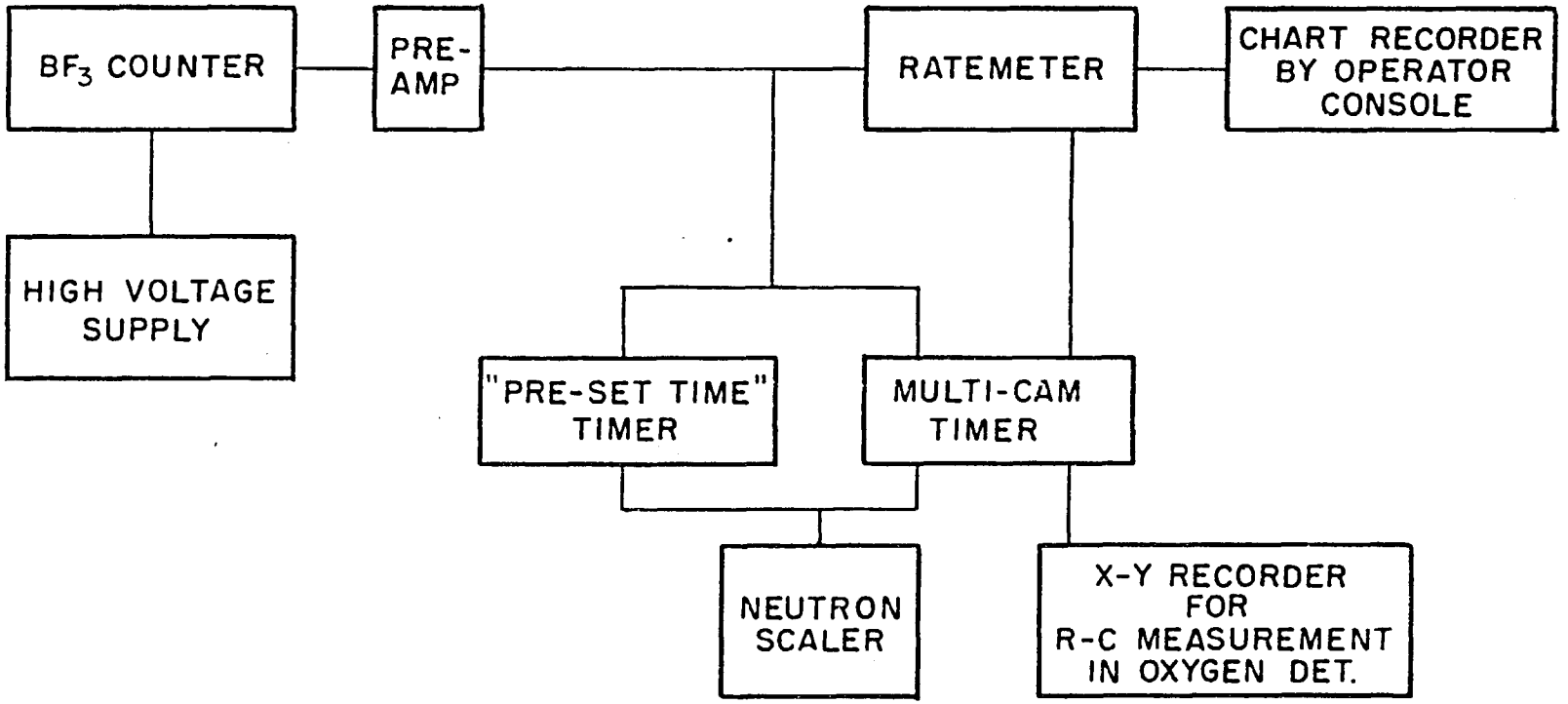

FIGURE 14. BLOCK DIAGRAM OF NEUTRON MONITORING SYSTEM.

time is greater than the half-life of the product isotope, it is necessary to have a flux monitoring system that follows the same growth law and decay law as the isotope being produced. The potential across a capacitor shunted by a resistance, when connected to a charging circuit, follows such a growth law; the time constant of the resistance-capacitor (R-C) network being equivalent to the mean life of the isotope. One of the time constant positions in the counting-rate meter circuit was modified to give a time constant of 10.3 seconds for use in the determination of oxygen, in which the irradiation time was about five half-lives(5). Although under normal irradiation conditions both the R-C method and the integral method of monitoring agreed in the determination of oxygen, under circumstances where the neutron output varied extensively the R-C method gave much more consistent results.

NUCLEAR DATA AND CALCULATED ANALYTICAL SENSITIVITIES

A neutron generator offers a choice for neutron activation analysis between 14 MeV neutron activation or activation with thermal neutrons. The thermal neutron flux is, of course, less than the initial unmoderated fast flux because of the thickness of moderator between the tritium target and the thermal neutron irradiation position. However, as the cross sections for activation usually increase with decrease in neutron energy, it is possible that a thermal neutron reaction may be more sensitive for analytical purposes than a fast neutron reaction, despite the lower thermal neutron flux. In order to assess the sensitivities that may be expected in activation analysis and the importance of interfering reactions from other components in a mixture, it is necessary to have fairly complete information on the nuclear parameters involved in the activation process for all target isotopes and also on the modes of decay of the radioactive isotopes produced on activation. In general there are five types of reactions that may be expected on fast neutron activation; viz., (n, 2n), (n, p), (n, α), (n, γ) and (n, n'). With thermal neutron activation the (n, γ) reaction is usually the only reaction encountered. The (n, p) and (n, α) reactions resulting from fast neutron activation often experience serious interference in the determination of an element Z in a Z-1 or Z-2 matrix from (n, 2n) or (n, γ) reactions with the matrix.

The amount of activity, $\frac{dN}{dt}$, produced on neutron irradiation of any nuclide is given by the equation

$$\frac{dN}{dt}(d/sec) = \frac{w\,A\,\sigma\,F\,f}{W}\left(1-e^{-\frac{0.693 \times T}{t_{1/2}}}\right) \qquad \text{(Eq 1)}$$

where w = weight of target element,

W = atomic weight of target element,

A = Avogadro's Number,

σ = cross section for activation in cm^2 (1 barn = 10^{-24} cm^2),

F = neutron flux in n/cm^2-sec,

f = fractional abundance of target isotope,

T = irradiation time,

$t_{1/2}$ = half-life of product nuclide.

The term in brackets in this equation is called the "build-up" factor. The "build-up" factor relates the ratio of the irradiation time to the half-life of the product nuclide to the amount of induced activity formed, and is shown graphically in Figure 15 as a function of $T/t_{1/2}$. It will be seen that, for irradiation times greater than five half-lives, only a very small increase occurs in the build-up factor and hence in the amount of induced activity formed. Thus, irradiation times greater than this value are not required, since they would lead to little further increase in sensitivity.

A knowledge of the various factors in equation (1) allows $\frac{dN}{dt}$ to be calculated for a weight w of a given element. Alternatively, if a value of $\frac{dN}{dt}$ is assumed, then the weight w of the element required to give this disintegration rate may be calculated. If a certain value of $\frac{dN}{dt}$ is established as the minimum disintegration rate that can be reliably measured, the weight w then represents the sensitivity of detection of the element for the given irradiation conditions. A number of such sensitivities have been calculated for the activation of most elements with thermal and with 14 MeV neutrons. For calculation purposes one gram of the target element has been considered and equation (1) becomes

$$R(d/sec/g) = \frac{A \sigma F f}{W} \left(1 - e^{-\frac{0.693 \times T}{t_{1/2}}}\right). \qquad \text{(Eq 2)}$$

Certain assumptions have been made to allow sensitivities to be calculated using equation (2). These assumptions are:

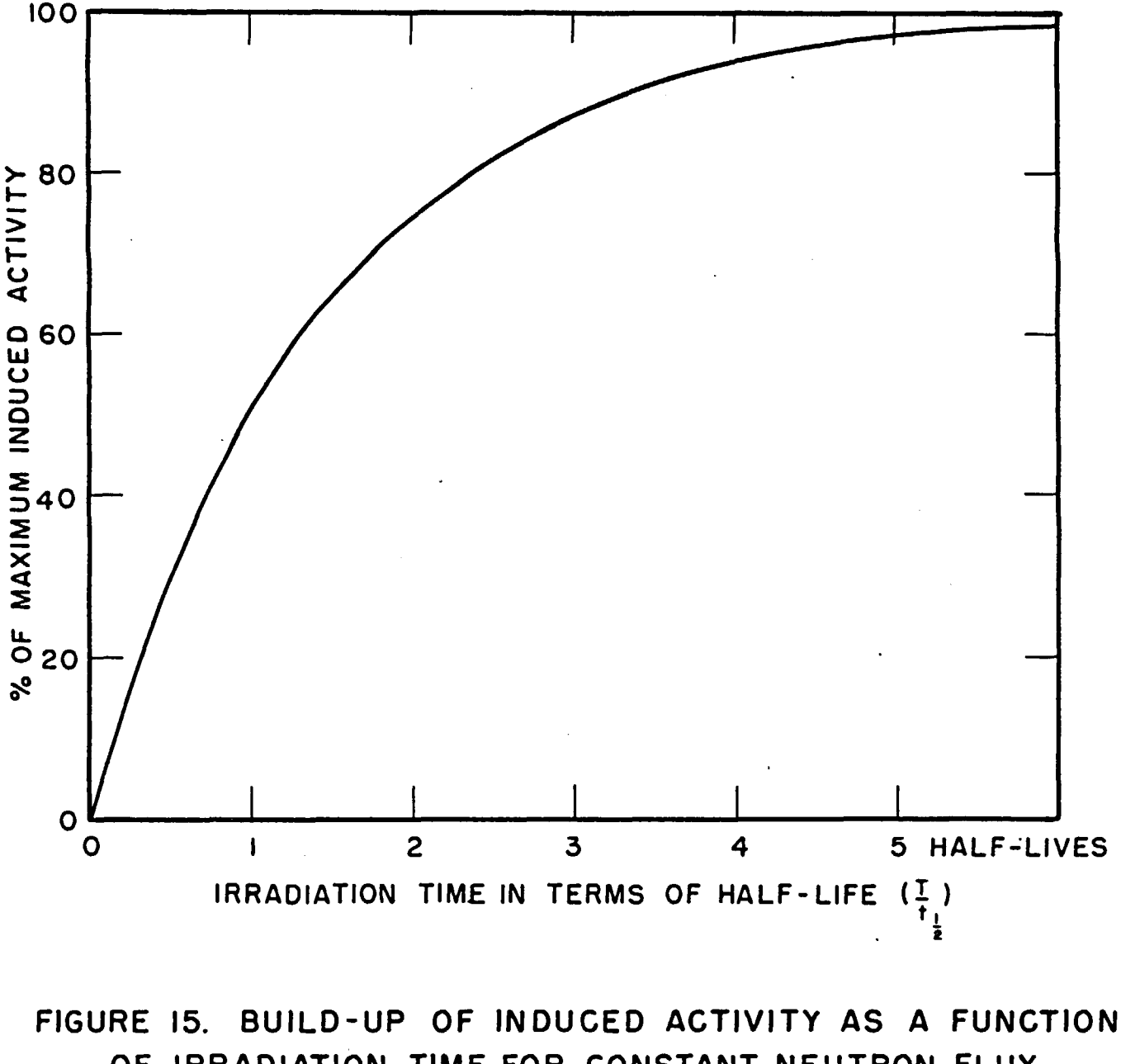

FIGURE 15. BUILD-UP OF INDUCED ACTIVITY AS A FUNCTION OF IRRADIATION TIME FOR CONSTANT NEUTRON FLUX.

(1) For a reasonable sample volume, the maximum average fast neutron flux is 5×10^8 n/cm^2 -sec and the maximum well-thermalised neutron flux is 1×10^8 n/cm^2 -sec. As the calculated sensitivity is a linear function of the neutron flux, fluxes greater or less than these values will result in a corresponding increase or decrease in the sensitivity. With improvements in generator design, higher neutron outputs may be anticipated. However, it should be borne in mind that prolonged operation at high beam currents leads to a decrease in neutron output because of target deterioration.

(2) The maximum irradiation time will be forty minutes or five half-lives, whichever is shorter. In general, this limitation on irradiation time precludes the formation of significant amounts of isotopes that have half-lives greater than a few days.

(3) Only isotopes that decay by gamma emission or by positron emission are considered (in positron emission 0.51 MeV gamma radiation is emitted). Gamma emitters are chosen because they may be identified and quantitatively measured by gamma-ray spectrometry.

(4) Sensitivity is arbitrarily defined as the weight of an element (in μ g) that will yield 1000 disintegrations in a counting period of ten minutes or five half-lives, whichever is shorter, following the irradiation. For those isotopes that decay significantly during the counting period, a correction has been applied to allow for this counting loss. Certain published sensitivity tables (17, 22) are based on the formation of a given amount of activity at the end of the irradiation period (e.g. 100 dpm) without consideration for isotopic decay during the measurement period. This approach is unrealistic because, for short-lived isotopes, decay during the measurement period is very significant. The sensitivity in μ g represents the ppm concentration of a given element that, in principle, could be determined in a one gram sample. For a sample weighing ten grams the sensitivity (in ppm) would be improved ten-fold.

(5) Where the decay scheme of the isotope is known, the sensitivity has been normalised to 100% emission of the most abundant gamma radiation. Thus, if the most abundant gamma-ray in the decay scheme of the particular isotope occurs in only 33% of the disintegrations, the sensitivity (for gamma-ray counting) has been decreased by a factor of three. No correction has been made for the decrease in sensitivity of a NaI (Tl) crystal with increase in gamma-ray energy (23), or for the presence of a beta absorber that is usually used in gamma-ray counting (24).

Matrix effects are not considered in these calculations but may be very important in (a) neutron self-shielding during irradiation for a nuclide of high neutron cross section, or for a nuclide in a matrix of high neutron cross section, (b) during scintillation counting by the self-absorption of gamma radiation within a sample. This effect is particularly marked at low gamma energies.

The calculated sensitivities, together with the relevant nuclear data, are given in Table 4. It should be emphasised that these sensitivities are calculated and are best considered as a guide to the order of magnitude of the sensitivity to be expected for a given element, and as to which nuclear reaction is probably the most suitable to employ for analytical purposes. In a sense these sensitivities are based on a thermodynamically ideal system in which the element to be detected at a low concentration is considered as separate from a matrix. Thus, although 1000 disintegrations from a gamma-emitting isotope may be readily determined with a NaI (Tl) detecting system, 1000 disintegrations would not be discernible against a high background from an active matrix. This detection difficulty applies particularly to the determination of short-lived isotopes, where chemical separation is not possible. A number of reactions listed in Table 4 are obviously not suitable for high-sensitivity analytical determinations. However, these reactions can be significant where the element is present as the matrix and may give rise to interfering reactions or emit gamma radiation of energy similar to the element being determined.

The information listed in Table 4 is largely self-explanatory. Most of the data relating to thermal neutron cross sections and isotope decay characteristics are reasonably accurate. The data on the fast neutron cross sections of the higher Z elements are not as reliable, measurements of the same fast neutron cross section by different authors being in variance by much more than the quoted experimental errors in the method (25). In addition, there are a number of fast neutron reactions, also with the higher Z elements, for which cross section data are not available, but which are more useful for analytical purposes than certain of the reactions listed.

The product isotopes in the table are listed in order of increasing half-lives, with the products (if any) of fast neutron reactions given first. R(d/sec/g) is included to allow sensitivity conditions other than 1000 disintegrations to be used if desired.

In those cases where the percentage of gamma-ray or positron emission in the decay scheme of the product isotope is not established, it has been assumed, for calculation purposes, that 100% emission does occur. Where only the relative gamma-ray emission is known, this is indicated by an 'x' after the gamma-ray energy. A dash between two gamma-ray energies indicates that a number of gamma-rays of low intensity are present.

The cross section data for this tabulation were taken mainly from the Brookhaven National Laboratory compilations (26), and also from summaries by Gardner (25) and Chatterjee (27), modified, where necessary, by more recent literature data. The decay scheme information was taken from the Nuclear Data Sheets (28), Okada (29), and recent literature references.

TABLE 4

Neutron Activation Data

Z	Target Isotope	% Abundance	F or T	σ(barns)	Reaction	Half-life	Gamma Energy (MeV)	R(d/sec/g)	Sensitivity (μg)
5	B 11	80.2	F	0.0033	B11(n,p) Be11	13.6 sec	2.12(32%), 6.8(4%), 4.6-8.0	7.1×10^4	2.2×10^3
7	N 14	99.63	F	0.0082	N14(n, 2n)N13	10.0 min	β^+	1.64×10^5	14
8	O 16	99.759	F	0.033	O16(n, p)N16	7.14 sec	6.13(73%), 7.12(5%)	6×10^5	2.2×10^2
	F 19	100	F	0.023	F19(n,α)N16	7.14 sec	6.13(73%), 7.12(5%)	3.52×10^5	3.8×10^2
9	F 19	100	F	0.0145	F19(n, p)O19	29.1 sec	0.2(96%), 1.36(54%)	2.2×10^5	1.1×10^2
	F 19	100	F	0.064	F19(n, 2n)F18	109.7 min	β^+(100%)	2.25×10^5	8
10	Ne 22	8.82	T	0.036	Ne22(n, γ)Ne23	38 sec	0.44(33%), 1.65(1%)	9.15×10^3	6×10^3
	Na 23	100	F	0.170	Na23(n,α)F20	11.56 sec	1.63(100%)	2.15×10^6	28
11	Na 23	100	F	0.037	Na23(n, p)Ne23	38 sec	0.44(33%), 1.65(1%)	4.66×10^5	1.2×10^2
	Na 23	100	T	0.525	Na23(n, γ)Na24	15.05 hr	1.37(100%), 2.75(100%)	4.12×10^4	40
	Mg 26	11.17	F	0.035	Mg26(n,α)Ne23	38 sec	0.44(33%), 1.65(1%)	4.66×10^4	1.2×10^3
12	Mg 25	10.13	F	0.063	Mg25(n, p)Na25	60 sec	0.40(15%), 0.58(15%), 0.98(15%)	7.65×10^4	1×10^3
	Mg 24	78.7	F	0.174	Mg24(n, p)Na24	15.05 hr	1.37(100%), 2.75(100%)	5.2×10^4	32
	Mg 26	11.17	T	0.027	Mg26(n, γ)Mg27	9.5 min	0.84(68%), 1.01(29%)	7×10^3	4.8×10^2
	Al 27	100	F	0.00056	Al 27(n, γ)Al 28	2.238 min	1.78(100%)	6×10^3	8.9×10^2
13	Al 27	100	F	0.066	Al 27(n, p)Mg27	9.5 min	0.84(68%), 1.01(29%)	7×10^5	5
	Al 27	100	F	0.112	Al 27(n,α)Na24	15.05 hr	1.37(100%), 2.75(100%)	3.73×10^4	45
	Al 27	100	T	0.21	Al 27(n, γ)Al 28	2.238 min	1.78(100%)	4.52×10^5	12
	Si 28	92.21	F	0.24	Si28(n, p)Al28	2.238 min	1.78(100%)	2.29×10^6	2.4
14	Si 29	4.70	F	0.1	Si29(n, p)Al29	6.6 min	1.28(85%), 2.43(15%)	4.86×10^4	65
	Si 30	3.09	F	0.123	Si30(n,α)Mg27	9.5 min	0.84(68%), 1.01(29%)	3.87×10^4	88
15	P 31	100	F	0.117	P31(n,α)Al28	2.238 min	1.78(100%)	1.1×10^6	5
	P 31	100	F	0.020	P31(n, 2n)P30	2.53 min	β^+(100%)	1.91×10^5	26
16	S 34	4.22	F	0.085	S34(n, p)P34	12.4 sec	2.1(25%)	3.25×10^4	6.9×10^3
	Cl 37	24.47	F	0.044	Cl 37(n,α)P34	12.4 sec	2.1(25%)	8.8×10^4	2.5×10^3
17	Cl 37	24.47	F	0.025	Cl 37(n, p)S37	5.0 min	3.13(10%)	5×10^4	6.1×10^2
	Cl 35	75.53	F	0.006	Cl 35(n, 2n)Cl 34^m	32.4 min	1.16(18%), 2.13(43%), 3.30(7%), β^+(100%)	2.2×10^4	83
	Cl 37	24.47	T	0.43	Cl 37(n, γ)Cl 38	37.3 min	1.64(31%), 2.16(47%)	9.3×10^4	41
18	A 40	99.6	T	0.61	A40(n,α)S37	5.0 min	3.13(10%)	7.68×10^5	40
	A 40	99.6	T	0.53	A40(n, γ)A41	110 min	1.27(99%)	1.77×10^5	10

(Continued)

TABLE 4 (Continued)

Z	Target Isotope	% Abundance	F or T	σ (barns)	Reaction	Half-life	Gamma Energy (MeV)	R(d/sec/g)	Sensitivity (μg)
19	K 39	93.08	F	0.006	K39(n, 2n)K38	7.7 min	2.16(100%), β^+(100%)	4.15×10^4	61
	K 41	6.88	F	0.030	K41(n, α)Cl 38	37.3 min	1.64(31%), 2.16(47%)	8.25×10^3	4.7×10^2
	K 41	6.88	F	0.069	K41(n, p)A41	110 min	1.27(99%)	8.1×10^3	2.1×10^2
	K 41	6.88	T	1.3	K41(n, γ)K42	12.5 hr	1.52(18%), 0.3, 1.9	5.1×10^3	1.8×10^3
20	Ca 44	2.06	F	0.025	Ca44(n, p)K44	22 min	1.13(100)[x], 2.07(60)[x], 2.55(12)[x], 3.66(6)[x]	2.77×10^3	7×10^2
	Ca 44	2.06	F	0.035	Ca44(n, α)A41	110 min	1.27(99%)	1.2×10^3	1.4×10^3
	Ca 48	0.185	T	1.1	Ca48(n, γ)Ca49	8.8 min	3.09(89%), 4.05(8%), 4.7 (3%)	2.92×10^3	9.2×10^2
21	Sc 45	100	F	0.13	Sc45(n, 2n)Sc44	3.92 hr	1.16(99%), β^+(95%)	9.55×10^4	17
	Sc 45	100	F	0.132	Sc45(n, α)K42	12.5 hr	1.52(18%), 0.3, 1.9	3.17×10^4	2.9×10^2
	Sc 45	100	T	10.4	Sc45(n, γ)Sc46[m]	20 sec	0.14	1.34×10^3	2.6
22	Ti 50	5.34	F	0.009	Ti50(n, p)Sc50	1.8 min	0.51(100%), 1.11(100%), 1.56(100%)	2.9×10^3	2.2×10^3
	Ti 50	5.34	F	0.0035	Ti50(n, γ)Ti51	5.8 min	0.32(95%), 0.62(1%), 0.94(5%)	1.14×10^3	2.7×10^3
	Ti 46	7.93	F	0.0133	Ti46(n, 2n)Ti45	3.08 hr	β^+(85%)	9.25×10^3	1.8×10^3
	Ti 48	73.94	F	0.055	Ti48(n, p)Sc48	43.2 hr	0.98(100%), 1.04(100%), 1.31(100%)	2.75×10^3	6×10^2
	Ti 50	5.34	T	0.14	Ti50(n, γ)Ti51	5.8 min	0.32(95%), 0.62(1%), 0.94(5%)	9.07×10^3	3.3×10^2
23	V 51	99.76	F	0.055	V51(n, p)Ti51	5.8 min	0.32(95%), 0.62(1%), 0.94(5%)	3.14×10^5	6.7
	V 51	99.76	F	0.018	V51(n, α)Sc48	43.2 hr	0.98(100%), 1.04(100%), 1.31(100%)	1.15×10^3	1.5×10^3
	V 51	99.76	T	4.5	V51(n, γ)V52	3.76 min	1.43(100%)	5.1×10^6	0.72
24	Cr 53	9.55	F	0.037	Cr53(n, p)V53	2.0 min	1.0	1.97×10^4	3×10^2
	Cr 52	83.76	F	0.105	Cr52(n, p)V52	3.76 min	1.43(100%)	4.85×10^5	7.4
25	Mn 55	100	F	0.031	Mn55(n, α)V52	3.76 min	1.43(100%)	1.64×10^5	22
	Mn 55	100	T	13.3	Mn55(n, γ)Mn56	2.58 hr	0.845(99%), 1.81(24%), 2.12(15%)	2.4×10^6	0.7
26	Fe 54	5.82	F	0.01	Fe54(n, 2n)Fe53	9 min	0.38, β^+(98%)	2.98×10^3	8×10^2
	Fe 56	91.66	F	0.105	Fe56(n, p)Mn56	2.58 hr	0.845(99%), 1.81(24%), 2.12(15%)	8.5×10^4	21
27	Co 59	100	F	0.029	Co59(n, α)Mn56	2.58 hr	0.845(99%), 1.81(24%), 2.12(15%)	2.4×10^4	73
	Co 59	100	T	20	Co59(n, γ)Co60[m]	10.35 min	0.059(99.7%), 1.33(0.3%)	1.89×10^7	0.12
28	Ni 62	3.66	F	0.0053	Ni62(n, p)Co62	13.9 min	1.17(82%), 1.47(18%), 1.73(18%), 2.03(7%)	8.55×10^2	3×10^3
	Ni 61	1.19	F	0.022	Ni61(n, p)Co61	1.65 hr	0.072(100%)	3.24×10^2	5.4×10^3
	Ni 64	1.08	T	1.52	Ni64(n, γ)Ni65	2.61 hr	0.37(4.6%), 1.12(17%), 1.48(24%)	2.77×10^3	2.53×10^3
29	Cu 63	69.09	F	0.5	Cu63(n, 2n)Cu62	9.8 min	0.66(2%), 0.85-2.24, β^+(98.2%)	1.58×10^6	1.5
	Cu 63	69.09	F	0.023	Cu63(n, α)Co60[m]	10.35 min	0.059(99.7%), 1.33(0.3%)	6.98×10^4	33
	Cu 65	30.91	F	0.026	Cu65(n, p)Ni65	2.61 hr	0.37(4.6%), 1.12(17%), 1.48(24%)	6.2×10^3	1.1×10^3
	Cu 65	30.91	F	1.0	Cu65(n, 2n)Cu64	12.8 hr	1.34(0.6%), β^+(19%)	5.25×10^4	1.6×10^2
	Cu 63	69.09	T	4.51	Cu63(n, γ)Cu64	12.8 hr	1.34(0.6%), β^+(19%)	1.05×10^5	83

(Continued)

TABLE 4 (Continued)

Z	Target Isotope	% Abundance	F or T	σ (barns)	Reaction	Half-life	Gamma Energy (MeV)	R(d/sec/g)	Sensitivity (μg)
	Zn 68	18.57	F	0.025	Zn68(n, p)Cu68	30 sec	0.81(17%), 1.08(95%), 1.24(3%), 1.88(5%)	2.06×10^4	1.2×10^3
	Zn 66	27.81	F	0.077	Zn66(n, p)Cu66	5.1 min	1.04(9%)	9.45×10^4	3.6×10^2
30	Zn 64	48.89	F	0.105	Zn64(n, 2n)Zn63	38.1 min	0.67(13%), 0.96(9%), 1.4(0.7%), β^+(90%)	1.18×10^5	16
	Zn 68	18.57	F	0.051	Zn68(n, α)Ni65	2.61 hr	0.37(4.6%), 1.12(17%), 1.48(24%)	7×10^3	1×10^3
	Zn 64	48.89	F	0.23	Zn64(n, p)Cu64	12.8 hr	1.34(0.6%), β^+(19%)	1.76×10^4	5×10^2
	Ga 69	60.4	F	0.105	Ga69(n, α)Cu66	5.1 min	1.04 (9%)	2.64×10^5	1.3×10^2
	Ga 71	39.6	F	0.7	Ga71(n, 2n)Ga70	21 min	0.17(0.2%), 1.04(0.5%)	8.75×10^5	4.6×10^2
31	Ga 69	60.4	F	0.55	Ga69(n, 2n)Ga68	68 min	1.08(100)^x, 1.25(3)^x, 1.89(4)^x, β^+(85%)	4.8×10^5	4.3
	Ga 69	60.4	T	1.4	Ga69(n, γ)Ga70	21 min	0.17(0.2%), 1.04(0.5%)	5.33×10^5	7.6×10^2
	Ga 71	39.6	T	5.0	Ga71(n, γ)Ga72	14.1 hr	0.63(19%), 0.84(88%), 2.20(29%), & others	5.44×10^4	35
	Ge 74	36.54	F	0.04	Ge74(n, α)Zn71	2.2 min	0.51(100%)	5.85×10^4	94
	Ge 70	20.52	F	0.129	Ge70(n, p)Ga70	21 min	0.17(0.2%), 1.04(0.5%)	8×10^4	5×10^3
	Ge 76	7.76	F	1.8	Ge76(n, 2n)Ge75	82 min	0.27(11%)	1.69×10^5	95
	Ge 73	7.76	F	0.137	Ge73(n, p)Ga73	4.8 hr	0.3, 0.74	4.07×10^3	4.1×10^2
32	Ge 72	27.43	F	0.065	Ge72(n, p)Ga72	14.1 hr	0.63(19%), 0.84(88%), 2.20(29%), &others	2.35×10^3	8×10^2
	Ge 70	20.52	F	0.70	Ge70(n, 2n)Ge69	40 hr	0.24 - 1.98, β^+	6.7×10^3	2.5×10^2
	Ge 74	36.54	T	0.04	Ge74(n, γ)Ge75^m	49 sec	0.139(100%)	1.17×10^4	1.2×10^3
	Ge 76	7.76	T	0.08	Ge76(n, γ)Ge77^m	54 sec	0.16(14%), 0.215(8%)	4.97×10^3	1.9×10^4
	Ge 74	36.54	T	0.21	Ge74(n, γ)Ge75	82 min	0.27(11%), 0.066 - 0.84	1.79×10^4	9×10^2
	As 75	100	F	0.035	As75(n, p)Ge75	82 min	0.27(11%), 0.066 - 0.84	4.1×10^4	3.8×10^2
33	As 75	100	F	0.029	As75(n, α)Ga72	14.1 hr	0.63(19%), 0.84(88%), 2.20(29%) & others	3.72×10^3	5.1×10^2
	As 75	100	T	5.4	As75(n, γ)As76	26.5 hr	0.56(45%), 0.66(6.3%), 1.22 - 2.08	7.53×10^4	49
	Se 82	9.19	F	1.5	Se82(n, 2n)Se81^m	57 min	0.10(8%)	2×10^5	1.1×10^2
34	Se 80	49.82	F	0.038	Se80(n, α)Ge77	11.3 hr	0.21(35%), 0.22(45%), 0.27(57%), 0.37(17%)	2.93×10^3	1×10^3
	Se 76	9.02	T	22	Se76(n, γ)Se77^m	17.7 sec	0.16	1.46×10^6	27
	Se 80	49.82	T	0.5	Se80(n, γ)Se81^m	57 min	0.10(8%)	7.27×10^4	3×10^2
	Br 79	50.54	F	0.793	Br79(n, 2n)Br78	6.4 min	0.62, β^+	1.46×10^6	1.9
	Br 81	49.46	F	0.107	Br81(n, α)As78	91 min	0.62(100)^x, 0.7(42)^x, 1.32(33)^x	5.2×10^4	33
35	Br 79	50.54	F	0.013	Br79(n, α)As76	26.5 hr	0.56(45%), 0.66(6.3%), 1.22 - 2.08	1.1×10^3	3.3×10^3
	Br 79	50.54	T	8.5	Br79(n, γ)Br80	17.6 min	0.62(14%), β^+(8%)	2.56×10^6	5.7
	Br 81	49.46	T	3.3	Br81(n, γ)Br82	36 hr	0.55(75%), 0.62(42%), 0.70(28%) 0.78(83%), 0.83(25%), 1.04(29%), 1.32(28) 1.48(17%)	1.57×10^4	1.3×10^2
36	Kr 84	56.90	T	0.1	Kr84(n, γ)Kr85^m	4.4 hr	0.15(74%), 0.305(15.5%)	4.27×10^3	5.3×10^2

(Continued)

TABLE 4 (Continued)

Z	Target Isotope	% Abundance	F or T	σ (barns)	Reaction	Half-life	Gamma Energy (MeV)	R(d/sec/g)	Sensitivity (μg)
	Rb 87	27.85	F	0.059	Rb87(n, α)Br84	32 min	0.27, 0.35, 0.43, 0.47, 0.52, 0.61, 0.74, 0.81, 0.88	3.34×10^4	56
37	Rb 85	72.15	F	0.142	Rb85(n, α)Br82	36 hr	0.55(75%), 0.62(42%), 0.70(28%) 0.78(83%), 0.83(25%), 1.04(29%) 1.32(28%), 1.48(17%)	4.6×10^3	4.3×10^2
	Rb 85	72.15	T	0.007	Rb85(n,γ)Rb86^m	61 sec	0.56	3.43×10^3	3.4×10^3
	Rb 87	27.85	T	0.12	Rb87(n,γ)Rb88	18 min	0.90(15%), 1.39(1.4%), 1.84(23%)2.11-4.9	1.84×10^4	4.8×10^2
	Sr 88	82.56	F	0.018	Sr88(n, p)Rb88	18 min	0.90(15%), 1.39(1.4%), 1.84(23%)2.11-4.9	4×10^4	2.2×10^2
38	Sr 88	82.56	F	0.087	Sr88(n, α)Kr85^m	4.4 hr	0.15(74%), 0.305(15.5%)	2.4×10^4	93
	Sr 84	0.56	T	0.6	Sr84(n, γ)Sr85^m	70 min	0.15(14%), 0.225(85%)	7.5×10^2	2.7×10^3
	Sr 86	9.86	T	1.65	Sr86(n, γ)Sr87^m	2.8 hr	0.39(79%)	1.69×10^4	1.3×10^2
	Zr 90	51.46	F	0.080	Zr90(n, 2n)Zr89^m	4.18 min	0.59(94%), 1.53(7%), β^+(1.8%)	1.3×10^5	27
	Zr 94	17.40	F	0.007	Zr94(n, p)Y94	17.0 min	0.56(6%), 0.92(43%), 1.15(5%), 1.36-3.6	3.2×10^3	1.5×10^3
40	Zr 90	51.46	F	0.003	Zr90(n, α)Sr87^m	2.8 hr	0.39(79%)	7.5×10^2	2.8×10^3
	Zr 92	17.11	F	0.022	Zr92(n, p)Y92	3.7 hr	0.48, 0.56, 0.93, 1.40, 1.84	1.4×10^3	1.2×10^3
	Zr 94	17.40	F	0.0047	Zr94(n, α)Sr91	9.7 hr	0.94(3%), 1.03(30%), 0.27-1.6	1.24×10^2	4×10^4
41	Nb 93	100	T	1.0	Nb93(n, γ)Nb94^m	6.6 min	0.042(100%), 0.87(0.1%)	6.26×10^5	4.3
	Mo 94	9.04	F	0.0074	Mo94(n, p)Nb94^m	6.6 min	0.042(100%), 0.87(0.1%)	2×10^3	1.3×10^3
	Mo 92	15.84	F	0.106	Mo92(n, 2n)Mo91	15.6 min	β^+(94%)	4.2×10^4	52
42	Mo 98	23.78	F	0.009	Mo98(n, p)Nb98	51.5 min	0.72(75)^x, 0.78(100)^x, 1.16(30)^x, 0.33-1.93	2.8×10^3	6.4×10^2
	Mo 97	9.46	F	0.110	Mo97(n, p)Nb97	72.0 min	0.66(100)^x, 1.02(1)^x	9.9×10^3	1.8×10^2
	Mo 100	9.63	F	0.014	Mo100(n, α)Zr97	17 hr	0.75(100%, Nb97^m), 0.66, 0.35-1.76	1.14×10^2	1.5×10^4
	Mo 100	9.63	T	0.20	Mo100(n, γ)Mo101	14.6 min	0.19(25%), 0.31-2.03	1×10^4	8.3×10^2
	Ru 101	17.07	F	0.002	Ru101(n, p)Tc101	14.0 min	0.31(91%), 0.54(5%), 0.13-0.94	8.7×10^3	2.6×10^3
44	Ru 96	5.51	F	0.48	Ru96(n, 2n)Ru95	1.65 hr	0.3, 0.34, 0.63, 0.81-2.25, β^+(20%)	1.9×10^4	5.4×10^2
	Ru 104	18.58	T	0.7	Ru104(n, γ)Ru105	4.45 hr	0.32(13%), 0.47(21%), 0.73(50%), 0.13-1.34	7.62×10^3	4.4×10^2
	Rh 103	100	F	0.0112	Rh103(n, α)Tc100	16 sec	0.54, 0.60, 0.71-1.8	3.16×10^4	1.4×10^3
45	Rh 103	100	T	140	Rh103(n, γ)Rh104	42.8 sec	0.56(2%), 1.24(0.1%)	7.9×10^7	10.3
	Rh 103	100	T	12	Rh103(n, γ)Rh104^m	4.29 min	0.052(96.2%), 0.077(96.2%), 0.56-1.53	6.78×10^6	0.52
	Pd 104	10.97	F	0.132	Pd104(n, p)Rh104	42.8 sec	0.56(2%), 1.24(0.1%)	3.96×10^4	2×10^4
	Pd 110	11.81	F	0.0138	Pd110(n, α)Ru107	4.8 min	0.22(17)^x, 0.86(8)^x, 0.93(5)^x, 1.03(4)^x, 1.29(5)^x	4.45×10^3	7×10^2
46	Pd 108	26.71	F	0.0031	Pd(108(n, α)Ru105	4.45 hr	0.32(13%), 0.47(21%), 0.72(50%), 0.13-1.34	2.3×10^2	1.4×10^4
	Pd 110	11.81	F	2.0	Pd110(n, 2n)Pd109	13.6 hr	0.088(4%), 0.31	2.2×10^4	1.9×10^3
	Pd 105	22.23	F	0.74	Pd105(n, p)Rh105	35 hr	0.08, 0.16, 0.22, 0.31, 0.32, 0.42, 0.55	6.1×10^3	2.7×10^2
	Pd 108	26.71	T	0.26	Pd108(n, γ)Pd109^m	4.8 min	0.18(100%)	3.79×10^4	83
	Pd 108	26.71	T	10.4	Pd108(n, γ)Pd109	13.6 hr	0.088(4%), 0.31	5×10^4	8.3×10^2

(Continued)

TABLE 4 (Continued)

Z	Target Isotope	% Abundance	F or T	σ (barns)	Reaction	Half-life	Gamma Energy (MeV)	R(d/sec/g)	Sensitivity (μg)
47	Ag 109	48.65	F	0.038	Ag109(n, α)Rh106	30 sec	0.51(20%), 0.62(11%), 0.87-2.66	4.98×10^4	1.9×10^3
	Ag 109	48.65	F	0.8	Ag109(n, 2n)Ag108	2.3 min	0.43(0.2%), 0.63(1%), β^+(0.1%)	1.1×10^6	5×10^2
	Ag 107	51.35	F	0.889	Ag107(n, 2n)Ag106	24.0 min	0.51(18%), 0.62-1.54, β^+(61%)	8.6×10^5	4.7
	Ag 109	48.65	T	89	Ag109(n, γ)Ag110	24.42 sec	0.66(<5%)	2.33×10^7	25
	Ag 107	51.35	T	45	Ag107(n, γ)Ag108	2.3 min	0.43(0.2%), 0.63(1%), β^+(0.1%)	1.25×10^7	43
48	Cd 110	12.39	T	0.2	Cd110(n, γ)Cd111^m	49 min	0.15(29)^x, 0.246(94)^x	5.48×10^3	3.3×10^2
	Cd 116	7.58	T	1.5	Cd116(n, γ)Cd117	2.9 hr	0.28, 0.33, 0.83, 1.27, 1.53, 2.25	8.9×10^3	1.9×10^2
49	In 115	95.72	T	155	In115(n, γ)In116^m	54 min	0.406(40%), 0.81(15%), 1.09(57%), 1.27(83%), 0.14-2.08	3.1×10^7	0.07
50	Sn 120	32.85	F	0.0038	Sn120(n, p)In120	50 sec	0.73, 0.85, 1.02, 1.18	3×10^3	4.6×10^3
	Sn 124	5.94	T	0.2	Sn124(n, γ)Sn125^m	9.7 min	0.33(99%), 1.42(2%), 0.59-1.04	5.65×10^3	4.1×10^2
	Sn 122	4.72	T	0.16	Sn122(n, γ)Sn123	41 min	0.15(88%)	1.9×10^3	1.1×10^3
51	Sb 121	57.25	F	1.056	Sb121(n, 2n)Sb120	15.7 min	1.18(1%), β^+(44%)	1.2×10^6	4
	Sb 121	57.25	T	0.19	Sb121(n, γ)Sb122^m	4.1 min	0.060(100%), 0.075(100%)	5.19×10^4	67
52	Te 128	31.79	F	0.8	Te128(n, 2n)Te127	9.4 hr	0.36(0.1%), 0.418(0.8%), 0.059-0.215	2.8×10^4	7.4×10^3
	Te 130	34.48	T	0.22	Te130(n, γ)Te131	25 min	0.15(100)^x, 0.448(24)^x, 0.595-1.14	2.39×10^4	80
	Te 128	31.79	T	0.13	Te128(n, γ)Te129	74 min	0.45(9%), 0.031-1.09	5.9×10^3	3.2×10^3
	Te 126	18.71	T	0.8	Te126(n, γ)Te127	9.4 hr	0.36(0.1%), 0.418(0.8%), 0.059-0.215	3.3×10^3	6.3×10^4
53	I 127	100	F	0.025	I 127(n, p)Te127	9.4 hr	0.36(0.1%), 0.418(0.8%), 0.059-0.215	2.8×10^3	7.5×10^4
	I 127	100	T	5.6	I 127(n, γ)I 128	25 min	0.44(17%), 0.54(1.8%), 0.97(0.3%)	1.7×10^6	6.4
54	Xe 136	8.87	T	0.15	Xe136(n, γ)Xe137	3.95 min	0.455(33%)	5.9×10^3	1.8×10^3
	Xe 134	10.44	T	0.2	Xe134(n, γ)Xe135	9.2 hr	0.25(~97%), 0.36(~0.1%), 0.6(~3%)	4.6×10^2	3.8×10^3
55	Cs 133	100	F	0.0018	Cs133(n, α)I 130	12.5 hr	0.41(30)^x, 0.53(100)^x, 0.66(90)^x, 0.74(80)^x, 1.15(40)^x	1.5×10^2	1.1×10^4
	Cs 133	100	T	3	Cs133(n, γ)Cs134^m	2.91 hr	0.127(13%)	1.94×10^5	66
56	Ba 138	71.66	F	0.013	Ba138(n, α)Xe135^m	15.6 min	0.53	1.7×10^4	1.2×10^2
	Ba 138	71.66	F	0.0025	Ba138(n, p)Cs138	32 min	0.46(23%), 1.01(25%), 1.43(73%), 2.21(18%), 0.14-3.34	2.26×10^3	1.1×10^3
	Ba 136	7.81	T	0.016	Ba136(n, γ)Ba137^m	2.6 min	0.662(100%)	5.29×10^2	9×10^3
	Ba 138	71.66	T	0.5	Ba138(n, γ)Ba139	85 min	0.167(21%), 1.43(2%)	4.35×10^4	1.9×10^2

(Continued)

TABLE 4 (Continued)

Z	Target Isotope	% Abundance	F or T	σ (barns)	Reaction	Half-life	Gamma Energy (MeV)	R(d/sec/g)	Sensitivity (μg)
57	La 139	99.91	F	0.005	La139(n, p)Ba139	85 min	0.167(21%), 1.43(2%)	3×10^3	2.8×10^3
	La 139	99.91	T	8.2	La139(n, γ)La140	40.2 hr	0.33(19%), 0.49(41%), 0.82(27%), 0.92(11%), 1.60(95%), 2.54(4%)	4.07×10^4	43
58	Ce 140	88.48	F	0.009	Ce140(n, α)Ba137^m	2.6 min	0.662(100%)	1.65×10^4	2.9×10^2
	Ce 142	11.07	F	0.008	Ce142(n, α)Ba139	85 min	0.167(21%), 1.43(2%)	5.3×10^2	1.6×10^4
	Ce 142	11.07	F	0.0094	Ce142(n, p)La142	92 min	0.65(100)^x, 0.89(30)^x, 1.03(20)^x, 1.8(15)^x, 2.08(30)^x, 2.4(55)^x, 2.9(15)^x, 3.4(5)^x	5.8×10^2	3×10^3
	Ce 142	11.07	T	0.94	Ce142(n, γ)Ce143	33 hr	0.29(43%), 0.057-1.10	5.9×10^2	6.6×10^3
59	Pr 141	100	F	1.24	Pr141(n, 2n)Pr140	3.4 min	β^+(54%)	2.5×10^6	2.8
	Pr 141	100	T	10.8	Pr141(n, γ)Pr142	19.1 hr	1.58(4%)	1.1×10^5	3.8×10^2
60	Nd 142	27.11	F	0.01	Nd142(n, α)Ce139^m	60 sec	0.75	5.5×10^3	2.1×10^3
	Nd 148	5.73	F	0.0035	Nd148(n, p)Pr148	2 min	0.3	4.4×10^2	1.5×10^4
	Nd 142	27.11	F	0.0135	Nd142(n, p)Pr142	19.1 hr	1.57(4%)	1.84×10^2	2.3×10^5
	Nd 150	5.62	T	1.5	Nd150(n, γ)Nd151	12 min	0.14-1.75	3.16×10^4	69
	Nd 148	5.73	T	3.7	Nd148(n, γ)Nd149	1.8 hr	0.03-0.65	2×10^4	87
62	Sm 152	26.72	F	0.0037	Sm152(n, p)Pm152	6 min	0.122, 0.24	1.9×10^3	1.5×10^3
	Sm 154	22.71	F	0.009	Sm154(n,α)Nd151	12 min	0.14-1.75	3.67×10^3	6×10^2
	Sm 152	26.72	F	0.01	Sm152(n,α)Nd149	1.8 hr	0.03-0.65	1.2×10^3	1.4×10^3
	Sm 154	22.71	T	5.5	Sm154(n, γ)Sm155	22 min	0.104(76%), 0.142(1%), 0.246(3%)	3.57×10^5	7.2
63	Eu 153	52.18	F	0.009	Eu153(n, α)PM150	2.7 hr	0.33(100)^x, 0.41(10)^x, 0.51(30)^x, 0.84(25)^x, 0.57-0.84	1.45×10^3	1.2×10^3
	Eu 151	47.82	F	0.48	Eu151(n, 2n)Eu150	12.8 hr	0.34, 0.41, 0.61-1.97	1.47×10^4	1.1×10^2
	Eu 151	47.82	T	1700	Eu151(n, γ)Eu152^m	9.3 hr	0.12(7%), 0.84(11%), 0.96(9%), 0.34-1.39	1.55×10^7	1
64	Gd 160	21.9	F	0.002	Gd160(n, α)Sm157	30 sec	0.57	7.75×10^2	3×10^4
	Gd 157	15.68	F	0.0113	Gd157(n, p)Eu157	15.15 hr	0.065-0.75	99	1.7×10^4
	Gd 160	21.9	F	1.5	Gd160(n, 2n)Gd159	18.0 hr	0.36(19%), 0.08-0.3	1.54×10^4	5.7×10^2
	Gd 160	21.9	T	0.8	Gd160(n, γ)Gd161	3.7 min	0.1(17)^x, 0.32(37)^x, 0.36(100)^x, 0.08-0.53	6.48×10^4	57
	Gd 158	24.87	T	3.9	Gd158(n, γ)Gd159	18.0 hr	0.36(19%), 0.08-0.3	9.1×10^3	9.6×10^2
65	Tb 159	100	F	0.0022	Tb159(n, p)Gd159	18.0 hr	0.36(19%), 0.08-0.3	1×10^2	8.6×10^4
	Tb 159	100	T	22	Tb159(n, γ)Tb160	73 d	0.087-1.27	2.16×10^3	7.7×10^2

(Continued)

TABLE 4 (Continued)

Z	Target Isotope	% Abundance	F or T	σ (barns)	Reaction	Half-life	Gamma Energy (MeV)	R(d/sec/g)	Sensitivity (μg)
	Dy 164	28.18	F	0.015	Dy164(n, α)Gd161	3.7 min	$0.1(17)^{x}$, $0.32(37)^{x}$, $0.36(100)^{x}$, 0.08-0.53	7.5×10^{3}	4.9×10^{2}
	Dy 163	24.97	F	0.003	Dy163(n, p)Tb163	16 min	$0.025(20)^{x}$, $0.235(12)^{x}$, $0.33(40)^{x}$, $0.51(14)^{x}$	1.34×10^{3}	1.9×10^{3}
66	Dy 162	25.53	F	0.0036	Dy162(n, α)Gd159	18.0 hr	0.36(19%), 0.08-0.30	38	2.4×10^{5}
	Dy 164	28.18	T	2000	Dy164(n, γ)$Dy165^{m}$	1.3 min	0.11(97%), 0.36(3%), 0.15, 0.52	2×10^{8}	0.045
	Dy 164	28.18	T	800	Dy164(n, γ)Dy165	2.3 hr	0.098(3.2%), 0.28(1.4%), 0.36(1.7%) 0.56(0.7%), 0.64(1.1%), 0.72(0.9%)	1.52×10^{7}	3.4
67	Ho 165	100	F	2.76	Ho165(n, 2n)Ho164	35 min	0.037, 0.073, 0.091	2.6×10^{6}	0.69
	Ho 165	100	T	60	Ho165(n, γ)Ho166	27 hr	0.08(6%), 0.67-1.83	3.73×10^{5}	75
	Er 168	27.07	F	0.001	Er168(n, α)$Dy165^{m}$	1.3 min	0.11(97%), 0.36(3%), 0.15, 0.52	4.7×10^{2}	1.9×10^{4}
	Er 168	27.07	F	0.0025	Er168(n, p)Ho168	3 min	0.85	1.2×10^{3}	3.6×10^{3}
	Er 167	22.94	F	0.003	Er167(n, p)Ho167	3.1 hr	0.057, 0.079, 0.083, 0.21, 0.24, 0.32, 0.13-0.53	1.76×10^{2}	9.4×10^{3}
68	Er 162	0.136	T	2.03	Er162(n, γ)Er163	75 min	0.30, 0.43, 1.1	3.1×10^{2}	5.7×10^{3}
	Er 170	14.88	T	9	Er170(n, γ)Er171	7.5 hr	0.112(22%), 0.124(9%), 0.296(23%) 0.308(69%)	2.86×10^{4}	84
69	Tm 169	100	T	130	Tm169(n, γ)Tm170	127 d	0.084(3%)	6.97×10^{3}	7.9×10^{3}
	Yb 176	12.73	T	0.4	Yb176(n, γ)$Yb177^{m}$	6.4 sec	0.104, 0.233	1.7×10^{4}	6.5×10^{3}
70	Yb 176	12.73	T	5.5	Yb176(n, γ)Yb177	1.9 hr	0.15(6.4%), 1.09(1.9%), 1.24(1.7%), 0.12-0.95	5.22×10^{4}	5×10^{2}
	Yb 174	31.84	T	60	Yb174(n, γ)Yb175	4.2 d	0.11(3%), 0.28(5%), 0.39(9%)	3.05×10^{4}	6×10^{2}
71	Lu 175	97.41	T	35	Lu175(n, γ)$Lu176^{m}$	3.7 hr	0.055, 0.088	1.37×10^{6}	1.2
	Hf 177	18.5	T	380	Hf 177(n, γ)$Hf 178^{m}$	3.5 sec	0.326, 0.41	2.29×10^{7}	8.7
72	Hf 178	27.14	T	40	Hf 178(n, γ)$Hf 179^{m}$	18.6 sec	0.16(100%), 0.217(100%)	3.54×10^{6}	11
	Hf 179	13.75	T	65	Hf 179(n, γ)$Hf 180^{m}$	5.5 hr	0.058(62%), 0.093(20%), 0.22(88%), 0.33(96%), 0.44(81%), 0.50(16%)	2.39×10^{5}	7.3
	Ta 181	99.987	F	0.0012	Ta181(n, α)Lu178	22 min	$0.34(100)^{x}$, $0.44(10)^{x}$	1.43×10^{3}	1.4×10^{3}
73	Ta 181	99.987	F	0.9	Ta181(n, 2n)$Ta180^{m}$	8.1 hr	0.102	8.55×10^{4}	20
	Ta 181	99.987	T	0.03	Ta181(n, γ)$Ta182^{m}$	16 min	0.147, 0.172, 0.184, 0.319, 0.356	8.2×10^{3}	2.5×10^{2}

(Continued)

TABLE 4 (Continued)

Z	Target Isotope	% Abundance	F or T	σ (barns)	Reaction	Half-life	Gamma Energy (MeV)	R(d/sec/g)	Sensitivity (μg)
74	W 186	28.41	F	0.0029	W186(n, p)Ta186	10 min	0.123(25)^{x}, 0.2(100)^{x}, 0.3(25)^{x}, 0.41(20)^{x}, 0.51(45)^{x}, 0.61(45)^{x}, 0.73(65)^{x}, 0.94(15)^{x}	1.26×10^{3}	1.8×10^{3}
	W 184	30.64	F	0.0049	W184(n, p)Ta184	8.7 hr	0.11(30)^{x}, 0.24(60)^{x}, 0.30(35)^{x}, 0.41(100)^{x}, 0.89(90)^{x}, 1.18(50)^{x}, 0.16-0.78	1×10^{2}	2×10^{3}
	W 182	26.41	T	20	W182(n, γ)W183^{m}	5.5 sec	0.06, 0.105, 0.155	1.67×10^{6}	76
	W 186	28.41	T	34	W186(n, γ)W187	24 hr	0.072(13%), 0.134(10%), 0.48(28%), 0.68(32%), 0.55-0.77	6.05×10^{4}	86
75	Re 187	62.93	F	0.00094	Re187(n, α)Ta184	8.7 hr	0.11(30)^{x}, 0.24(60)^{x}, 0.30(35)^{x}, 0.41(100)^{x}, 0.89(90)^{x}, 1.18(50)^{x}, 0.16-0.78	39	4.2×10^{4}
	Re 187	62.93	F	0.0039	Re187(n, p)W187	24 hr	0.072(13%), 0.134(10%), 0.48(28%), 0.68(32%), 0.55-0.77	76	6.8×10^{4}
	Re 187	62.93	T	66	Re187(n, γ)Re188^{m}	20 min	0.064, 0.105	3.92×10^{6}	0.5
	Re 187	62.93	T	75	Re187(n, γ)Re188	18 hr	0.155(15%), 0.45-1.96	4.12×10^{5}	27
	Re 185	37.07	T	120	Re185(n, γ)Re186	90 hr	0.137(11%)	7.35×10^{4}	2.1×10^{2}
76	Os 192	41.0	T	1.6	Os192(n, γ)Os193	32 hr	0.139(3%), 0.28(1.3%), 0.46(4%)	2.98×10^{3}	1.4×10^{4}
77	Ir 191	37.3	F	0.0024	Ir191(n, α)Re188	18 hr	0.155(15%), 0.45-1.96	38.2	2.9×10^{5}
	Ir 193	62.7	F	0.0027	Ir193(n, p)Os193	32 hr	0.139(3%), 0.28(1.3%), 0.46(4%)	38	1.46×10^{6}
	Ir 191	37.3	T	610	Ir191(n, γ)Ir192^{m}	1.4 min	0.058(99%)	6.86×10^{7}	0.12
	Ir 193	62.7	T	130	Ir193(n, γ)Ir194	19 hr	0.29(5%), 0.33(24%), 0.64(6.2%), 0.62-2.05	6.18×10^{5}	11
78	Pt 195	33.8	F	0.0029	Pt 195(n, p)Ir195	2.3 hr	0.1(100)^{x}, 0.13(50)^{x}, 0.33(60)^{x}, 0.37(40)^{x}, 0.43(30)^{x}, 0.66(20)^{x}	2.7×10^{2}	6.2×10^{3}
	Pt 198	7.21	F	2.8	Pt 198(n, 2n)Pt 197	20 hr	0.077(100%), 0.19(1.5%)	7.2×10^{3}	2.3×10^{2}
	Pt 194	32.9	F	0.0039	Pt 194(n, p)Ir194	19 hr	0.29(5%), 0.33(24%), 0.64(6.2%), 0.62-2.05	48	1.45×10^{5}
	Pt 198	7.21	T	0.028	Pt 198(n, γ)Pt 199^{m}	14 sec	0.032(100%), 0.39(100%)	6×10^{2}	8.2×10^{4}
	Pt 198	7.21	T	3.9	Pt 198(n, γ)Pt 199	30 min	0.074-0.96	5.2×10^{4}	36
	Pt 196	25.3	T	0.87	Pt 196(n, γ)Pt 197	20 hr	0.077(100%), 0.19(1.5%)	1.56×10^{3}	1.07×10^{3}
79	Au 197	100	T	98.8	Au197(n, γ)Au198	2.7 d	0.41(95.6%), 0.68(1.1%), 1.09(0.26%)	2.14×10^{5}	8.1
80	Hg 201	13.22	F	0.0021	Hg201(n, p)Au201	26 min	0.55	2.7×10^{2}	6.9×10^{3}
	Hg 202	29.80	F	0.001	Hg202(n, α)Pt 199	30 min	0.074-0.96	2.68×10^{2}	7.0×10^{3}
	Hg 200	23.13	F	0.0036	Hg200(n, p)Au200	48.4 min	0.37(24%), 1.23(24%)	7.1×10^{2}	1.1×10^{4}
	Hg 204	6.85	T	0.43	Hg204(n, γ)Hg205	5.2 min	0.205	8.54×10^{3}	3.54×10^{2}
	Hg 198	10.02	T	0.018	Hg198(n, γ)Hg199^{m}	42 min	0.158, 0.368	2.78×10^{2}	6.5×10^{3}
	Hg 196	0.146	T	420	Hg196(n, γ)Hg197^{m}	24 hr	0.135(31%), 0.164(4.5%), 0.28(3%), 0.41(3%)	3.5×10^{3}	1.54×10^{3}
	Hg 196	0.146	T	880	Hg196(n, γ)Hg197	65 hr	0.077(20%), 0.191, 0.269	2.73×10^{3}	3.05×10^{3}

(Continued)

TABLE 4 (Concluded)

Z	Target Isotope	% Abundance	F or T	σ (barns)	Reaction	Half-life	Gamma Energy (MeV)	R(d/sec/g)	Sensitivity (μg)
81	Tl 205	70.5	F	0.003	Tl 205(n, p)Hg205	5.2 min	0.205	3×10^3	1×10^3
	Tl 203	29.5	F	0.00037	Tl 203(n, α)Au200	48.4 min	0.37(24%), 1.23(24%)	91	8×10^4
82	Pb 208	52.3	F	0.00096	Pb208(n, p)Tl 208	3.1 min	0.51(30%), 0.56(77%), 2.61(100%), 0.04-1.09	7.05×10^2	5.9×10^3
	Pb 208	52.3	F	0.0016	Pb208(n, α)Hg205	5.2 min	0.205	1.17×10^3	2.6×10^3
90	Th 232	100	T	7.33	Th232(n, γ)Th233	22.4 min	Many	1.34×10^6	1.5
92	U 238	99.3	T	2.74	U238(n, γ)U239	23.5 min	0.074, 0.38-0.99	4.74×10^5	4.1

- - - -

EMPIRICAL SENSITIVITY DATA

Empirical sensitivity data have been obtained for sixty-six elements, under standard irradiation and counting conditions, by irradiating a known weight of either the element or a pure compound of the element. The weight of sample used for these tests was dependent on the neutron activation cross section of the particular element and was normally a few hundred milligrams. The sample for irradiation was contained in a standard, 5-ml capacity, polythene irradiation vial. In order for this relatively small weight of sample to occupy a volume representative of the whole capsule, the sample was placed in a polythene-tube insert in the vial. The internal diameter of the insert was about 0.1 inch and the outside diameter such that it was a close fit in the irradiation capsule.

All of the irradiations were performed using the pneumatic transfer facility. For an isotope with a short half-life, the sample was counted in the transfer tube, following the irradiation, with a decay time of about one second. For an isotope with a reasonably long half-life, the sample was counted on top of the 3" x 3" NaI (Tl) scintillation detector, using a 1200 mg/cm^2 beta absorber. The decay time before counting, in this case, was usually one minute.

The identities of the isotopes produced were confirmed, if necessary, by half-life as well as by gamma-ray energy measurements. The photopeak counts were then taken for the most intense gamma-rays emitted by the isotope and normalised to a fast flux of 5×10^8 n/cm^2 -sec or a thermal flux of 1×10^8 n/cm^2 -sec, depending on the irradiation position that was used. The nuclear reaction and the gamma-ray photopeak that offer the highest analytical sensitivity for a given element are listed in Table 5. Where two photopeaks from the same isotope offer comparable sensitivities, both photopeaks are listed. Similarly, where two different reactions with the same element give comparable sensitivities, both reactions are listed. Other reactions with a given element that offer lesser sensitivities, have not been included in Table 5. The sensitivity data are usually the average of at least two determinations.

The irradiation times and the measurement times used in these empirical sensitivity tests do not represent the maximum times that could have been used. However, the various times that were used may be extended to other values by simple calculation.

The sensitivity data given in Table 5 are relevant to the experimental arrangements used for these determinations. The use of a second scintillation detector, for example, would result in an increase in sensitivity. However, the relative sensitivities from this table should be approximately the

same for other detector assemblies.

A number of fast neutron reactions were found to offer good analytical sensitivity but are not included in Table 4, through lack of published cross section data. These reactions are listed separately in Table 6.

TABLE 5

Empirical Sensitivity Data

Z	Target Element	F or T	Time			Product Isotope	Half-life	Photopeak Measured (MeV)	No. of μg to Give 100 Photopeak Counts
			Irradiation	Decay	Counting				
5	B	F	40 sec	1.5 sec	40 sec	Be 11	13.6 sec	2.12	2.5×10^4
7	N	F	5 min	1 min	10 min	N 13	10 min	β^+	35
8	O	F	40 sec	1.5 sec	40 sec	N 16	7.14 sec	4.5-6.5	7×10^2
9	F	F	2 min	1 sec	2 min	O 19	29.1 sec	0.2	1.35×10^2
	F	F	10 min	4 min	15 min	F 18	109.7 min	β^+	31
11	Na	F	2 min	1 sec	2 min	Ne 23	38 sec	0.44	2.3×10^2
	Na	T	15 min	4 min	30 min	Na 24	15.05 hr	1.37	2.4×10^2
12	Mg	F	2 min	1 sec	2 min	Ne 23, Na 25	38 sec, 60 sec	0.44, 0.4	1.4×10^3
	Mg	F	15 min	4 min	30 min	Na 24	15.05 hr	1.37	1.5×10^2
13	Al	F	5 min	1 min	10 min	Mg 27	9.5 min	0.84	50
								1.01	1.7×10^2
14	Si	F	2.3 min	1 min	4.6 min	Al 28	2.23 min	1.78	45
15	P	F	2.3 min	1 min	4.6 min	Al 28	2.23 min	1.78	70
	P	F	2.3 min	1 min	4.6 min	P 30	2.53 min	β^+	1.6×10^2
16	S	F	1 min	1 sec	1 min	P 34	12.4 sec	2.1	8.7×10^4
17	Cl	F	10 min	1 min	20 min	Cl 34^m	32.4 min	β^+	1.9×10^2
19	K	F	10 min	1 min	15 min	K 38	7.7 min	β^+	1.9×10^2
20	Ca	F	10 min	1 min	15 min	K 44	22 min	1.13	9×10^3
21	Sc	F	10 min	1 min	20 min	Sc 44	3.92 hr	β^+	26
	Sc	T	1 min	1 sec	1 min	Sc 46^m	20 sec	0.14	27
22	Ti	F	10 min	1 min	20 min	Sc 50, Ti 45	1.8 min, 3.08 hr	0.51, β^+	3.2×10^2
23	V	F	5 min	1 min	10 min	Ti 51	5.8 min	0.32	70
	V	T	5 min	1 min	10 min	V 52	3.76 min	1.43	13
24	Cr	F	3 min	1 min	3 min	V 52	3.76 min	1.43	3×10^2
25	Mn	T	10 min	1 min	20 min	Mn 56	2.58 hr	0.845	10
								1.81	75
26	Fe	F	10 min	1 min	20 min	Mn 56	2.58 hr	0.845	1.4×10^2

(Continued)

TABLE 5 (Continued)

Z	Target Element	F or T	Time			Product Isotope	Half-life	Photopeak Measured (MeV)	No. of μg to Give 100 Photopeak Counts
			Irradiation	Decay	Counting				
27	Co	T	5 min	1 min	10 min	Co 60^m	10.35 min	0.059	40
28	Ni	F	10 min	1 min	20 min	Co 60^m, Co 61	10.35 min, 1.65 hr	0.059, 0.072	9.4×10^2
29	Cu	F	5 min	1 min	10 min	Cu 62	9.8 min	β^+	6
30	Zn	F	5 min	1 min	10 min	Zn 63	38.1 min	β^+	70
31	Ga	F	10 min	1 min	20 min	Ga 68	68 min	β^+	8
32	Ge	F	1 min	1 sec	2 min	Ge 75^m	49 sec	0.139	3.3×10^2
33	As	T	15 min	1 min	30 min	As 76	26.5 hr	0.56	2×10^2
34	Se	F	30 sec	1 sec	60 sec	Se 77^m	17.7 sec	0.16	1.9×10^2
35	Br	F	20 sec	1 sec	20 sec	Br 79^m	5.1 sec	0.21	4.6×10^2
	Br	F	3.2 min	1 min	6.4 min	Br 78	6.4 min	β^+	8
37	Rb	F	1 min	1 sec	2 min	Rb 86^m	61 sec	0.56	1×10^2
	Rb	F	5 min	1 min	10 min	Rb 84^m	21 min	0.22, 0.25	12
38	Sr	T	10 min	1 min	20 min	Sr 87^m	2.8 hr	0.39	2.1×10^2
39	Y	F	1 min	1 sec	1 min	Y 89^m	16 sec	0.91	1×10^2
40	Zr	F	5 min	1 min	10 min	Zr 89^m	4.18 min	0.59	1.5×10^2
41	Nb	F	10 min	1 min	20 min	Y 90^m	3.14 hr	0.2	1.8×10^3
42	Mo	F	5 min	1 min	10 min	Mo 91	15.6 min	β^+	1.3×10^2
45	Rh	T	1 min	1 sec	1 min	Rh 104	42.8 sec	0.56	80
46	Pd	T	4 min	1 min	8 min	Pd 109^m	4.8 min	0.18	2.3×10^2
47	Ag	F	5 min	1 min	10 min	Ag 106	24 min	β^+	2
48	Cd	T	10 min	1 min	20 min	Cd 111^m	49 min	0.25	1×10^2
49	In	T	10 min	1 min	20 min	In 116^m	54 min	0.41	1.4
								1.09	1.5
								1.27	1.3
50	Sn	F	5 min	1 min	10 min	Sn 125^m	9.7 min	0.33	2.2×10^3
	Sn	F	5 min	1 min	10 min	Sn 123	41 min	0.15	1.4×10^3
51	Sb	F	5 min	1 min	10 min	Sb 120	15.7 min	β^+	18

(Continued)

TABLE 5 (Concluded)

Z	Target Element	F or T	Time			Product Isotope	Half-life	Photopeak Measured (MeV)	No. of μg to Give 100 Photopeak Counts
			Irradiation	Decay	Counting				
52	Te	T	5 min	1 min	10 min	Te 131	25 min	0.15	1.8×10^3
53	I	T	10 min	1 min	20 min	I 128	25 min	0.44	32
55	Cs	T	15 min	1 min	30 min	Cs 134^m	2.91 hr	0.127	1.5×10^2
56	Ba	F	2.6 min	1 min	5.2 min	Ba 137^m	2.6 min	0.662	27
57	La	T	20 min	1 min	40 min	La 140	40.2 hr	0.49	2.3×10^2
58	Ce	F	1 min	1 sec	2 min	Ce 139^m	1 min	0.75	70
59	Pr	F	3 min	1 min	6 min	Pr 140	3.4 min	β^+	8
60	Nd	F	2 min	1 min	4 min	Nd 141^m	64 sec	0.76	3×10^2
62	Sm	T	5 min	1 min	10 min	Sm 155	22 min	0.104	60
63	Eu	T	15 min	1 min	30 min	Eu 152^m	9.3 hr	0.12	3.5
64	Gd	T	3 min	1 min	6 min	Gd 161	3.7 min	0.32, 0.36	1.7×10^3
66	Dy	T	1 min	1 sec	2 min	Dy 165^m	1.3 min	0.11	20
67	Ho	T	15 min	1 min	30 min	Ho 166	27 hr	0.08	48
68	Er	T	15 min	1 min	30 min	Er 171	7.5 hr	0.3	2.6×10^2
70	Yb	T	10 min	1 min	20 min	Yb 177	1.9 hr	0.15	1.3×10^3
71	Lu	T	15 min	1 min	30 min	Lu 176^m	3.7 hr	0.055	15
72	Hf	T	1 min	1 sec	1 min	Hf 179^m	18.6 sec	0.22	60
73	Ta	T	10 min	1 min	20 min	Ta 180^m, Ta 182^m	8.1 hr, 16 min	0.057	4.5×10^2
74	W	T	15 min	1 min	20 min	W 187	24 hr	0.48 0.68	6.5×10^2 7.5×10^2
75	Re	T	5 min	1 min	10 min	Re 188^m	20 min	0.064	95
77	Ir	T	15 min	1 min	30 min	Ir 194	19 hr	0.33	25
78	Pt	T	10 min	1 min	20 min	Pt 199	30 min	0.48, 0.54	2.3×10^2
79	Au Au	F T	40 sec 20 min	1.5 sec 1 min	40 sec 75 min	Au 197^m Au 198	7.3 sec 2.7d	0.28 0.41	4×10^2 8
80	Hg	F	10 min	1 min	20 min	Hg 199^m	44 min	0.16	60
82	Pb	F	15 min	1 min	30 min	Pb 204^m, Tl 208 Pb 204^m	67 min, 3.1 min 67 min	0.9, 0.86 0.38	7×10^2 1.1×10^3

TABLE 6

Empirically Determined Fast Neutron Reactions That Offer High Analytical Sensitivities

Z	Element	Reaction	Half-life	Gamma Energy (MeV)
28	Ni	Ni60(n,p)Co60	10.35 min	0.059(99.7%), 1.33(0.3%)
32	Ge	Ge76(n,2n)Ge75^{m}	49 sec	0.139(100%)
35	Br	Br79(n,n')Br79^{m}	5.1 sec	0.21
37	Rb	Rb85(n,2n)Rb84^{m}	21 min	0.216(32)^{x}, 0.25(62)^{x}, 0.46(32)^{x}
		Rb87(n,2n)Rb86^{m}	61 sec	0.56
39	Y	Y89(n,n'), Y89^{m}	16 sec	0.91
41	Nb	Nb93(n,α)Y90^{m}	3.14 hr	0.2, 0.48
50	Sn	Sn124(n,2n)Sn123	40 min	0.15(88%)
56	Ba	Ba138(n,2n)Ba137^{m}	2.6 min	0.662(100%)
58	Ce	Ce140(n,2n)Ce139^{m}	1 min	0.75
60	Nd	Nd142(n,2n)Nd141^{m}	64 sec	0.76
79	Au	Au197(n,n')Au197^{m}	7.3 sec	0.13(99%), 0.28(99%)
80	Hg	Hg199(n,n')Hg199^{m}	44 min	0.16, 0.37
82	Pb	Pb204(n,n')Pb204^{m}	67 min	0.38, 0.9

CONCLUSIONS

A neutron generator offers the individual laboratory the possibility of having a self-contained activation analysis system that can be used for the quantitative determination of many elements. Except in a few very favourable cases, high sensitivity in the less than parts per million range will not be achieved with a neutron generator. However, there are a number of cases where its unique capabilities are superior to conventional analytical techniques and will allow a rapid, non-destructive determination to be made that is difficult or slow by other methods. The determination of oxygen by fast neutron activation has been widely exploited, and there is no reason why this type of quantitative, non-destructive determination should not be extended to certain other elements. The fact that a given element may be determined by alternative methods should not preclude the possibility of the determination being performed by activation analysis. Since there are at least 250 - 300 isotopes that could be formed in significant amounts by neutron activation with a neutron generator, in general it is not possible to say which elements can be best determined by this technique without reference to the matrix in which the element is contained. Each sample really represents a specific problem in itself. Fortunately, it is one of the advantages of neutron activation analysis that a preliminary screening may be made very rapidly (based on data such as given in Table 4 and Table 5) to assess the possibility of the determination. For certain determinations, e.g. hafnium in steel, silica in iron oxide, and nitrogen in carbon, where a nuclide of high cross section is present in a low cross section matrix, it is fairly obvious that activation will provide a suitable method. In other cases, it may be necessary to perform trial irradiations of the components of a mixture to decide upon the feasibility of using activation analysis. The relative contributions of the various components in a mixture, to the total induced activity of the mixture, can usually be optimised for the isotope of interest by suitable selection of the irradiation time, and the decay time before counting. Since activation analysis is a relative method of analysis, it will be necessary in all determinations to have a standard of known chemical composition that is similar to the samples under investigation. In all determinations that involve the measurement of positron-emitters, care has to be exercised in the interpretation of the results, in view of the large number of isotopes that decay in this manner (see Appendix 1). Thus, for example, the presence of copper would produce very serious interference in the determination of nitrogen by fast neutron activation, since copper-62 and nitrogen-13, both positron-emitters, have very similar half-lives.

There are two factors that currently limit the range of activation analysis with a neutron generator. The first factor is the relatively limited

life of the tritium target at high beam currents. This factor essentially restricts activation to isotopes with half-lives not greater than a few hours. Longer irradiations would permit the use of isotopes with half-lives of many hours or days with the additional possibility of chemical separation. Present developments in the design of various types of long-lived targets, target replenishment techniques (10), or sealed generator tubes (30), could well help to solve this problem. The second limiting factor is associated with the poor resolution of a sodium iodide scintillation detector (resolution, 5.9% at 1.33 MeV). As nearly all the gamma radiation to be measured following activation has an energy of less than 1.5 MeV, the resolution of some of the photopeaks that could arise from the activation of a complex mixture is not normally possible. This fact tends to restrict the application of the neutron generator to relatively simple mixtures or to mixtures in which the main components have low-activation cross sections. Improvements in the detection sensitivity of high-resolution lithium-drift germanium detectors (31) (resolution, 0.33% at 1.33 MeV) would be of great advantage in this respect.

The accuracy that may be obtained in activation analysis can be no better than the statistical accuracy of the recorded counts. As the concentration of an element decreases, the number of counts measured following activation will also decrease. The standard deviation, σ, for a measured number of counts, N, is given by $\sqrt{N}$. Thus, for 100 counts the standard deviation will be $\pm$ 10%.

Other errors of some significance are also present. In fast neutron activation in particular, the neutron flux distribution across a sample will be non-uniform (Figure 16) and will decrease with distance from the tritium target. For a counting system having only one NaI (Tl) detector, the side of the capsule of higher activity may not always be in the same position with respect to the detector. This error can be avoided by rotating the sample during irradiation (32) or by repeating the determination a number of times. For samples of high-neutron absorption cross sections, absorption of neutrons within the sample itself can also cause non-uniform flux gradients.

In general, activation analysis with a neutron generator can supplement rather than supplant existing analytical techniques. The high sensitivity associated with activation analysis using a nuclear reactor will not be obtained with a neutron generator. The techniques employed in activation analysis are very different from those used in conventional analytical methods and they offer an alternative approaches to the determination of many elements.

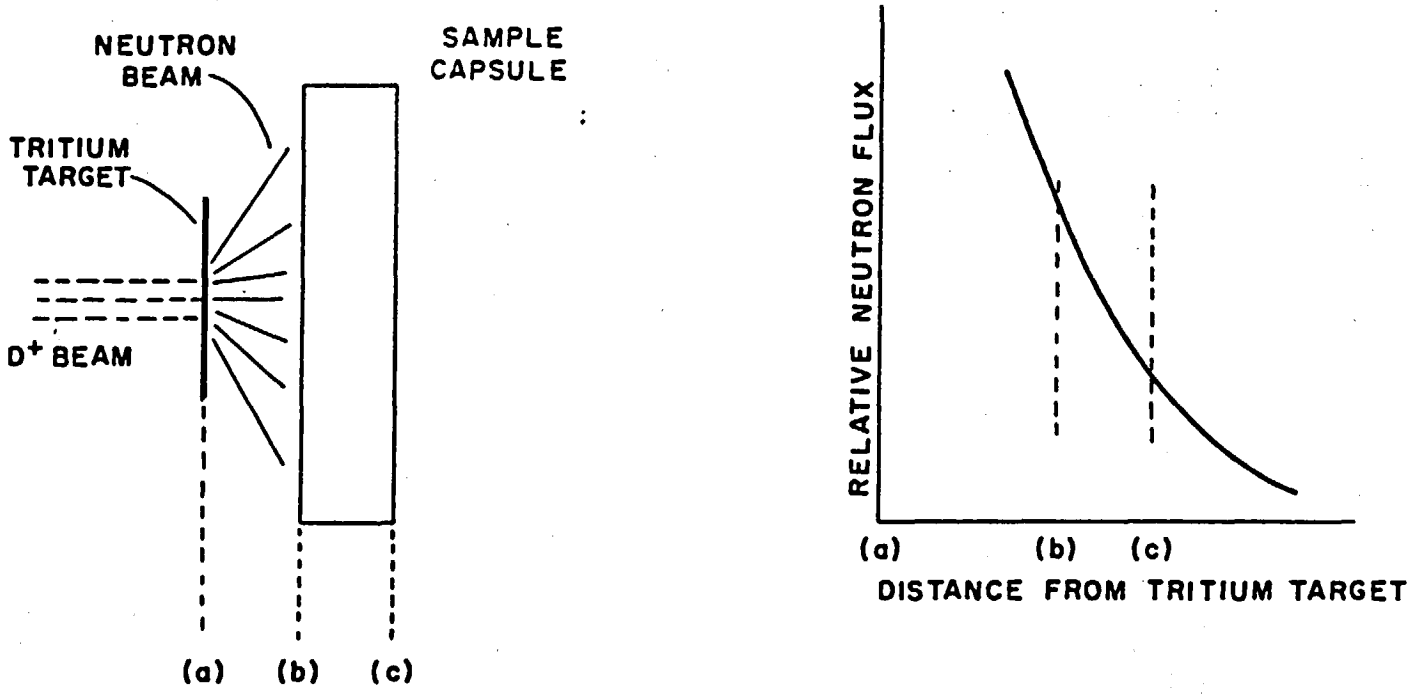

FIGURE 16. VARIATION OF FAST NEUTRON FLUX ACROSS SAMPLE CAPSULE.

ACKNOWLEDGEMENTS

It is a pleasure to acknowledge the assistance received in this work from Mr. C. McMahon, who has been associated with the neutron generator project since its inception. The author also wishes to thank Mr. A.F. Seeley for his significant contribution to the design and construction of the bulk shielding around the generator.

The neutron generator investigation was initiated by Dr. G.G. Eichholz, former Head of the Physics and Radiotracer Subdivision.

REFERENCES

(1) Leddicotte, G.W., Anal. Chem., 34, 143R (1962).

(2) Sayre, E.V., Ann. Rev. Nucl. Sci., 13, 145 (1963).

(3) Leddicotte, G.W., Anal. Chem., 36, 419R (1964).

(4) Bowen, H.J.M. and Gibbons, D., "Radioactivation Analysis", Oxford University Press, Oxford (1963).

(5) Dibbs, H.P., Canada Department of Mines and Technical Surveys, Mines Branch Tech. Bull. TB 55 (1964).

(6) Gorski, L., Kusch, W. and Wojtkowska, J., Talanta, 11, 1135 (1964).

(7) Hull, D.E. and Gilmore, J.T., Anal. Chem., 36, 2072 (1964).

(8) Yule, H.P., Lukens, H.R. and Guinn, V.P., U.S.AEC Report GA-5073 (1964).

(9) Moak, C.D., Reese, H. and Good, W.M., Nucleonics, 9(3), 18 (1951).

(10) Hollister, H., Nucleonics, 22(6), 68 (1964).

(11) Bramlitt, E.T. and Fink, R.W., Phys. Rev. 131, 2652 (1963).

(12) Houghton, G., J. Sci. Instr., 33, 199 (1956).

(13) National Bureau of Standards, Handbook 75 (1961).

(14) Price, D.B., Horton, C.C. and Spinney, K.T., "Radiation Shielding", Pergamon Press, London (1957).

(15) Hodge, N. and Sowden, R.G., Nucleonics, 19(11), 158 (1961).

(16) Hawkins, R.C. and Edwards, W.J., Atomic Energy of Canada, Ltd., Report CRDC-847 (1958).

(17) Koch, R.C., "Activation Analysis Handbook", Academic Press, New York (1960).

(18) Dibbs, H.P., Canada Department of Mines and Technical Surveys, Mines Branch Tech. Bull. TB 40 (1962).

(19) Volborth, A. and Banta, H.E., Anal. Chem., 35, 2203 (1963).

(20) Veal, D.J. and Cook, C.F., Anal. Chem., 34, 178 (1962).

(21) Coleman, R.F. and Perkins, J.L., Analyst, 84, 233 (1959).

(22) Gillespie, A.S. and Hill, A.W., Nucleonics, 19(11), 170 (1961).

(23) Miller, W.F. and Snow, W.J., Nucleonics, 19(11), 174 (1961).

(24) Heath, R.L., U.S. AEC Report IDO-16880 (1964).

(25) Gardner, D.G., Nucl. Phys., 29, 373 (1962).

(26) Hughes, D.J. and Schwartz, R.B., Brookhaven National Laboratory Report BNL 325 (1958).
Hughes, D.J., Magurno, B.A. and Brussel, B.K., Supplement No. 1 to BNL 325 (1960).
Stehn, J.R., Goldberg, M.D., Magurno, B.A. and Wiener-Chasman, R., Supplement No. 2 to BNL 325 (1964).

(27) Chatterjee, A., Nucleonics, 22(8), 108 (1964).

(28) Nuclear Data Sheets, National Academy of Sciences - National Research Council, Washington.

(29) Okada, M., Nucleonics, 22(8), 110 (1964).

(30) Lenihan, J.M.A., Nucleonics, 23(2), 65 (1965).

(31) Shirley, D.A., Nucleonics, 23(3), 62 (1965).

(32) Anders, O.U. and Briden, D.W., Anal. Chem., 36, 287 (1964).

====

HPD:gt

APPENDIX 1

Positron Emitters

A large number of positron-emitting isotopes are produced by fast neutron activation, quite often from an (n, 2n) reaction that results in a neutron-deficient isotope. Although the annihilation radiation from the decay of a positron-emitting isotope may be counted specifically by two single-channel gamma-ray spectrometers arranged in coincidence, or as a 0.51 MeV photopeak with a gamma-ray spectrometer, it is obviously not possible to characterise the isotope by this energy alone. Characterisation will depend upon the measurement of the half-life of the isotope and/or the measurement of other gamma radiation emitted in the isotopic decay process. As an aid in the identification of positron-emitting isotopes, Table 7 lists by half-life the positron-emitters likely to be encountered in activation analysis using a 14 MeV neutron source. Also given in this table are the energies of other gamma-rays associated with the decay of the particular isotope; a dash in this column indicates that the isotope is a pure positron-emitter. In those cases where the isotope is formed by other than an (n, 2n) reaction, the target nuclide and the production process are listed after the isotope.

TABLE 7

Positron Emitters Produced on Fast Neutron Activation Ordered by Half-life

(Production process (n, 2n) unless otherwise shown)

Isotope	Half-life	Other Gamma Energies (MeV)
Cl 34	1.5 sec	–
A 35	1.8 sec	1.19(5%), 1.73(2%)
S 31	2.6 sec	1.27(1%)
Si 27	4.2 sec	0.84(0.2%), 1.01(0.2%)
Ne 19	18 sec	–
Mo 91^{m}	65 sec	0.65(60%), 1.54(22%), 1.21(16%)
Ag 108	2.3 min	0.43(0.2%), 0.63 (1%)
Ag 108 (Cd 108;n, p)	2.3 min	0.43(0.2%), 0.63(1%)
P 30	2.53 min	–
Pr 140	3.4 min	–
Zr 89^{m}	4.18 min	0.59(94%), 1.53(7%)
Br 78	6.4 min	0.62
Br 78 (Kr 78;n, p)	6.4 min	0.62
K 38	7.7 min	2.16(100%)
Sm 143	9.0 min	–
Fe 53	9.0 min	0.38
La 136 (Ce 136;n, p)	9.5 min	0.83
Cu 62	9.8 min	0.66(2%), 0.85-2.24
N 13	10 min	–
Ho 162^{m} (Er 162;n, p)	11.8 min	0.08
In 112	14 min	0.16, 0.62
In 112 (Sn 112;n, p)	14 min	0.16, 0.62
Mo 91	15.6 min	–
Sb 120	15.7 min	1.18(1%)
Br 80	17.6 min	0.62(14%)
Ag 106	24 min	0.51(18%), 0.62-1.54
Ag 106 (Cd 106;n, p)	24 min	0.51(18%), 0.62-1.54
Cs 130 (Ba 130;n, p)	30 min	–
Cl 34^{m}	32.4 min	1.16(18%), 2.13(43%), 3.30(7%)
Sn 111	35 min	–
Zn 63	38.1 min	0.67(13%), 0.96(9%), 1.4(0.7%)
Cr 49	42 min	0.06, 0.09, 0.15
Se 73^{m}	44 min	0.09, 0.25, 0.58
Cd 105	55 min	0.03-2.32
Ga 68	68 min	1.08, 1.25, 1.89
Kr 77	72 min	0.02-0.87
Ru 95	99 min	0.3, 0.34, 0.63, 0.81-2.25
F 18	109.7 min	–
Xe 123	111 min	0.148
Nd 141	2.5 hr	1.14(1%), 1.3(0.5%)
Ba 129	2.6 hr	0.13-1.45
Er 161	3 hr	0.065-1.12
Ti 45	3.08 hr	–
Ir 190	3.2 hr	0.19, 0.36, 0.55, 0.62
Sc 44	3.92 hr	1.16(99%)
Se 73	7.1 hr	0.066(100%), 0.36(99%), 0.86, 1.31
Pd 101	8.5 hr	0.29(15%), 0.59(15%), 0.72-1.28
Cu 64 (Cu 63;n, γ)	12.8 hr	1.34(0.6%)
Cu 64 (Zn 64;n, p)	12.8 hr	1.34(0.6%)
Te 119	16 hr	0.65, 1.76
Sr 83	34 hr	0.04-0.165
Ni 57	37 hr	0.125, 1.38, 1.90
Ge 69	40 hr	0.24-1.98

APPENDIX 2

Gamma-Ray Spectra

In the course of the determination of the empirical sensitivity data given in Table 5, a number of gamma-ray spectra were obtained of isotopes formed by fast neutron activation, and thermal neutron activation, that are not conveniently available in the literature. For reference purposes these spectra are given in Figures 17-44. The irradiation time (I. T.), the decay time before counting (D. T.), and the counting time (C. T.) are given at the top right-hand corner of each figure. Also included on each figure are the isotopes produced, their half-lives, and their gamma energies as determined from the significant photopeaks. Where a compound was irradiated, the target element of interest is underlined in the title to the figure.

(Figures 17-44 follow,)
(on pages 59-86.)

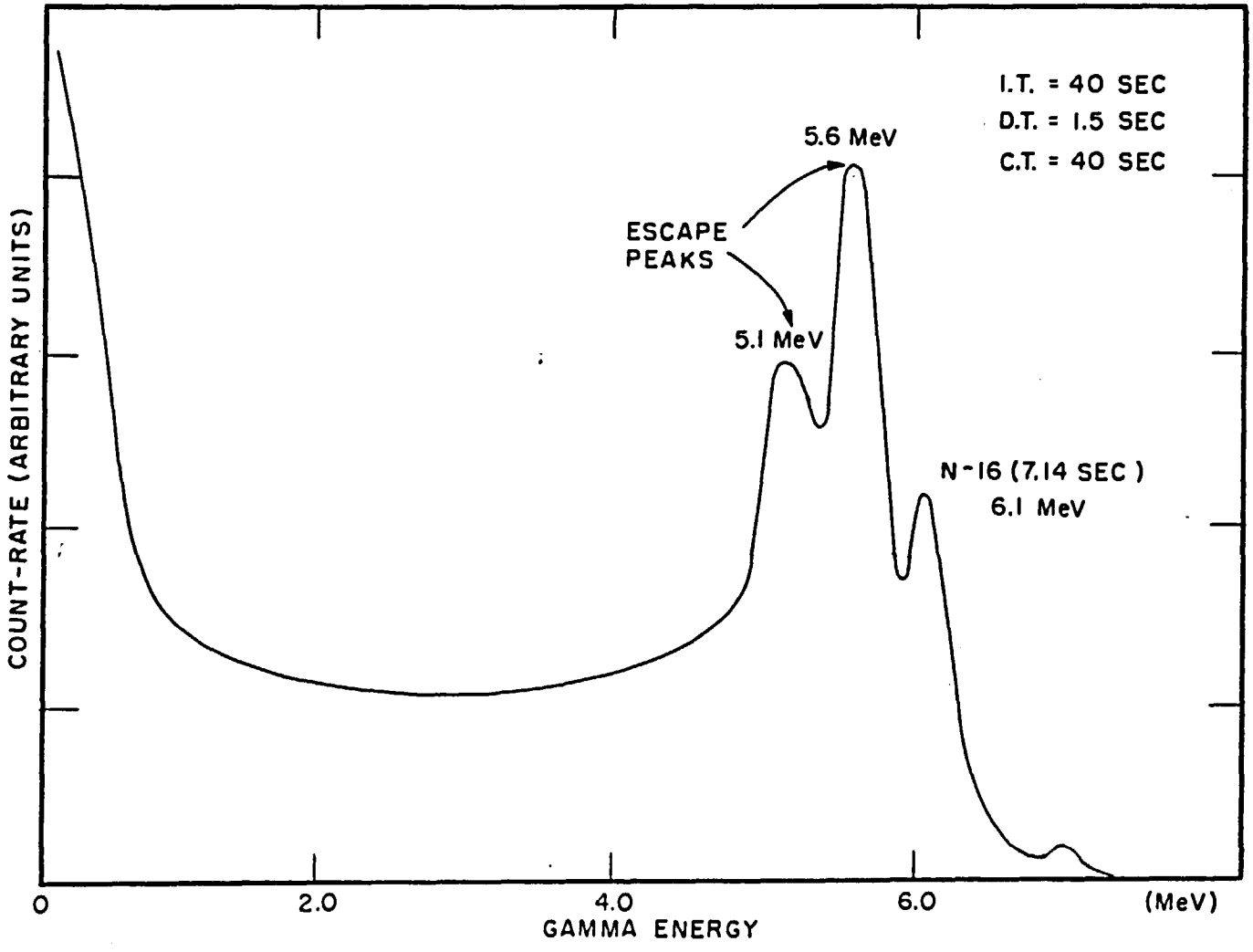

FIGURE 17. GAMMA-RAY SPECTRUM FOLLOWING FAST NEUTRON IRRADIATION OF $C_6H_5CO_2H$.

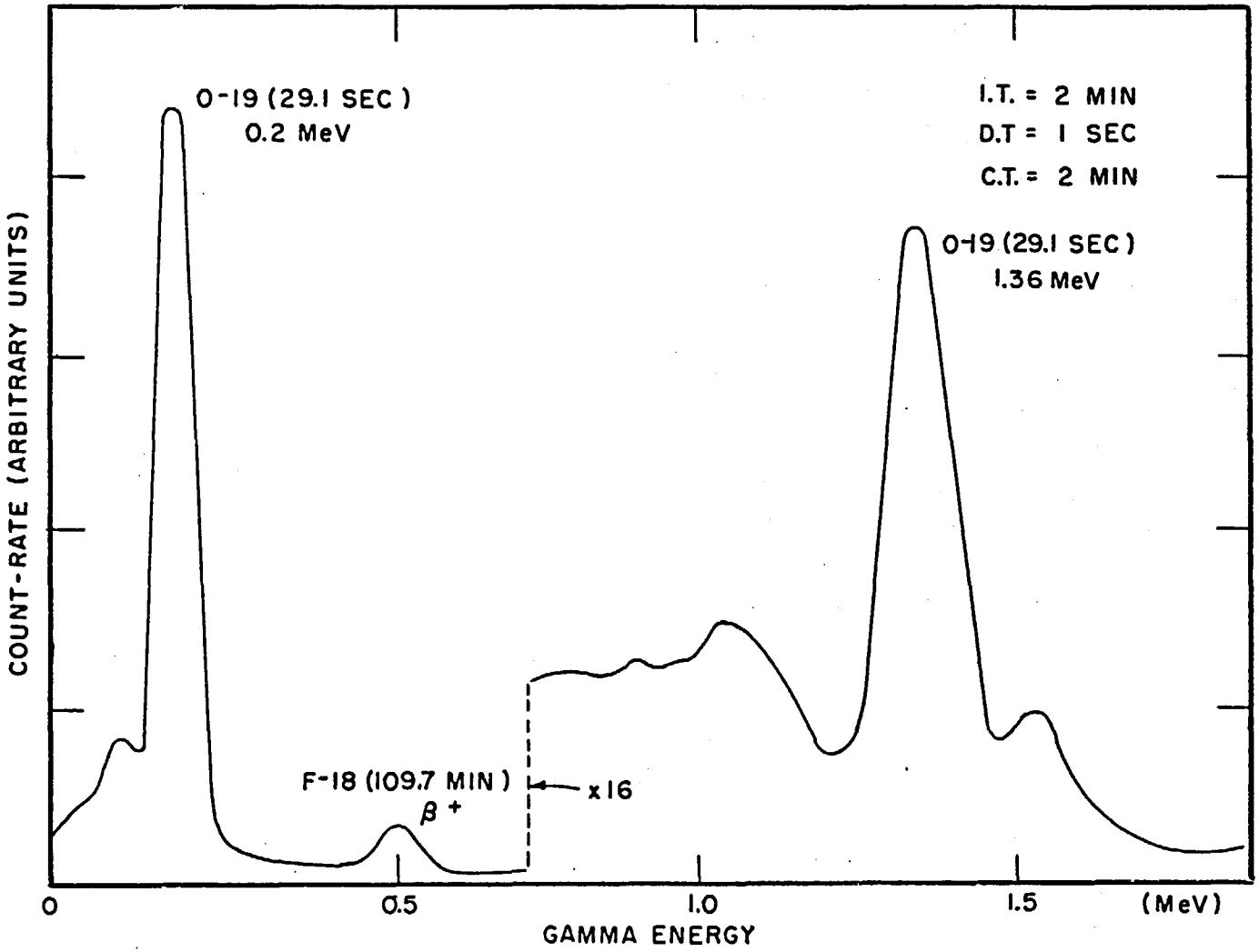

FIGURE 18. GAMMA-RAY SPECTRUM FOLLOWING FAST NEUTRON IRRADIATION OF LiF.

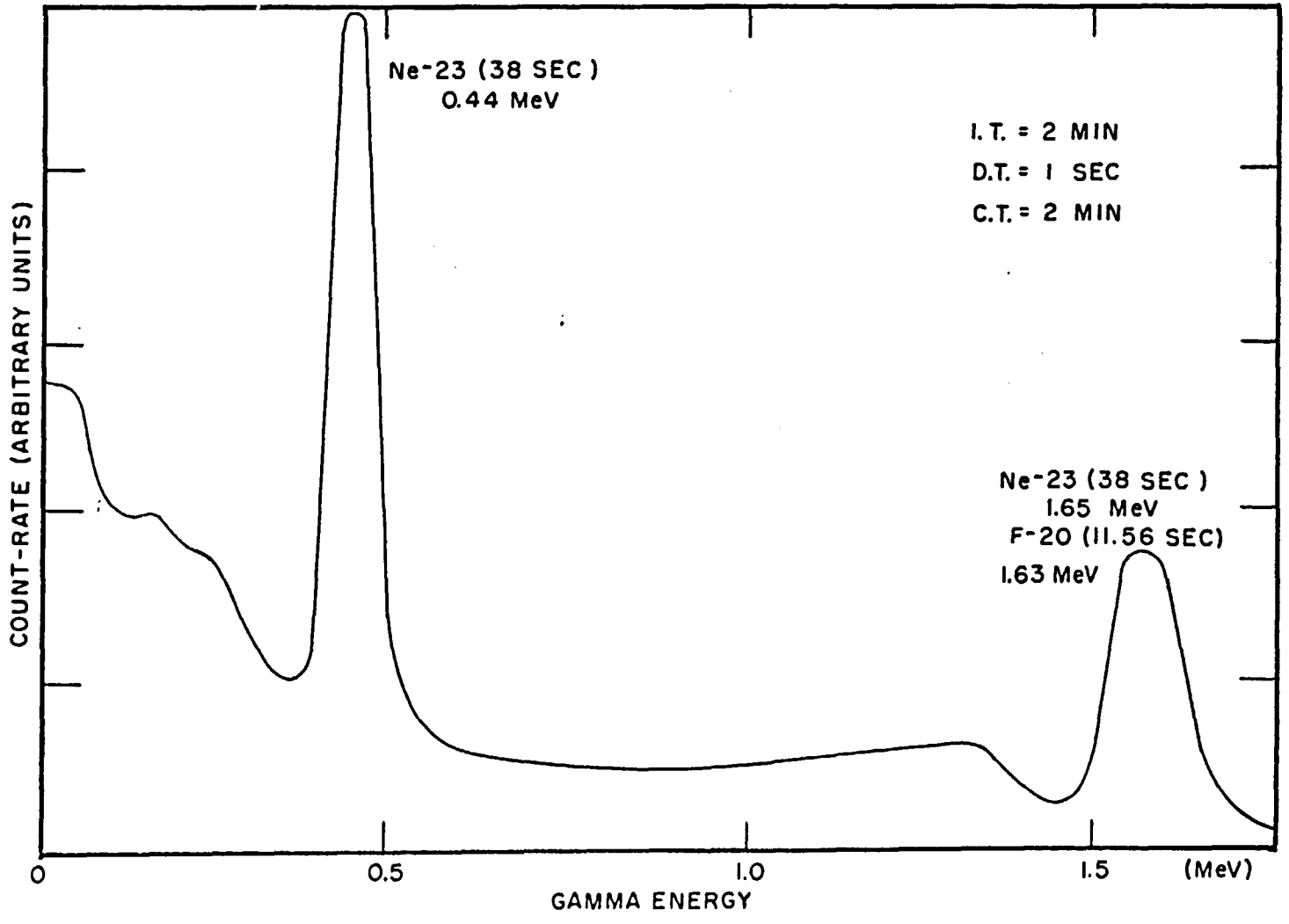

FIGURE 19. GAMMA-RAY SPECTRUM FOLLOWING FAST NEUTRON IRRADIATION OF Na_2CO_3.

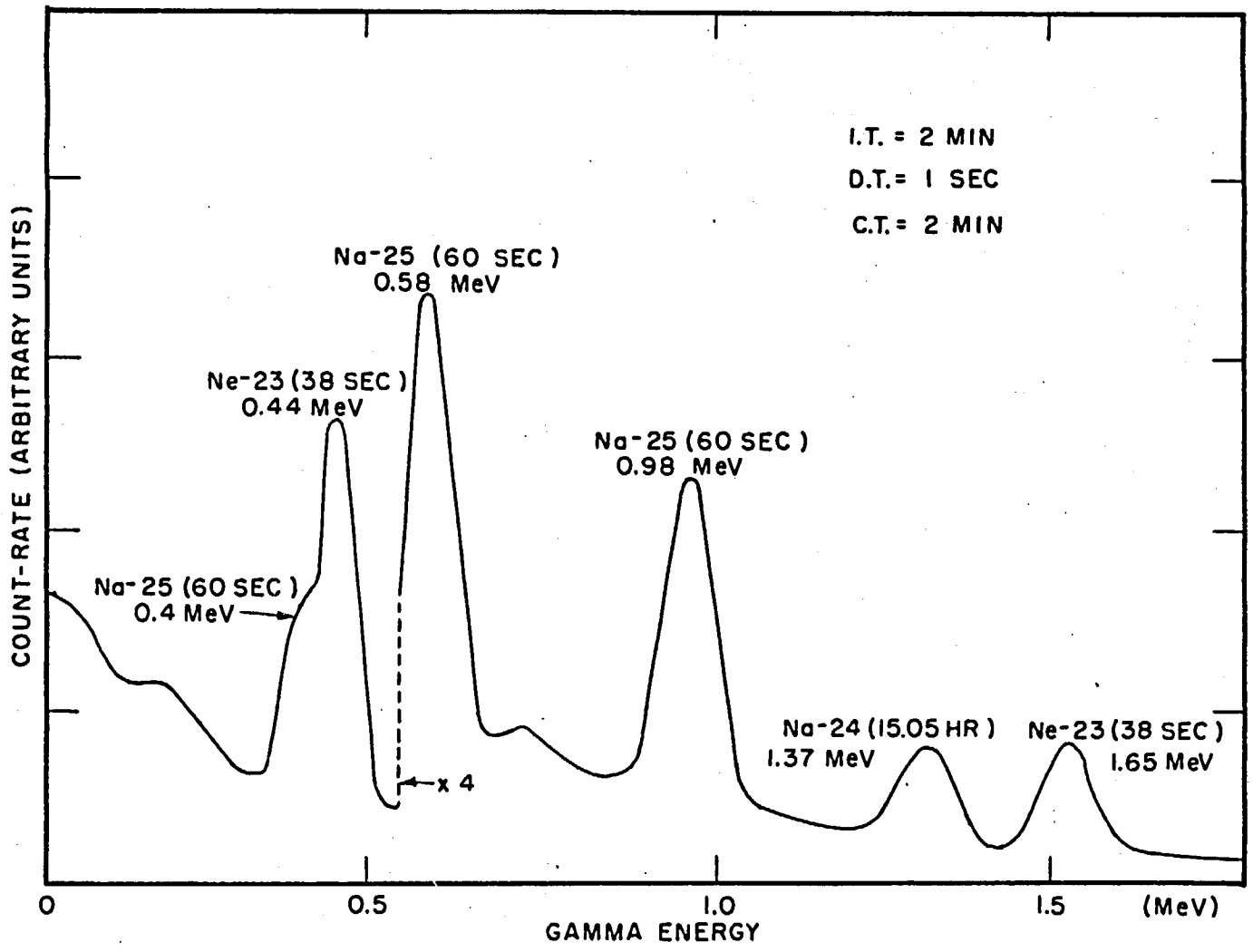

FIGURE 20. GAMMA-RAY SPECTRUM FOLLOWING FAST NEUTRON IRRADIATION OF MgO.

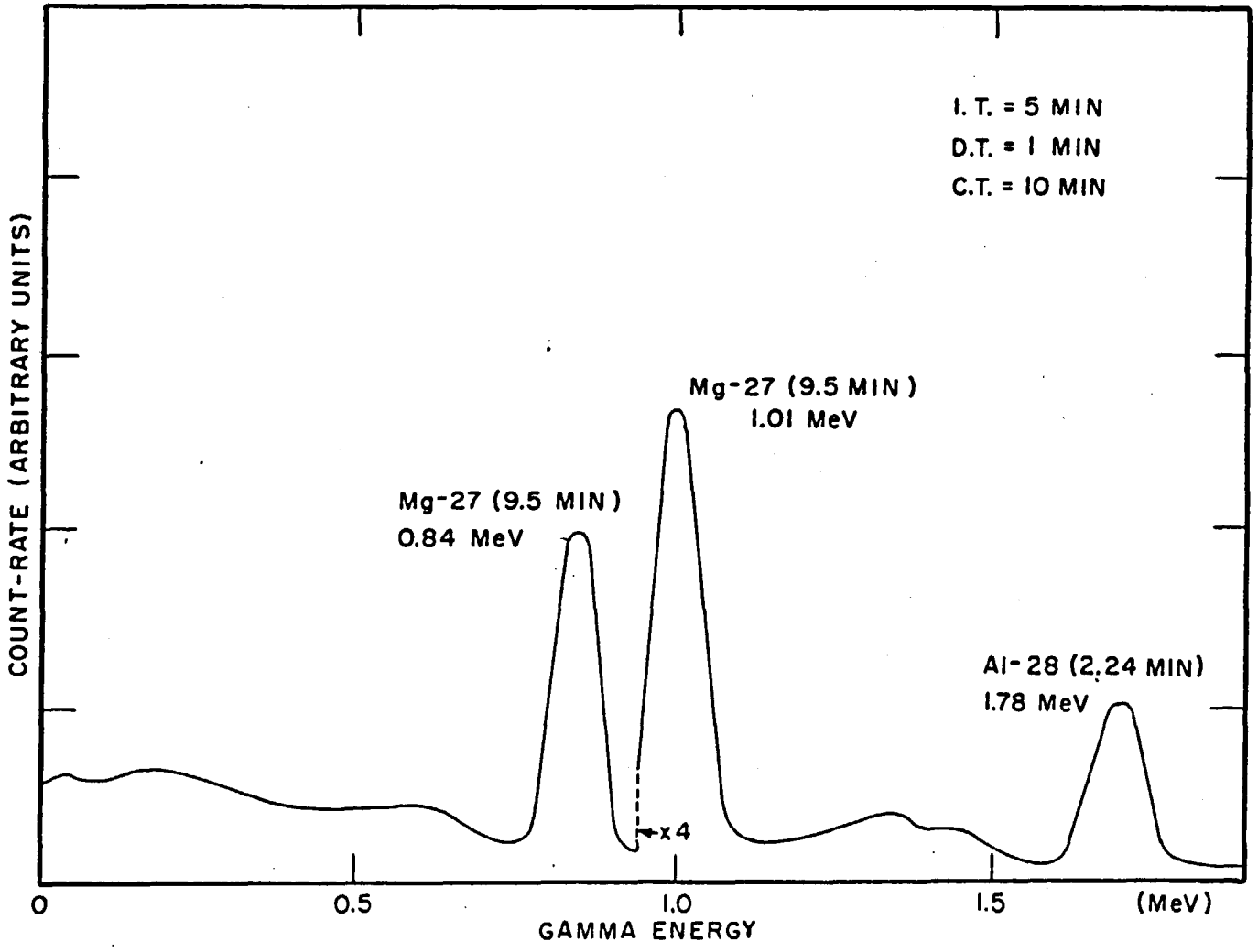

FIGURE 21. GAMMA-RAY SPECTRUM FOLLOWING FAST NEUTRON IRRADIATION OF $\underline{Al_2O_3}$.

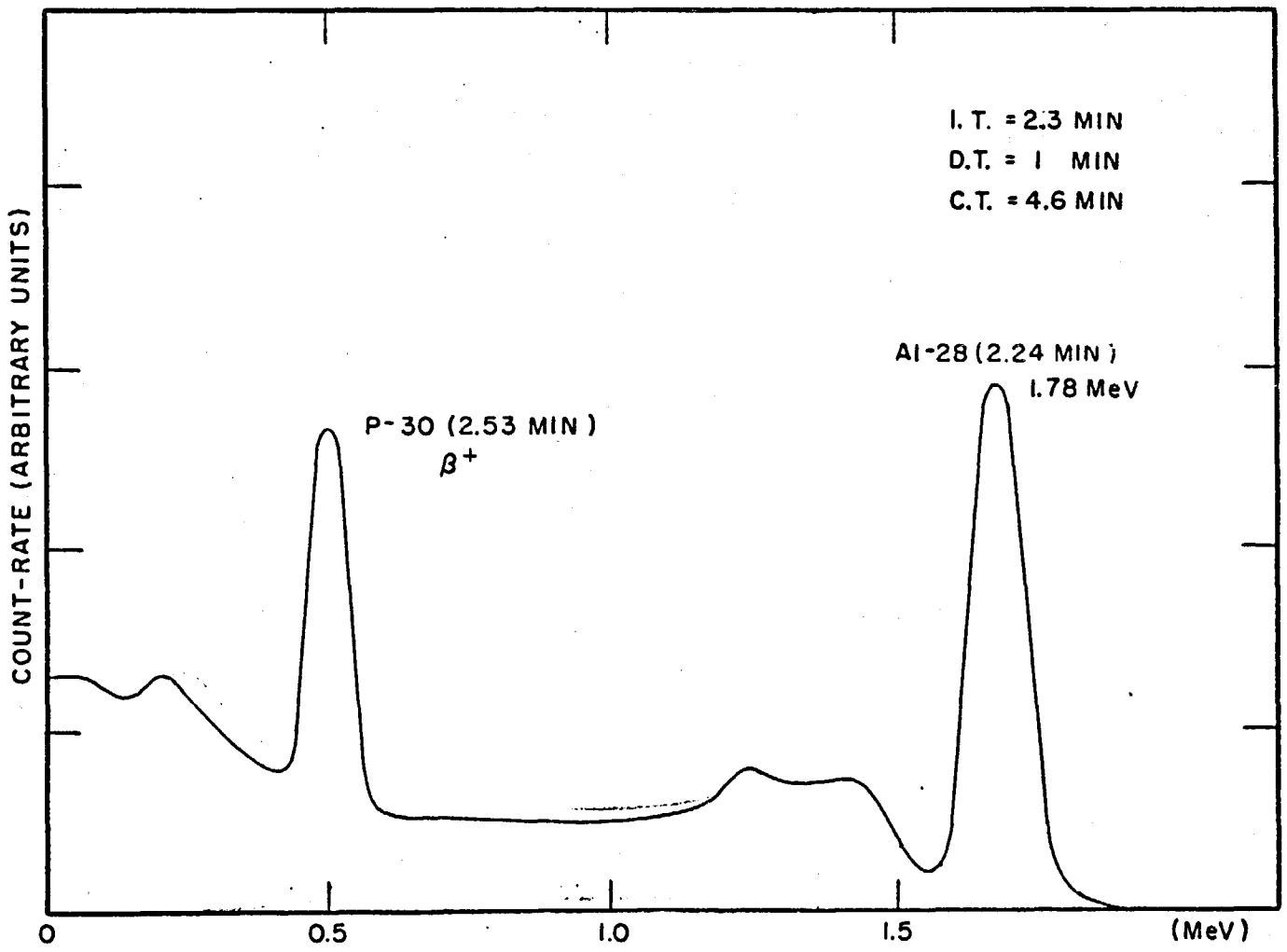

FIGURE 22. GAMMA-RAY SPECTRUM FOLLOWING FAST NEUTRON IRRADIATION OF $CaH\underline{P}O_4$.

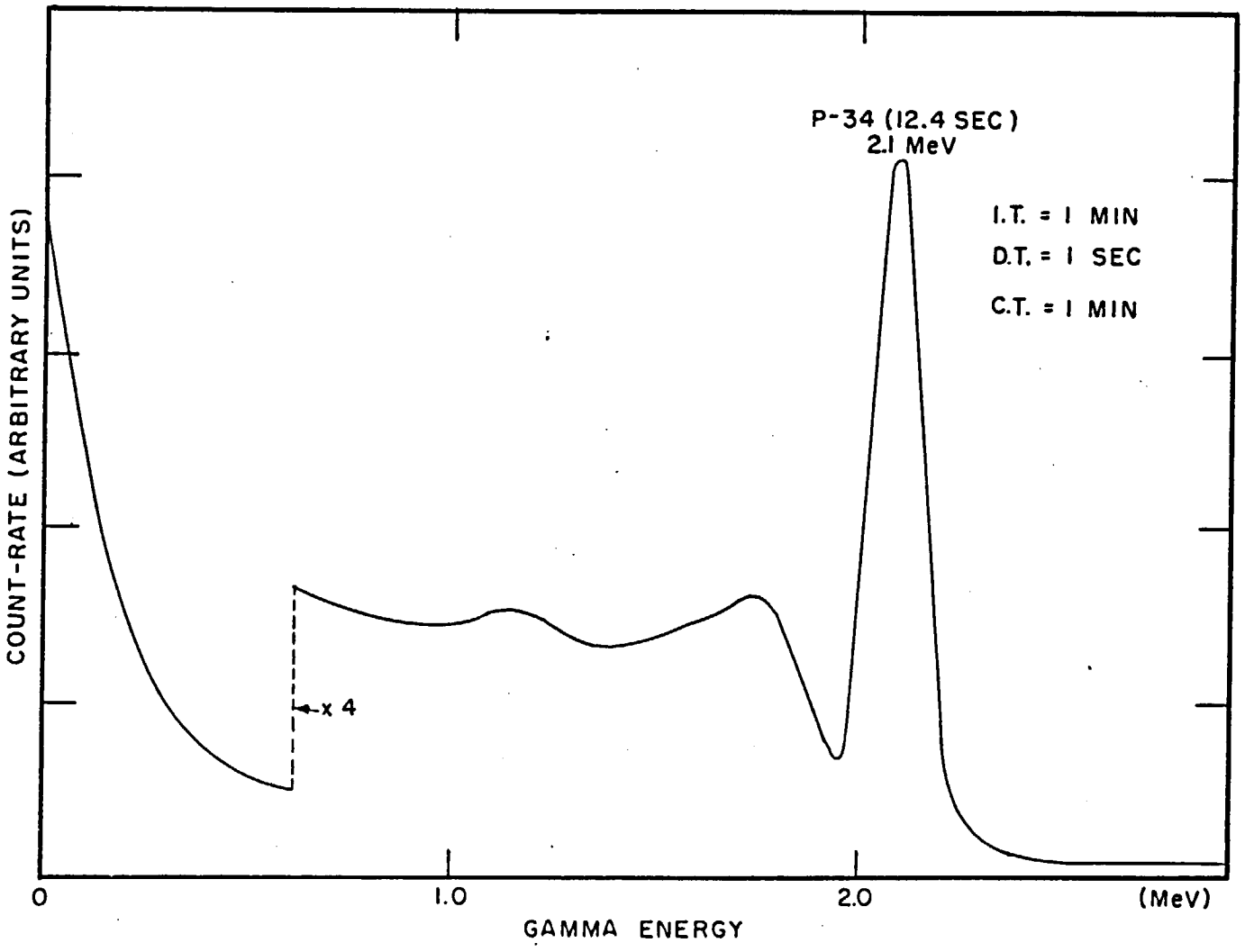

FIGURE 23 GAMMA-RAY SPECTRUM FOLLOWING FAST NEUTRON IRRADIATION OF SULPHUR.

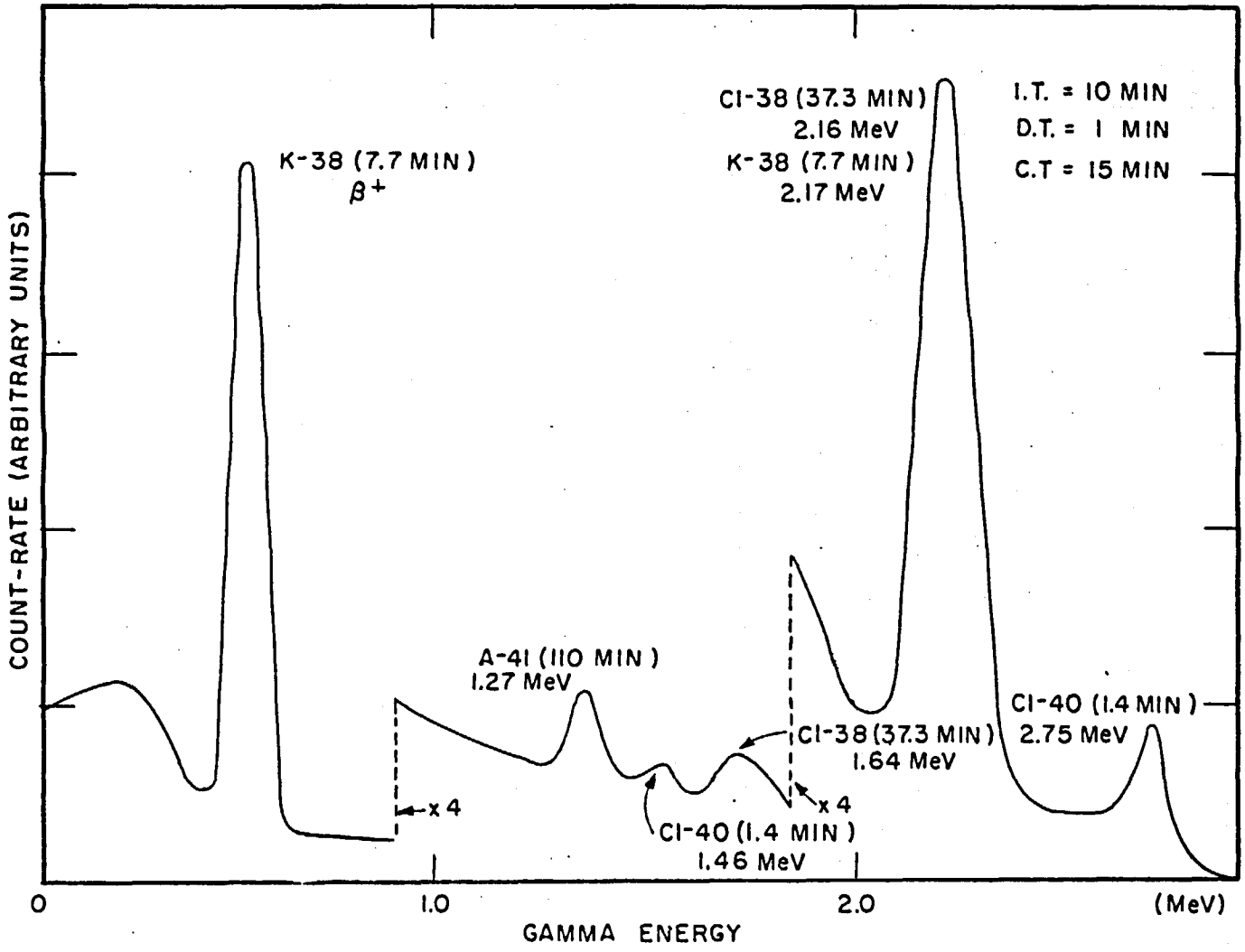

FIGURE 24. GAMMA-RAY SPECTRUM FOLLOWING FAST NEUTRON IRRADIATION OF K_2CO_3.

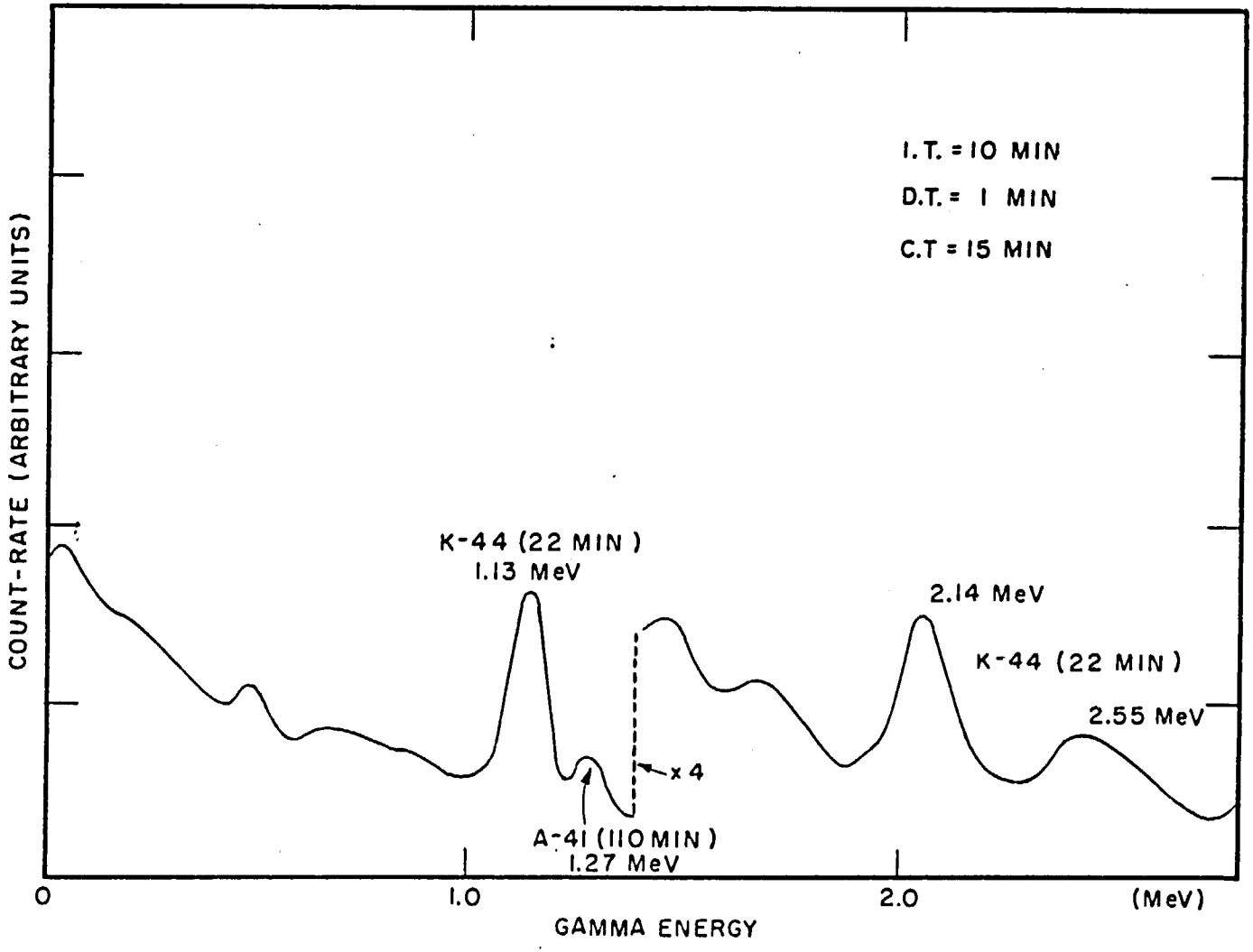

FIGURE 25. GAMMA-RAY SPECTRUM FOLLOWING FAST NEUTRON IRRADIATION OF CALCIUM.

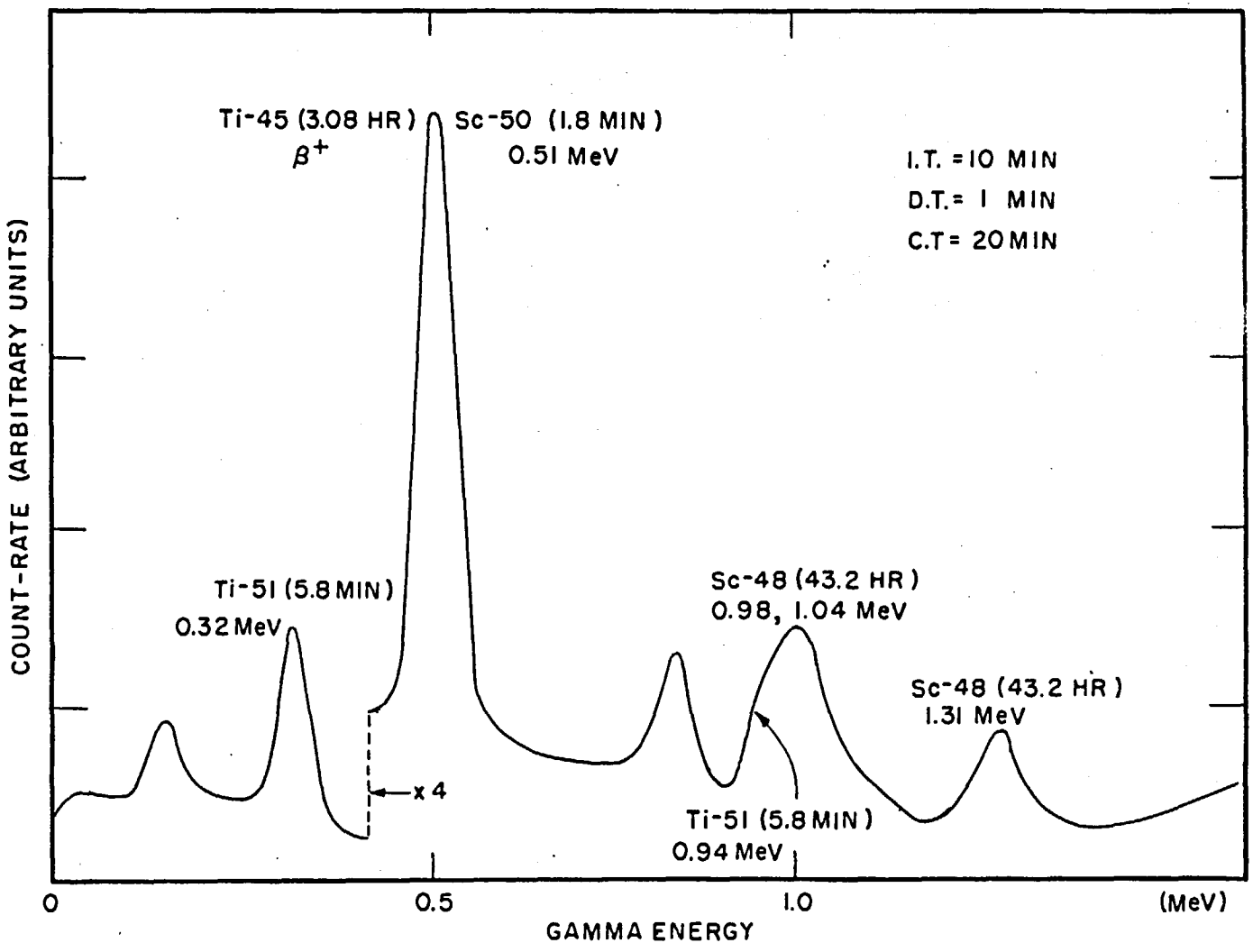

FIGURE 26. GAMMA-RAY SPECTRUM FOLLOWING FAST NEUTRON IRRADIATION OF $\underline{TiO_2}$.

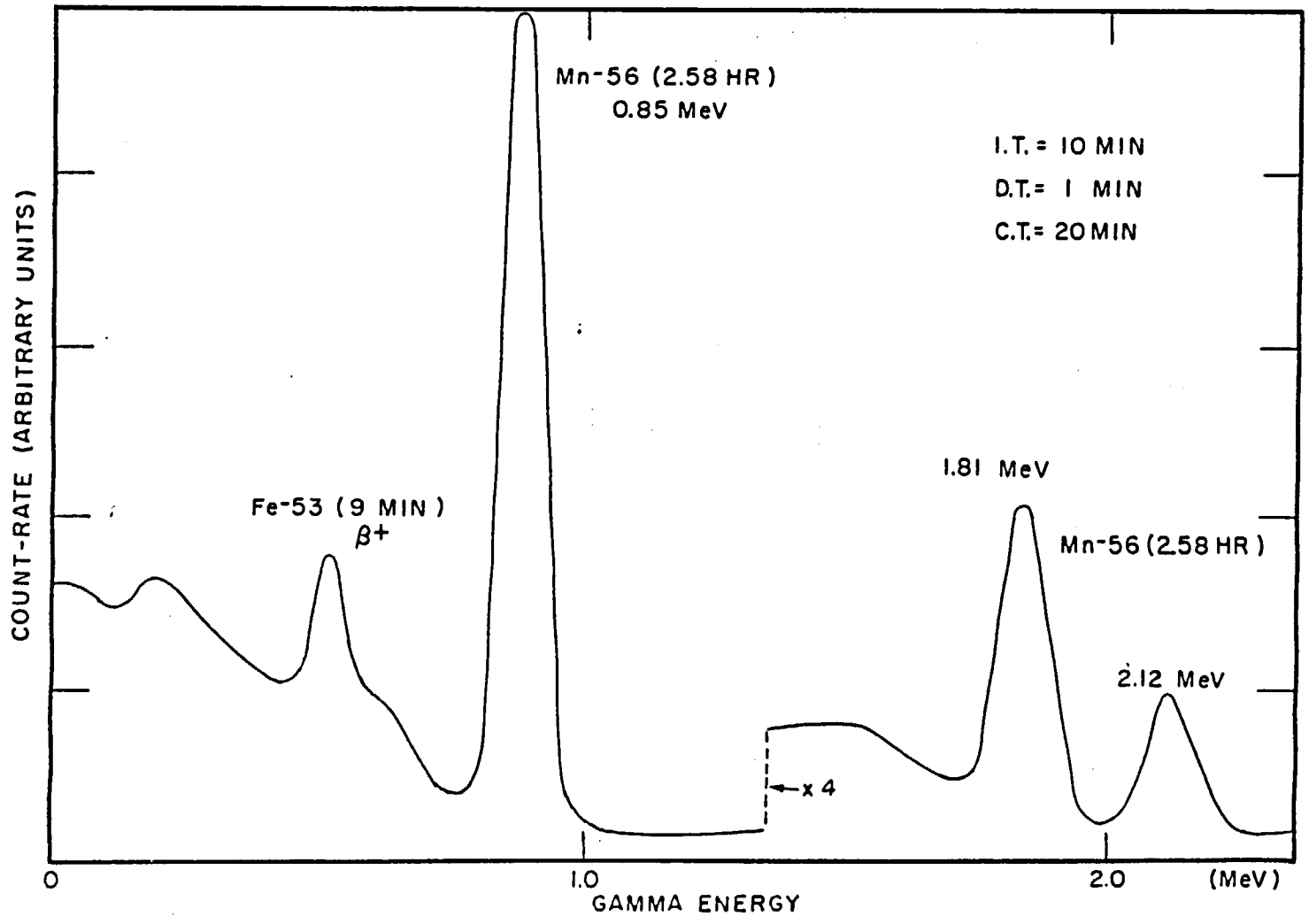

FIGURE 27. GAMMA-RAY SPECTRUM FOLLOWING FAST NEUTRON IRRADIATION OF IRON.

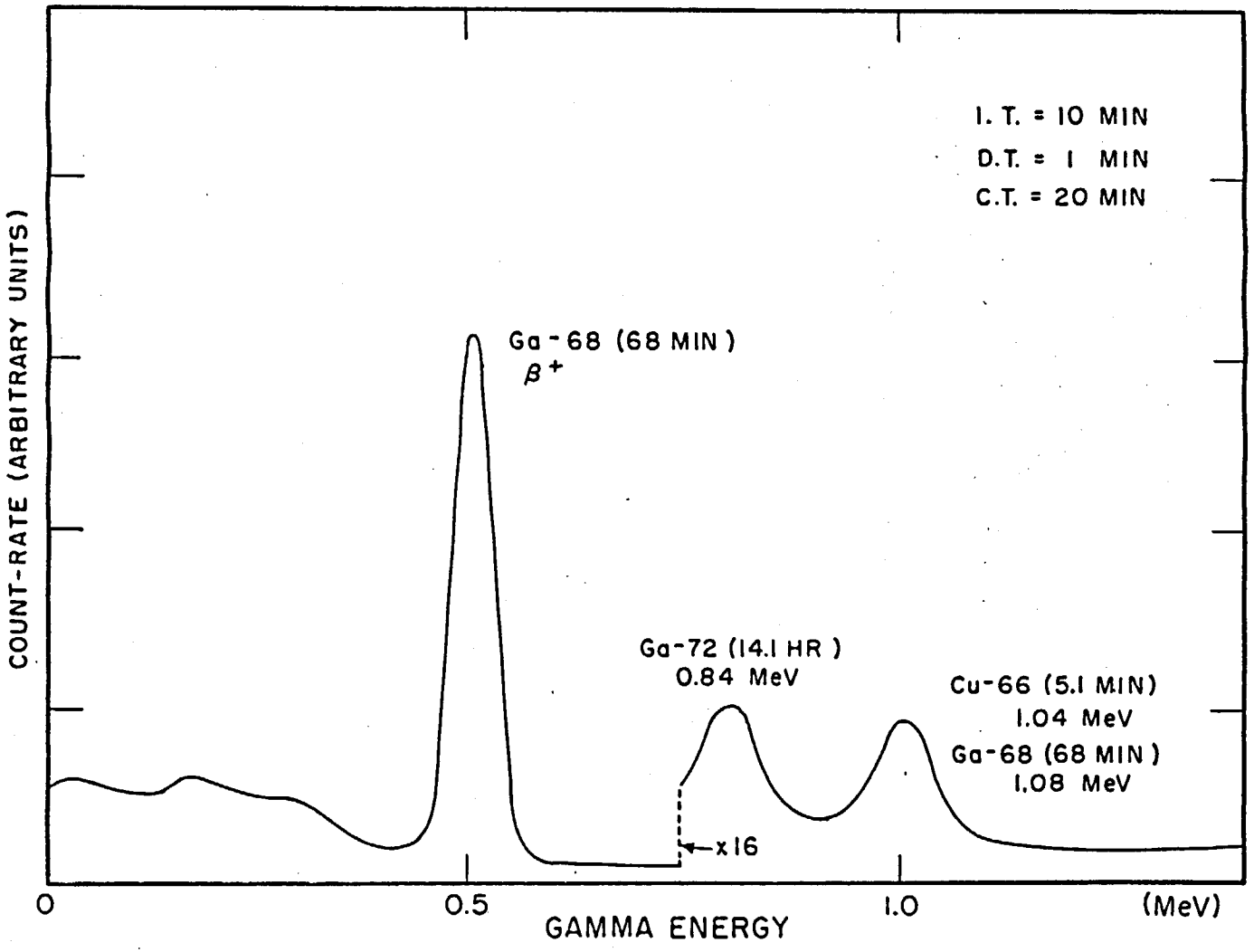

FIGURE 28. GAMMA-RAY SPECTRUM FOLLOWING FAST NEUTRON IRRADIATION OF GALLIUM.

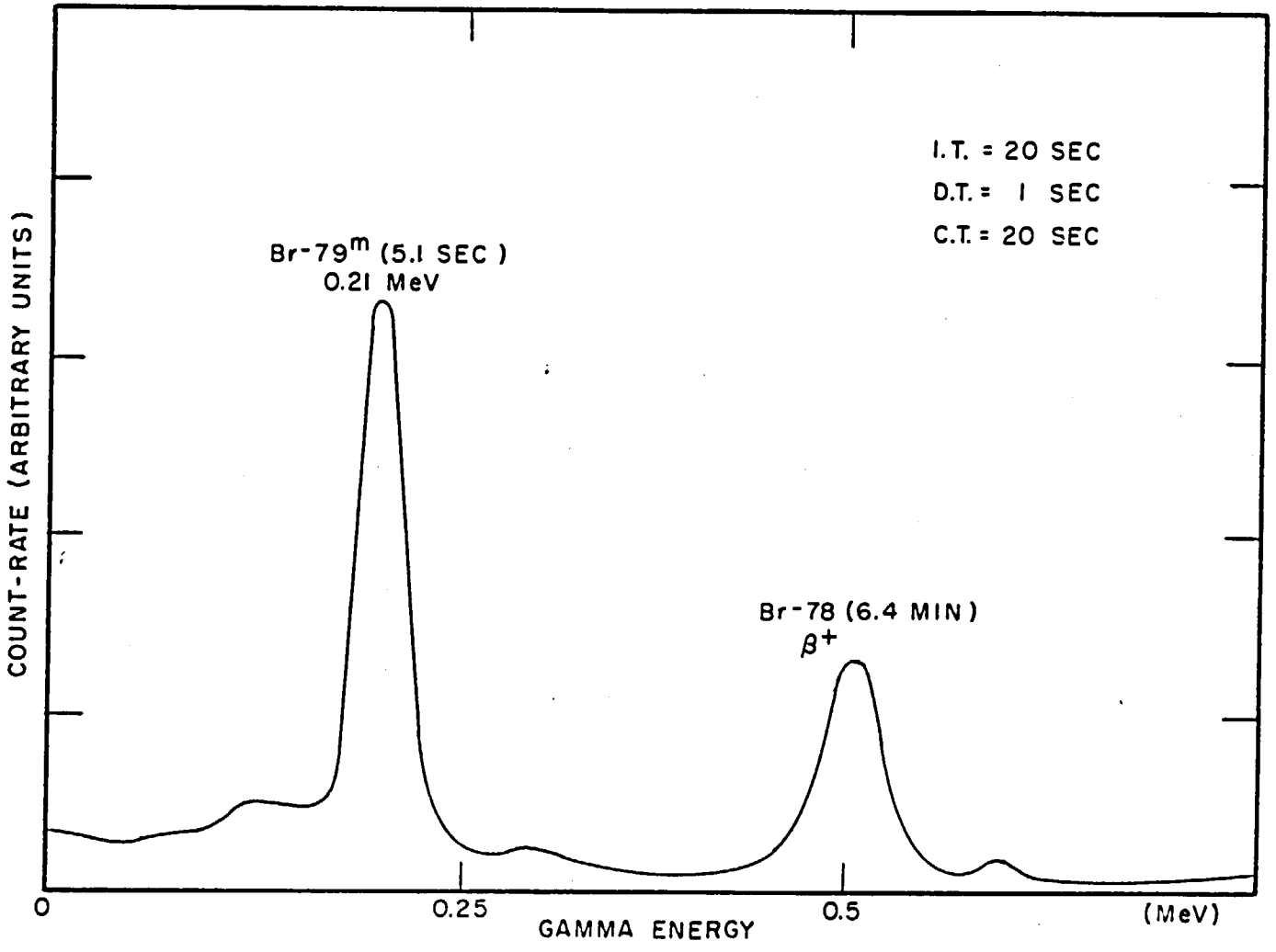

FIGURE 29. GAMMA-RAY SPECTRUM FOLLOWING FAST NEUTRON IRRADIATION OF DI-BROMO ANTHRACENE.

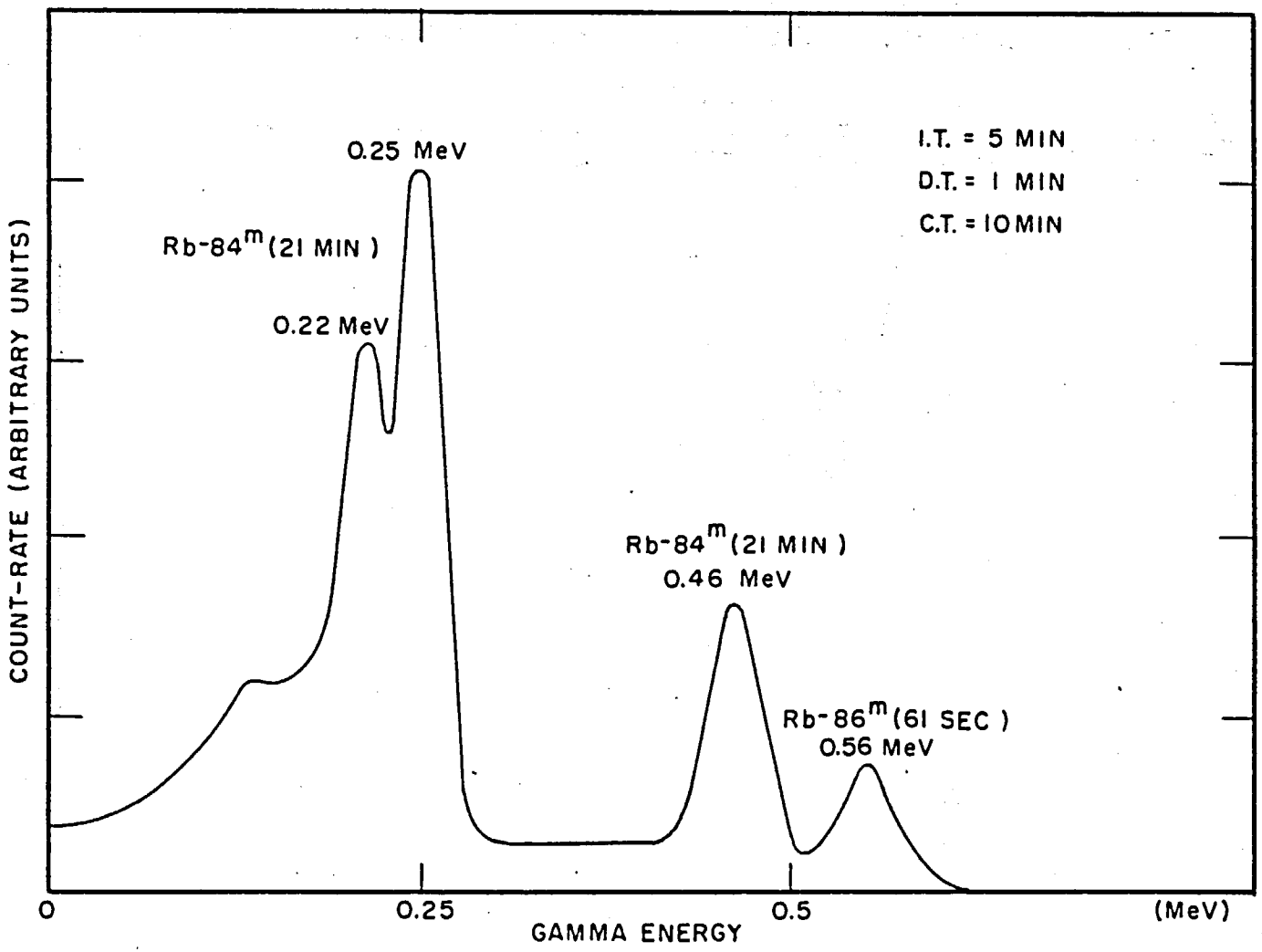

FIGURE 30. GAMMA-RAY SPECTRUM FOLLOWING FAST NEUTRON IRRADIATION OF $\underline{Rb}_2CO_3$.

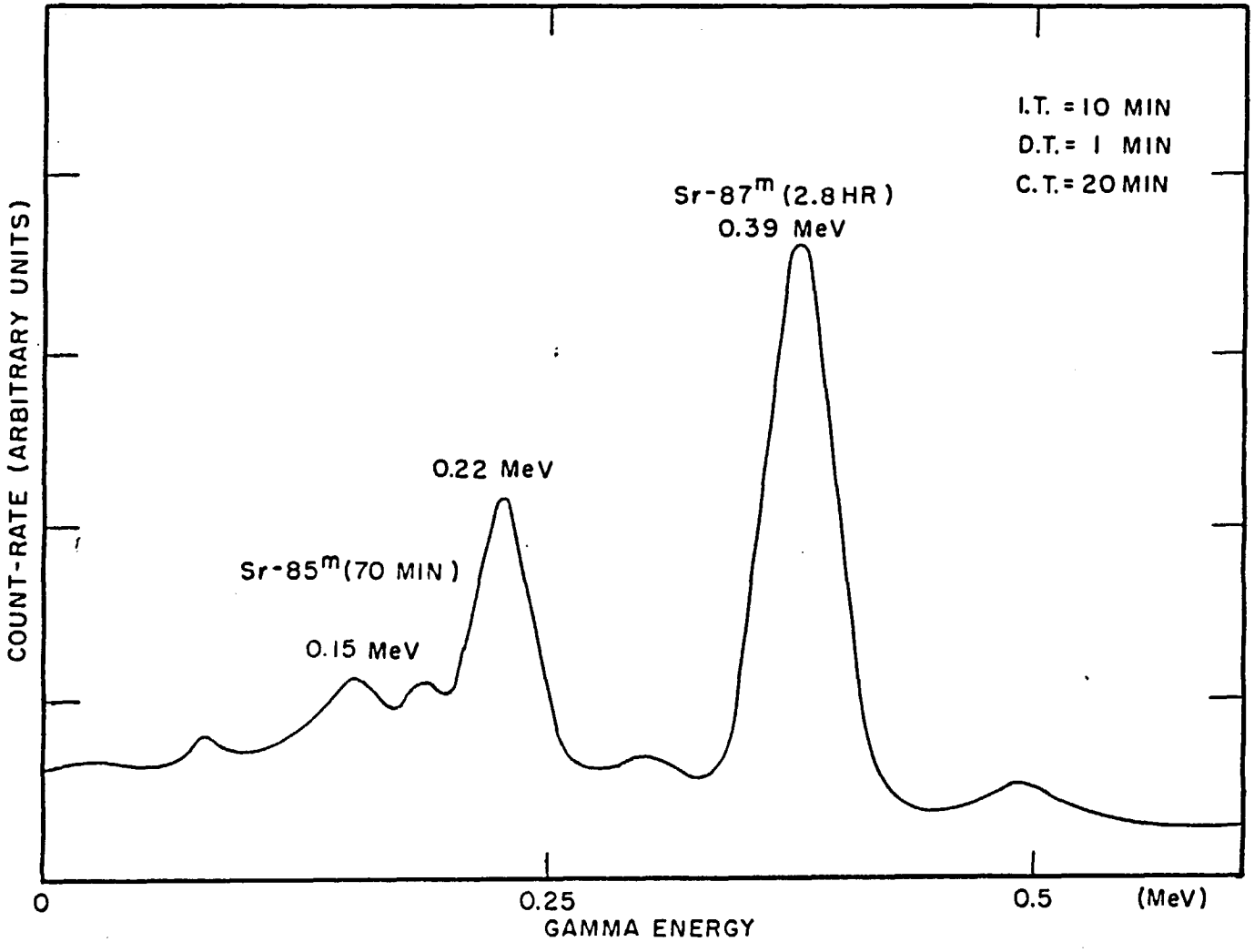

FIGURE 31. GAMMA-RAY SPECTRUM FOLLOWING THERMAL NEUTRON IRRADIATION OF $\underline{Sr}CO_3$.

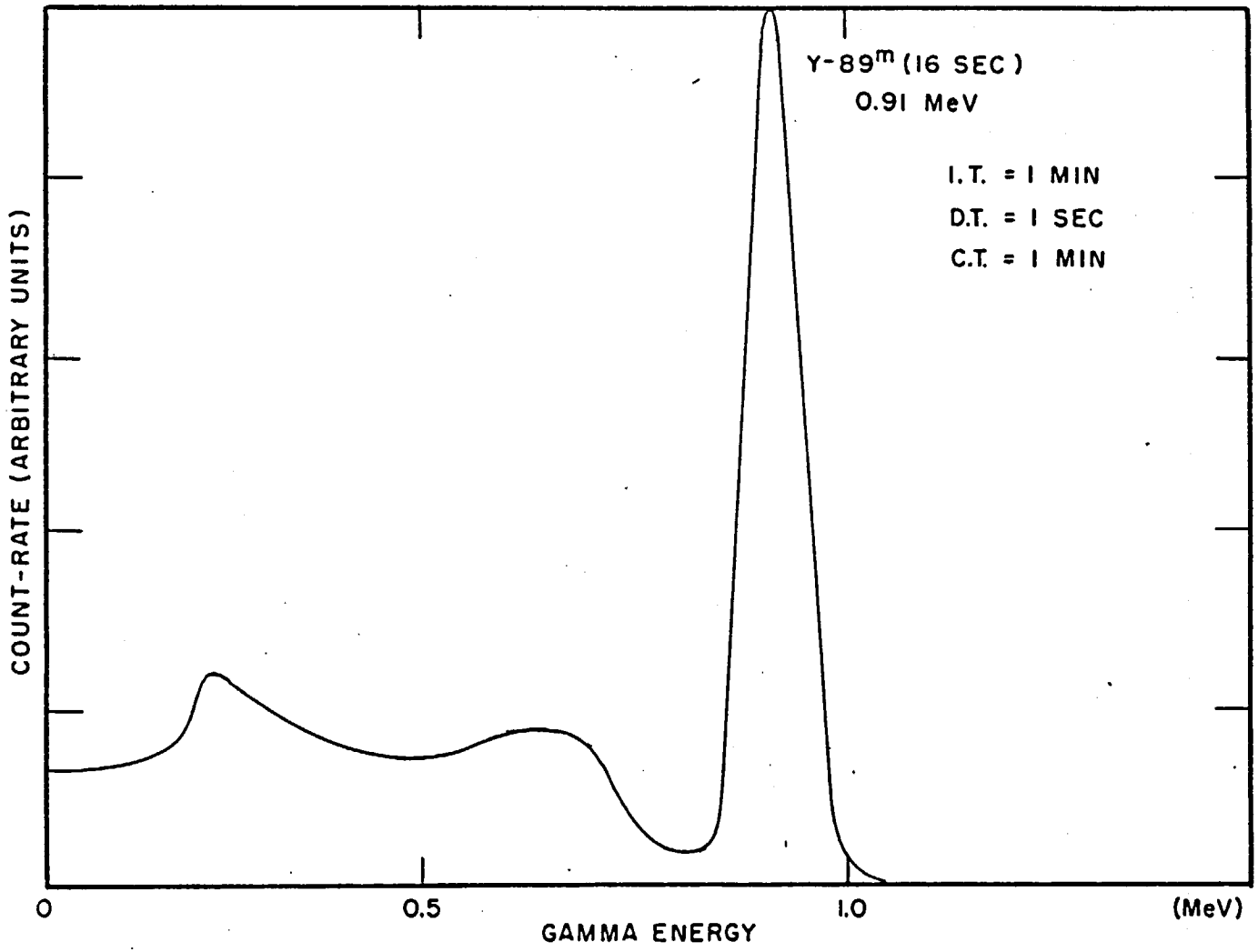

FIGURE 32. GAMMA-RAY SPECTRUM FOLLOWING FAST NEUTRON IRRADIATION OF YTTRIUM.

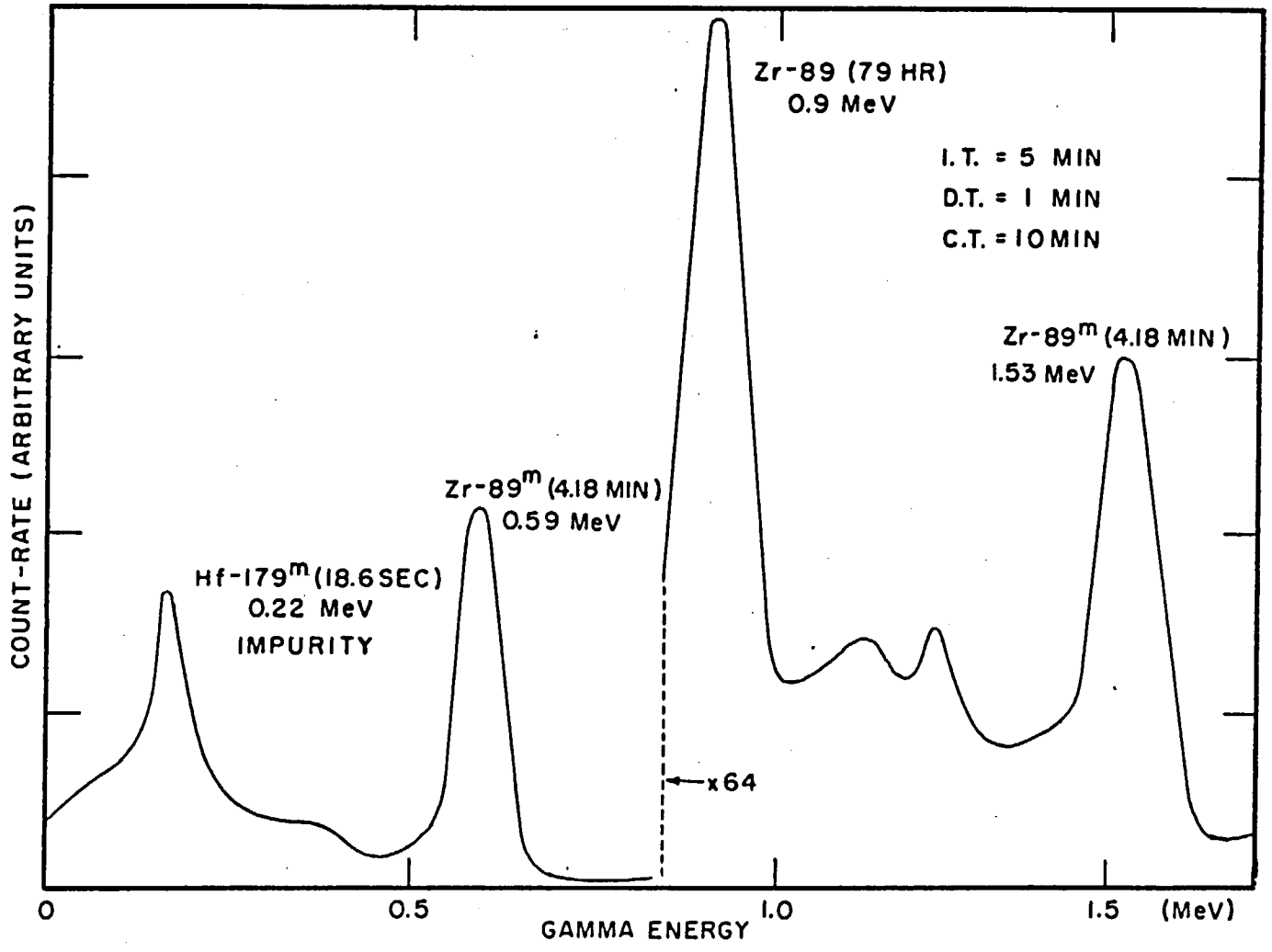

FIGURE 33. GAMMA-RAY SPECTRUM FOLLOWING FAST NEUTRON IRRADIATION OF ZIRCONIUM.

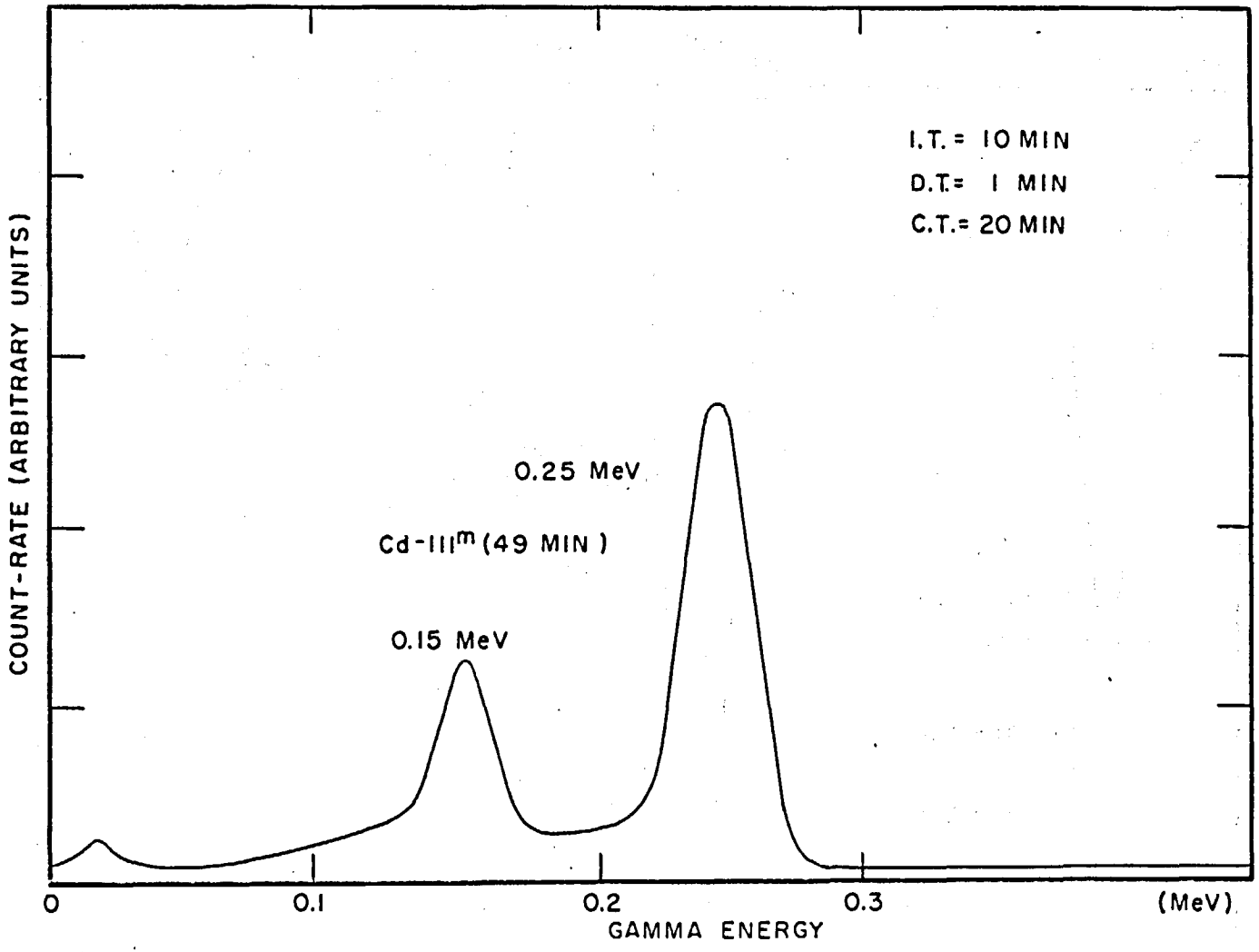

FIGURE 34. GAMMA-RAY SPECTRUM FOLLOWING THERMAL NEUTRON IRRADIATION OF CADMIUM.

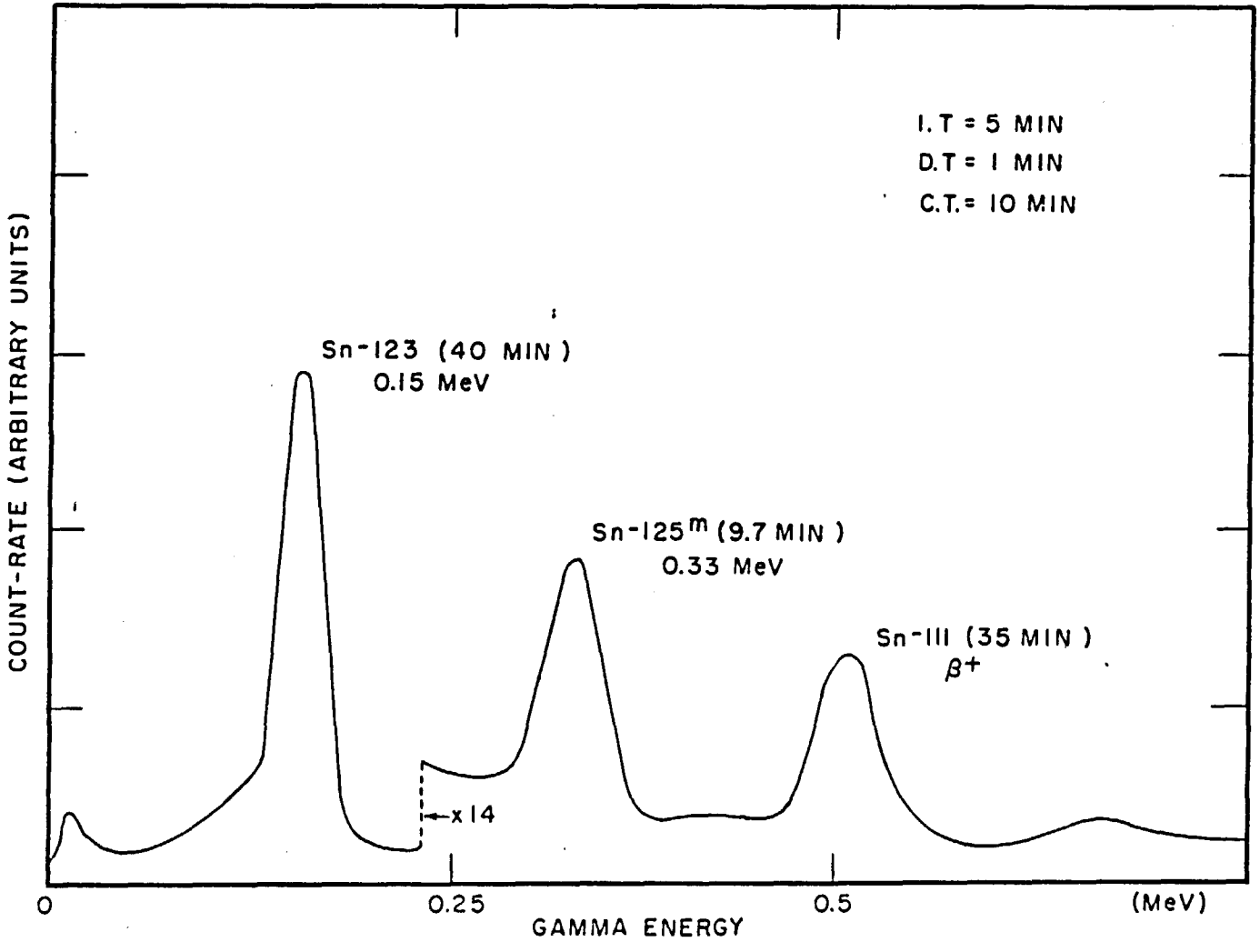

FIGURE 35. GAMMA-RAY SPECTRUM FOLLOWING FAST NEUTRON IRRADIATION OF TIN.

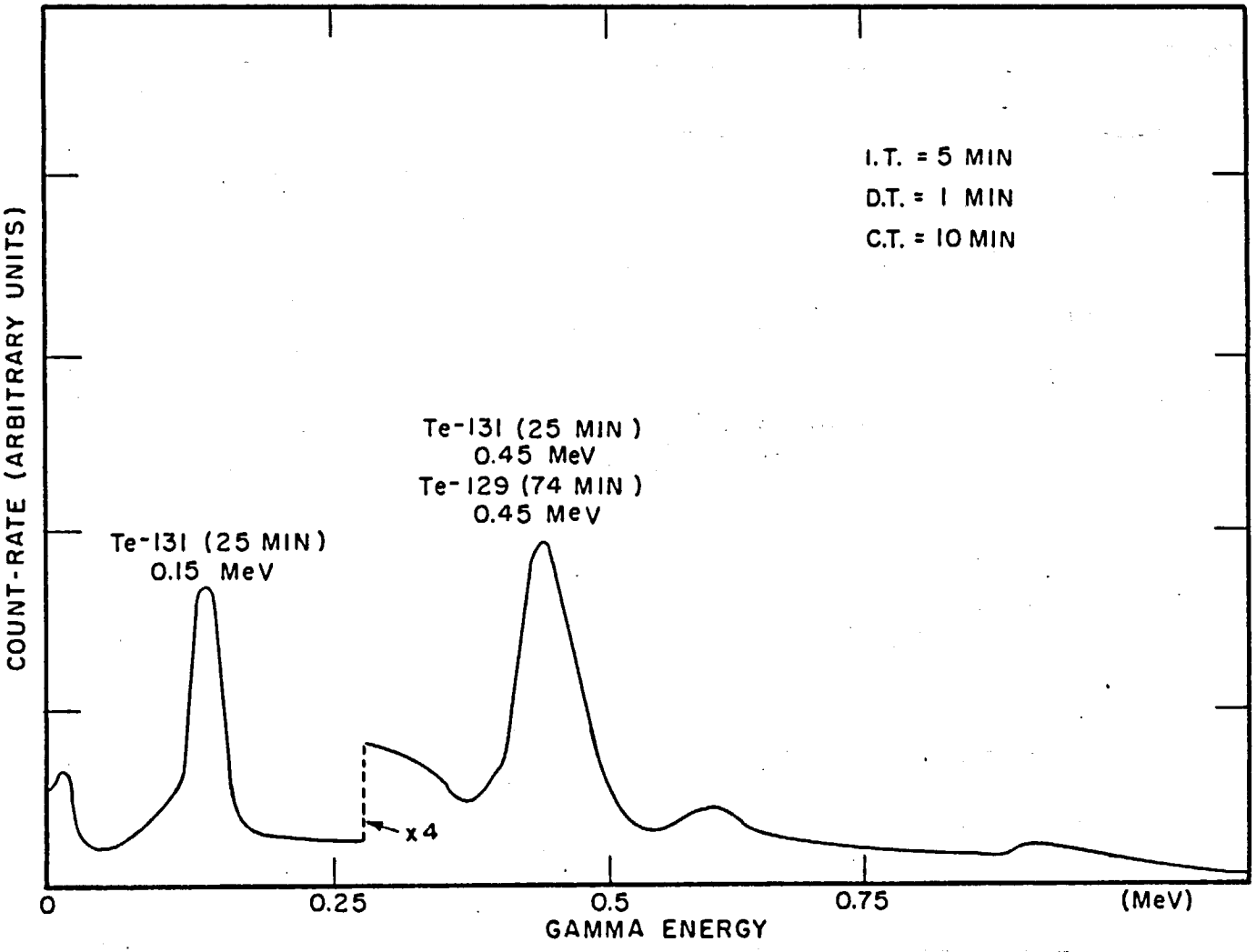

FIGURE 36. GAMMA-RAY SPECTRUM FOLLOWING THERMAL NEUTRON IRRADIATION OF TELLURIUM.

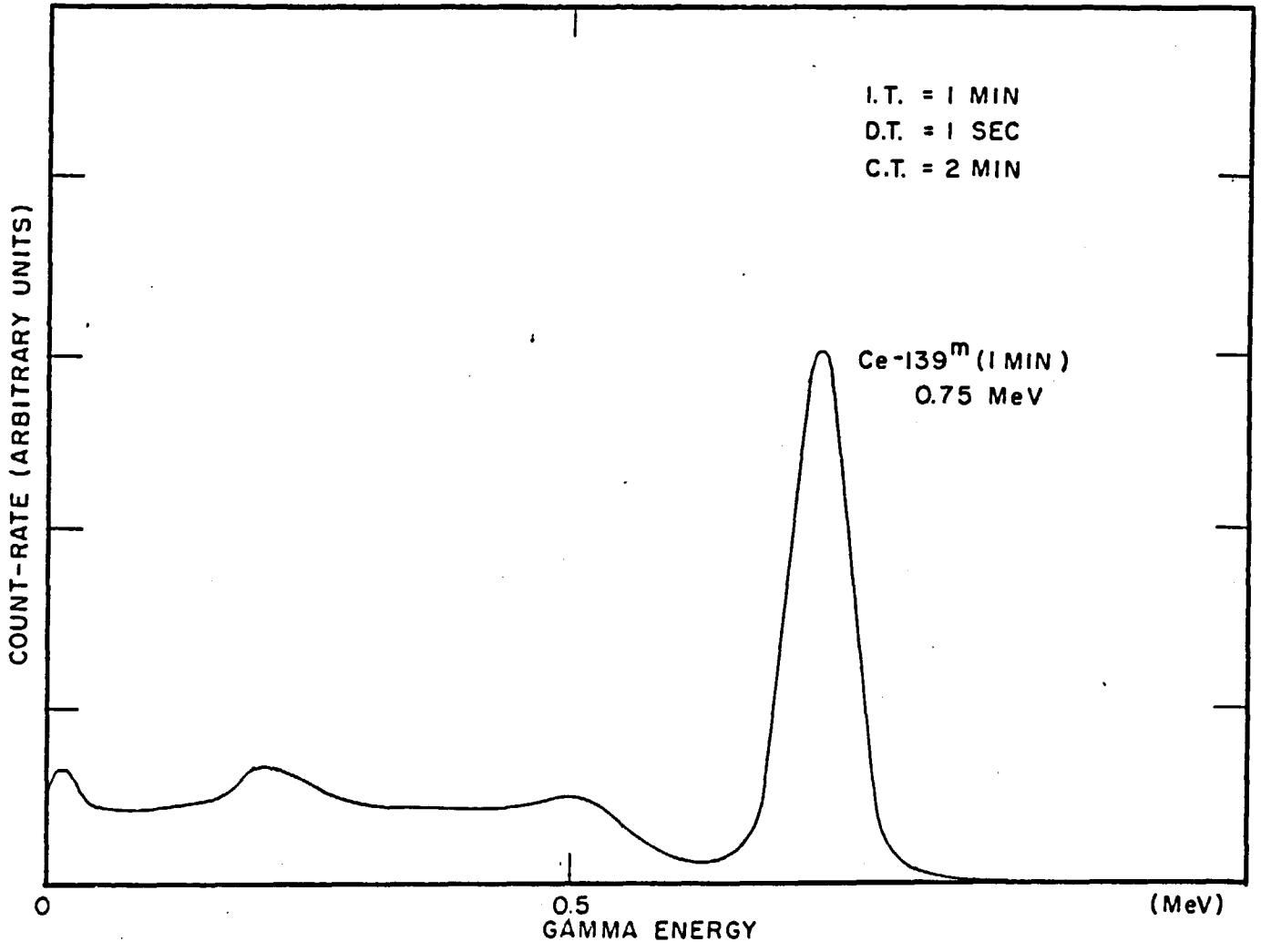

FIGURE 37. GAMMA-RAY SPECTRUM FOLLOWING FAST NEUTRON IRRADIATION OF $\underline{CeO_2}$.

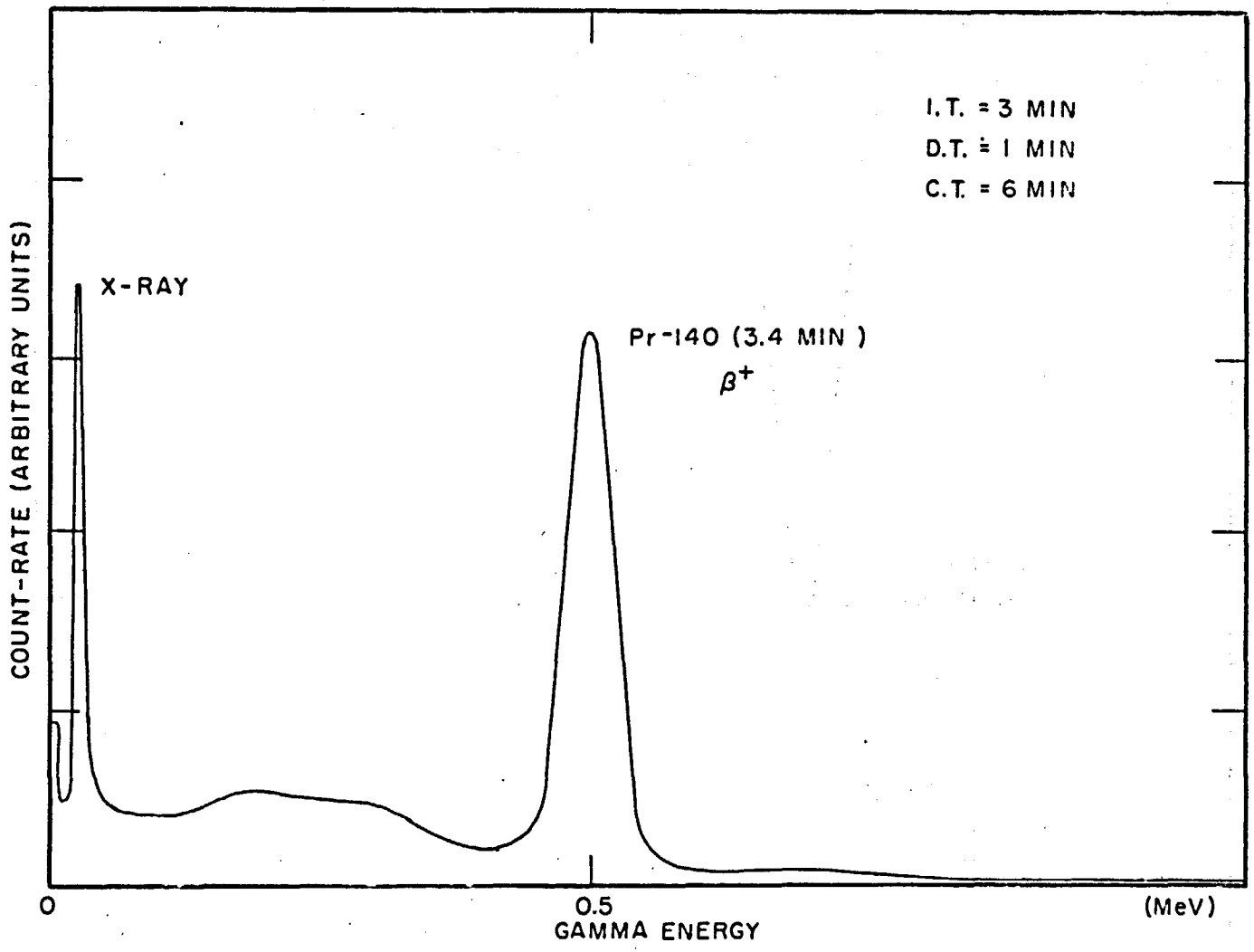

FIGURE 38. GAMMA-RAY SPECTRUM FOLLOWING FAST NEUTRON IRRADIATION OF $\underline{Pr}O_2$.

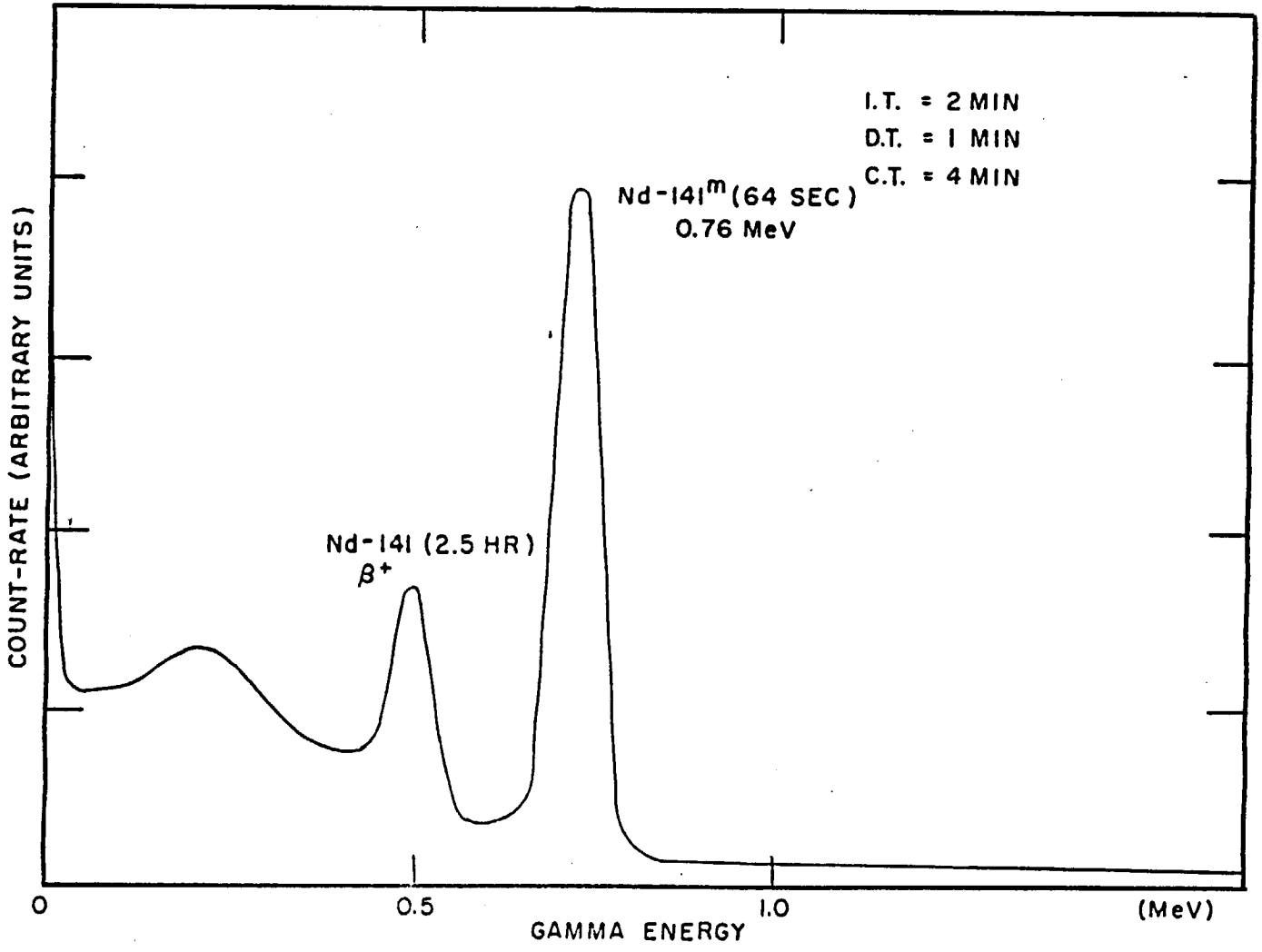

FIGURE 39. GAMMA-RAY SPECTRUM FOLLOWING FAST NEUTRON IRRADIATION OF $\underline{Nd}_2O_3$.

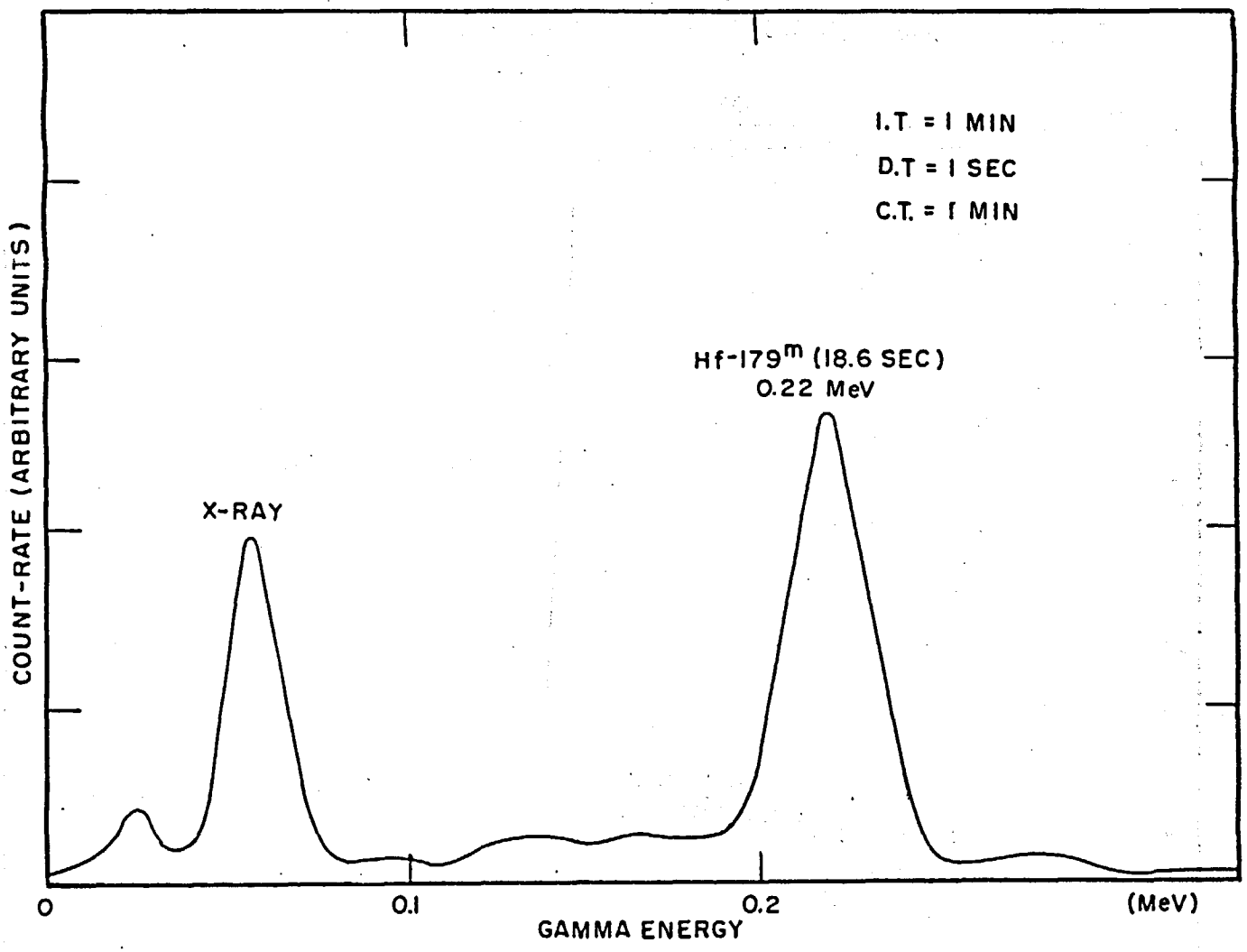

FIGURE 40. GAMMA-RAY SPECTRUM FOLLOWING THERMAL NEUTRON IRRADIATION OF HAFNIUM.

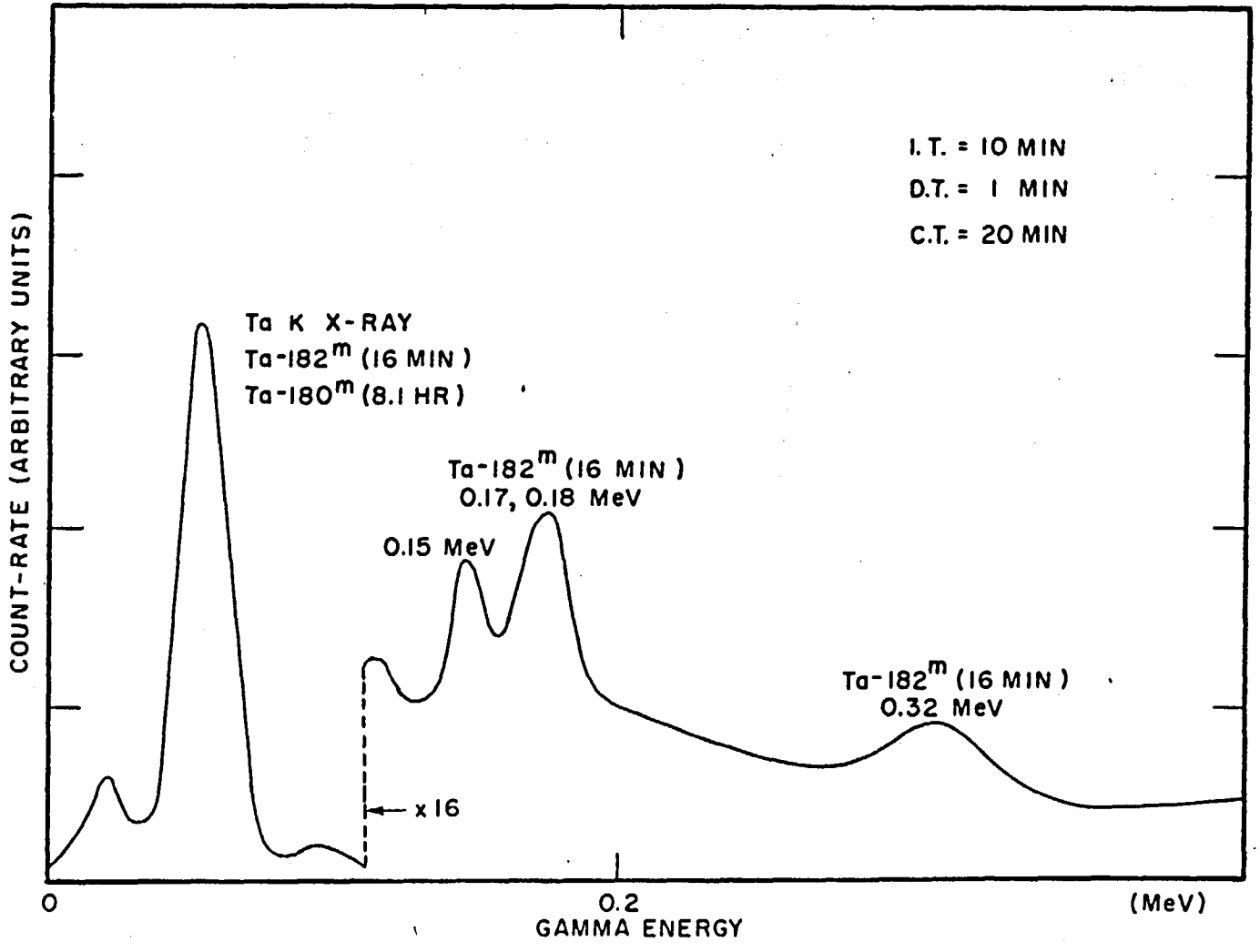

FIGURE 41. GAMMA-RAY SPECTRUM FOLLOWING THERMAL NEUTRON IRRADIATION OF TANTALUM.

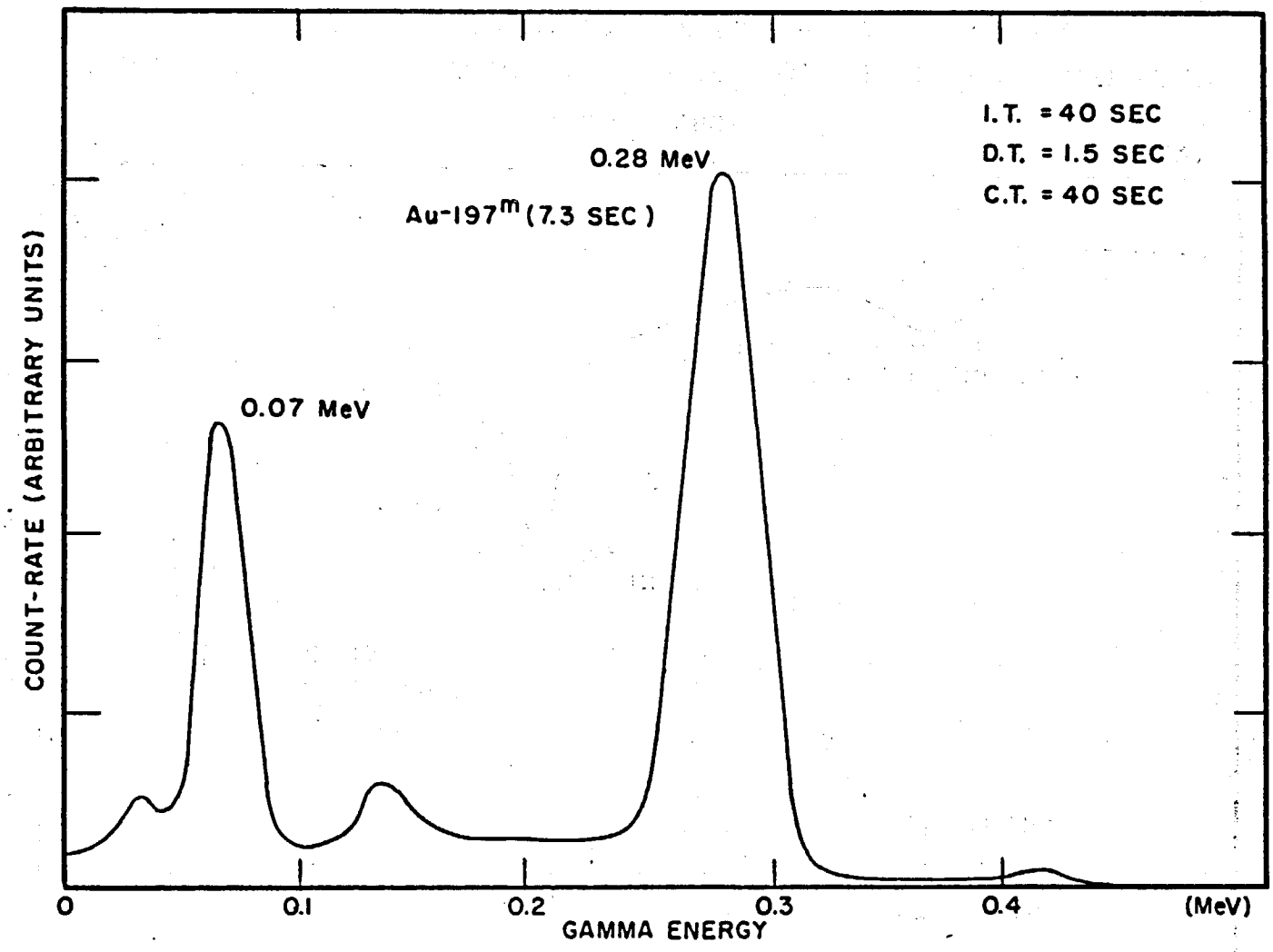

FIGURE 42. GAMMA-RAY SPECTRUM FOLLOWING FAST NEUTRON IRRADIATION OF GOLD.

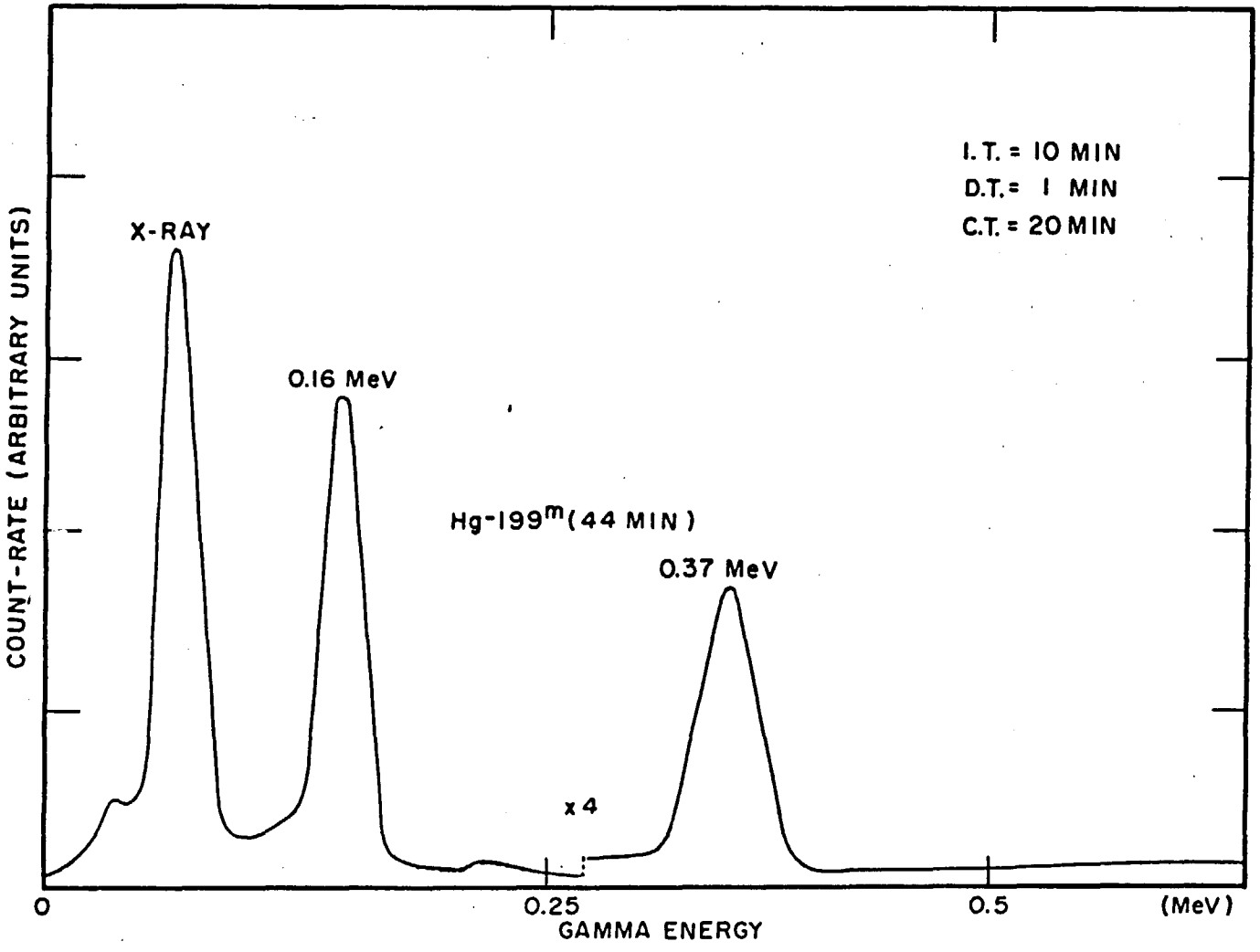

FIGURE 43. GAMMA-RAY SPECTRUM FOLLOWING FAST NEUTRON IRRADIATION OF HgO.

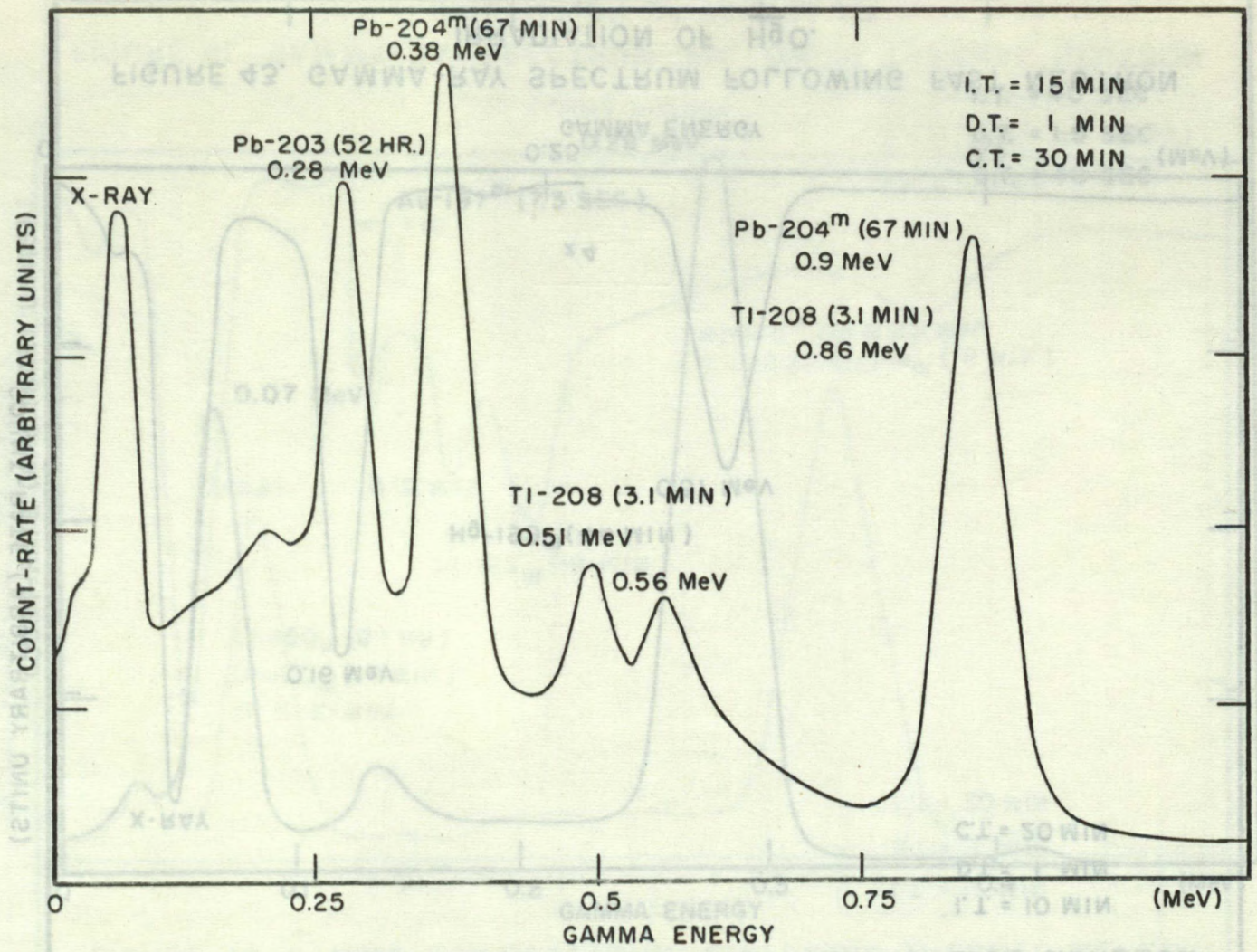

FIGURE 44. GAMMA-RAY SPECTRUM FOLLOWING FAST NEUTRON IRRADIATION OF LEAD.

====

HPD:gt